Environmental Technology Management (ETM):

Performance and Reaction Activity Changes of a NO_X Storage/Reduction Catalyst as a Function of Regeneration Mixture and Thermal Degradation

by

Meshari AL-Harbi

A thesis
presented to the University of Waterloo
in fulfillment of the
thesis requirement for the degree of

Master of Applied Science
in
Chemical Engineering

Waterloo, Ontario, Canada, 2008

© Meshari AL-Harbi 2008

AUTHOR'S DECLARATION

I hereby declare that I am the sole author of this thesis. This is a true copy of the thesis, including any required final revisions, as accepted by my examiners.

 I understand that my thesis may be made electronically available to the public.

Meshari AL-Harbi

Abstract

With steadily increasing emissions regulations being imposed by government agencies, automobile manufacturers have been developing technologies to mitigate NO_X emissions. Furthermore, there has been increasing focus on CO_2 emissions. An effective approach for CO_2 reduction is using lean burn engines, such as the diesel engine. An inherent problem with lean-burn engine operation is that NO_X needs to be reduced to N_2, but there is an excess of O_2 present. NO_X storage and reduction (NSR) is a promising technology to address this problem. This technology operates in two phases; where in the lean phase, normal engine operation, NO_X species are stored as nitrates, and in a reductant rich phase, relative to O_2, the NOx storage components are cleaned and the NO_X species reduced to N_2.

In this study, the effects of reductant type, specifically CO and/or H_2, and their amounts as a function of temperature on the trapping and reduction of NO_X over a commercial NSR catalyst have been evaluated. Overall, the performance of the catalyst improved with each incremental increase in H_2 concentration. CO was found ineffective at 200°C due to precious metal site poisoning. The addition of the H_2 to CO-containing mixtures resulted in improved performance at 200°C, but the presence of the CO still resulted in decreased performance in comparison to activity when just H_2 was used. At 300-500°C, H_2, CO, and mixtures of the two were comparable for trapping and reduction of NO_X, although the mixtures led to slightly improved performance.

Although NSR technology is very efficient in reducing NO_X emissions, a significant challenge that questions their long-term durability is poisoning by sulfur compounds

inherently present in the exhaust. Therefore, during operation, NSR catalysts require an intermittent high-temperature exposure to a reducing environment to purge the sulfur compounds from the catalyst. This desulfation protocol ultimately results in thermal degradation of the catalyst. As a second phase of this study, the effect of thermal degradation on the performance of NSR technology was evaluated. The catalyst performance between a 200 to 500°C temperature range, using H_2, CO, and a mixture of both H_2 and CO as reductants was tested before and after different high-temperature aging steps. Tests included water-gas shift (WGS) reaction extent, NO oxidation, NO_X storage capacity, oxygen storage capacity (OSC), and NO_X reduction efficiency during cycling. The WGS reaction extent was affected by thermal degradation, but only at low temperature. NO oxidation did not show a consistent trend as a function of thermal degradation. The total NO_X storage capacity was tested at 200, 350 and 500°C. Little change was observed at 500°C with thermal degradation and a steady decrease was observed at 350°C. At 200°C, there was also a steady decrease of NO_X storage capacity, except after aging at 700°C, where the capacity increased. There was also a steady decrease in oxygen storage capacity at test temperatures between 200 and 500°C after each increase in thermal degradation temperature, except again when the sample was degraded at 700°C, where an increase was observed. In the cycling experiments, a gradual drop in NO_X conversion was observed after each thermal degradation temperature, but when the catalyst was aged at 700°C, an increase in NO_X conversion was observed. These data suggest that there was redispersion of a trapping material component during the 700°C thermal degradation treatment while the oxygen storage capacity data indicate redispersion of oxygen storage components. It therefore seems

likely that it is these oxygen storage components that are becoming ''activated'' as trapping materials at low temperature.

Acknowledgements

Dedication

To my families especially

my beloved parents

and

my beloved wife

Table of Contents

List of Figures

xiii

List of Tables

Chapter 1: Introduction

1.1 Overview

Environmental Technology Management (ETM) focuses on providing a comprehensive understanding of the environmental issues for air, water, and land and solutions for those issues. The focus of this research is on a technology for controlling NO_X pollution and preventing its introduction into the environment.

Climate change is a significant environmental issue facing the world today. Global warming and climate change have created need for reducing automotive emissions of greenhouse gasses. Globally, concerns have been raised about the increase in carbon dioxide level, the principal greenhouse gas, in the atmosphere. There is approximately 30 percent more carbon dioxide in the atmosphere today than there was in 1750 [1]. This increase in carbon dioxide concentration has caused, and is causing, the earth's atmosphere to warm up. Carbon dioxide is emitted to the atmosphere from either natural sources such as volcanic eruptions, or human-related sources such as the combustion of fossil fuels such as coal, oil and gas in power plants, automobiles, industrial facilities and other sources. For automobiles, one of the suggested approaches for mitigation and reduction of CO_2 emissions is the use of lean burn engines, such as diesel engines.

Despite the fact that using diesel engines can contribute to a reduction of carbon dioxide relative to gasoline engine use, their NO_X emissions require special attention. The inherent challenge is reducing NO_X to N_2 in the oxidizing environment of lean-burn engine exhaust gas. Several technologies have been proposed to mitigate such diesel

engine emissions. These include three way catalytic (TWC) converters, continuous selective catalytic reduction (SCR), and nitrogen storage/reduction (NSR) catalysis. Each of these technologies will be described in this chapter.

1.2 Air Pollutants

Air pollutants are any substances, particles, liquids, or gaseous, that are released into the air and lead to a deterioration of the atmosphere, which in turn will affect the life of humans, plants, and animals. Pollutants are classified as either primary or secondary.

Primary pollutants are substances that are released directly into the air from their sources. Common examples of primary pollutants include sulfur dioxide (SO_2), carbon monoxide (CO), nitrogen oxides (NO_X), particulate matter less than 10 μm in diameter (PM-10), particulate lead (Pb), and volatile organic compounds (VOCS). In table 1, some primary pollutants are listed, starting from 1970, as cited by the Environmental Protection Agency (EPA)[2].

Secondary pollutants are not directly emitted from sources, but form in the atmosphere as a result of chemical and photochemical reactions of other emitted molecules. Common examples of secondary pollutants are ground level ozone (O_3), peroxy acetyl nitrate (PAN), and hydrogen peroxide (H_2O_2).

These pollutants, whether primary or secondary, have harmful effects on human, plant, and animal life. SO_2, for example, can react with water to form sulfuric acid which can corrode buildings, statues, and bridges as well as lead to lower pH levels in bodies of water. Also, sulfur dioxide is irritating to the respiratory system, eyes, and can result in

severe diseases[3]. Another example is CO, which is a poisonous gas that can be produced as a result of incomplete combustion of hydrocarbons in motor vehicle engines. It has significant effects on human health. It can cause shortage of breath, dizziness, severe headaches, and at high concentration can cause death.

Table 1-1 National air pollutant emissions estimates for major pollutants (EPA)

	Millions of Tons Per Year								
	1970	1975	1980	1985	1990	1995	2000	2005	2006
Carbon Monoxide (CO)	197	184	178	170	144	120	102	91	88
Nitrogen Oxides (NO$_X$)	27	26	27	26	25	25	22	19	18
Particulate Matter (PM) $\quad$ PM$_{10}$ $\quad$ PM$_{2.5}$	12 NA	7 NA	6 NA	4 NA	3 2	3 2	2 2	2 1	2 1
Sulfur Dioxide (SO$_2$)	31	28	26	23	23	19	16	15	14
Volatile Organic Compounds (VOC)	34	30	30	27	23	22	17	15	15
Lead	0.221	0.16	0.074	0.023	0.005	0.004	0.002	0.003	0.002
Totals	302	276	267	249	218	189	159	142	137

1.2 Regulations and Standards

With a dramatic increase in the number of cars world wide over the last several decades, government environmental agencies have been continuously imposing tighter regulations

to mitigate emissions from vehicle engines. Overall, automobile manufacturers have made remarkable progress in reducing pollutant emissions via advanced engine design and advanced exhaust aftertreatment technologies.

Basically, air quality standards are set by accounting for the assessment of the effects of each pollutant on public health and the environment. In fact, since the Clean Air Act (CAA) legislation began in 1955, there have been noteworthy reductions in emission levels.

Table 1-2 California (CARB) Emissions Standards

Year	Emission (g/mile)			
	HC	NO_X	CO	PM
1993	0.25	0.40	3.40	
1994	0.25	0.40	3.40	
2003	0.25	0.40	3.40	
2004	0.125	0.40	3.40	0.08
2005	0.075	0.40	3.40	0.08
2006	0.04	0.20	1.70	0.04
2007	0	0	0	0

Although public awareness related to air pollutants regulation has been gradually increasing over the last decade, statistics show that more than thousands die yearly because of air pollutants[4]. Therefore, public and governments efforts are still focused on reducing air pollution to protect human health. In table 2, a summary of some common pollutant legislation history is listed.

1.4 NO_X

NO_X is a generic term pertaining to compounds of nitric oxide (NO), nitrogen dioxide (NO_2), and other oxides of nitrogen, all of which are highly reactive gases. Most of the nitrogen oxides are colorless and odorless, except for NO_2, which appears as a yellowish-brown cloud with a biting odor. In our research, NO_X is used as a generic term for mono-nitrogen oxides, NO and NO_2.

1.5 Effect of NO_X

NO_X is one of the major contributors to ground-level ozone, which forms when NO_X reacts with highly reactive VOCs in the presence of sunlight. Ozone damages vegetation, kills trees, irritates the respiratory system, throat, eyes, or nose, and causes severe headaches.

VOCs + NO_X + Sunlight → Ozone

In addition, NO_X is a major component of smog. Smog is a mixture of poisonous gases caused by a reaction between sunlight and pollutants such as ozone, NO_X, and VOCs. Smog has adverse effects on plants, animals, and humans.

Furthermore, NO_X can react with atmospheric water to form acid which falls to earth as rain, fog, or dry particles. This acid rain leads to corrosion of statues and buildings, damages crops and forests, and changes the acidity of lakes and streams, consequently,

killing fishes and other plants and animals. The following figures illustrate the effect of acid rain on statues:
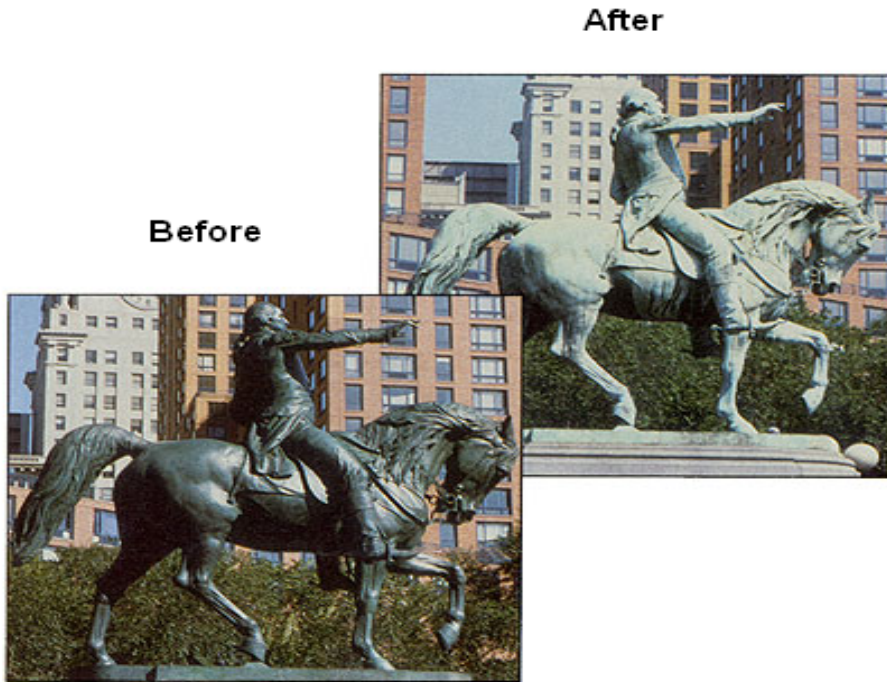
Figure 1-1 Effect of acid rain on statues

1.6 Sources of NO$_X$

The major sources of NO$_X$, as shown in Figure 2, are combustion of fuel at high temperature in motor vehicles, electric utilities, and other industrial, commercial, and residential sources.
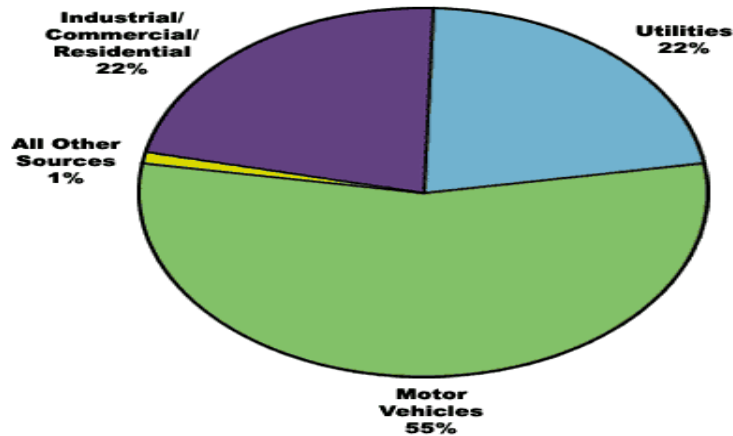
Figure 1-2 Major sources of NO$_X$ emissions (EPA)

1.7 Diesel Engine

Diesel engines operate via internal combustion. Combustion of the fuel and air takes place in enclosed space called a combustion chamber. Air is forced and compressed into the cylinder, and then the fuel is injected into it. The compressed air is hot enough to ignite the diesel fuel without the use of a sparkplug, unlike gasoline engine which needs a spark to initiate fuel ignition. The resulting combustion causes increased heat and expansion in the cylinder via increased pressure from the combustion process, which moves the piston downward creating power. The remaining gases are vented through an exhaust valve. This piston motion is transmitted by means of connecting rods to the crankshaft that converts linear motion to rotary motion for use as power in a variety of applications. A picture of diesel engine operation is shown in Figure 3.
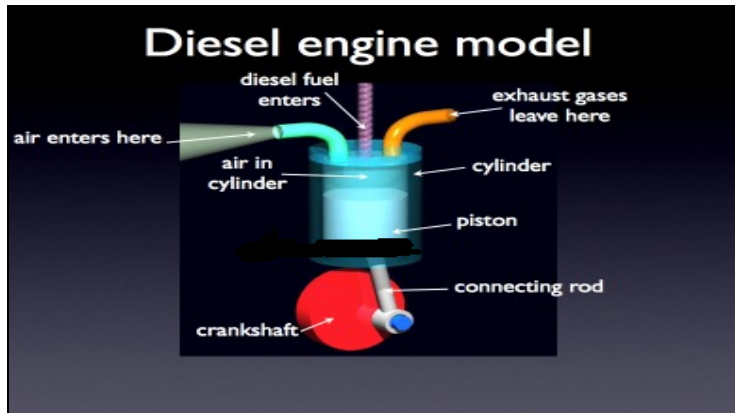
Figure 1-3 Diesel Engine operations taken from the RKM website

1.8 NO$_X$ Reduction Technologies

Although diesel engine use is promising from a fuel economy standpoint, the high NOx emissions remains an important technical issue for its use today. Fortunately, numerous technologies have been developed to reduce NO$_X$ emissions from diesel and/or lean-burn engine exhaust. Examples of the most common technologies that have been applied are summarized in Figure 4.
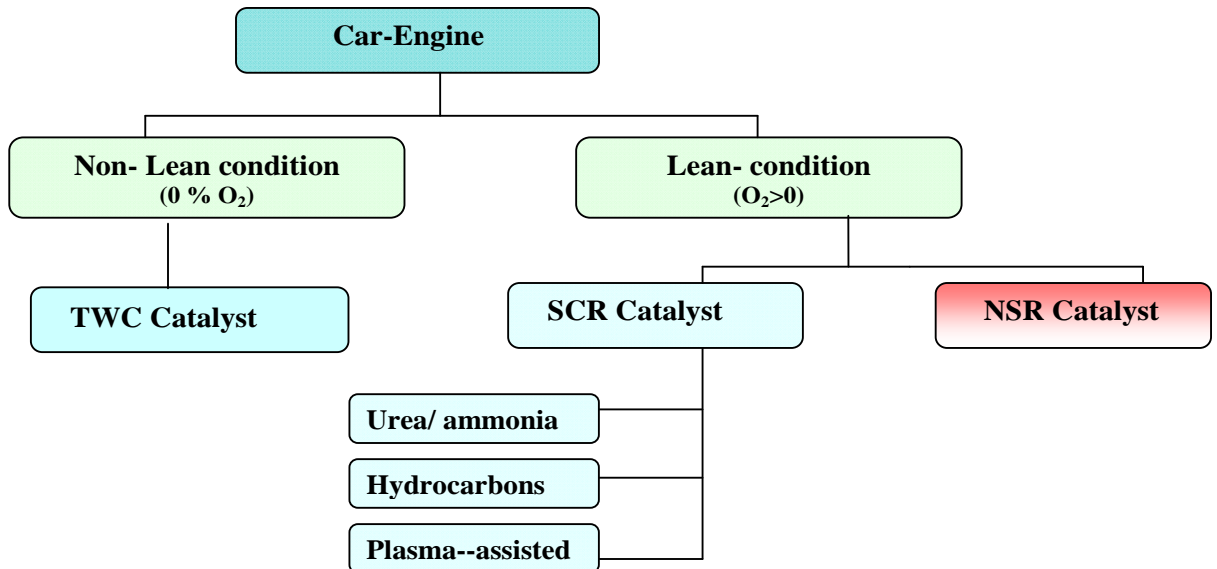
Figure 1-4 NO$_X$ emission control technologies

1.8.1 Three way catalytic (TWC) converter

The three way catalytic (TWC) converter is a device equipped in the exhaust pipe of most gasoline vehicles. It has a honeycomb structure, as shown in Figure 5. The TWC converter contains precious metals, such as platinum and rhodium, for chemically converting some pollutants in the exhaust gases, such as carbon monoxide, unburned hydrocarbons, and oxides of nitrogen, into harmless compounds. The chemical reactions occurring on the TWC can be described as follows:

$$2\ NO_X \rightarrow xO_2 + N_2$$

$$2CO + O_2 \rightarrow 2CO_2$$

$$2C_xH_y + (2x + y/2)\ O_2 \rightarrow 2xCO_2 + yH_2O$$
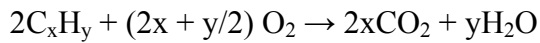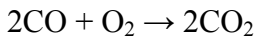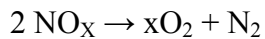
TWC converters have been used in cars since 1970 and have had a significant impact in the reduction of NO_X, CO and hydrocarbons emitted in engine exhaust. The TWC converter is designed for use in exhaust that is free of oxygen, in other words the engine operates with a stoichiometric air to fuel ratio.

$CO_2 + H_2O$
N_2
CO_2

HC
NOx
CO
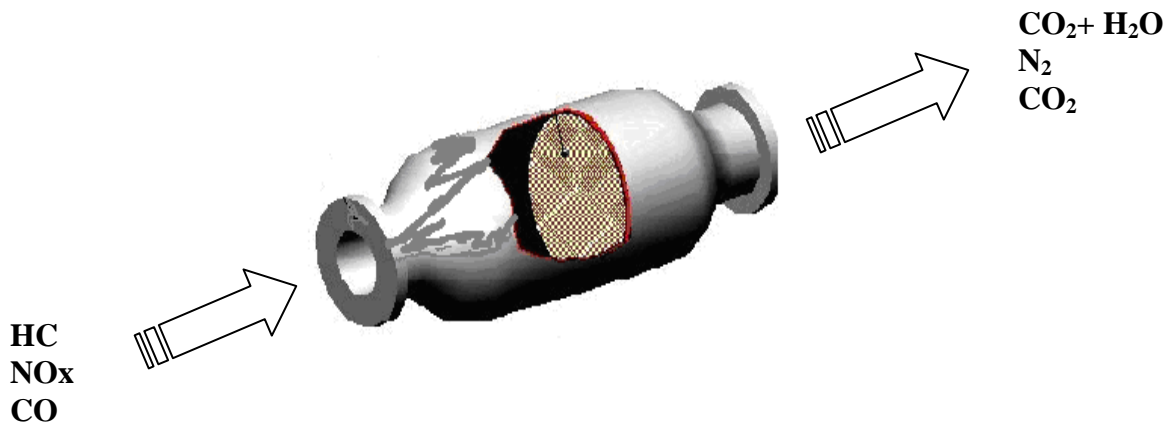
Figure 1-5 Three way catalytic converter (TWC)

Although the TWC can reduce a small fraction of lean-burn engine NO_X emissions, the reduction is not significant enough to meet today's regulations. This is due to its design focus on operation at the stoichiometric air/fuel ratio; where little to no oxygen is present during reaction. Another issue associated with TWC technology is its sensitivity toward lead, zinc, and sulfur. Thus, this catalyst can be poisoned when using fuels that have high amounts of these impurities. Due to its low conversion in lean-burn exhaust, alternate technologies have been developed to reduce NO_X emissions in oxygen-containing environments.

1.8.2 Selective catalytic reduction (SCR)

Selective catalytic reduction (SCR) is a process where a reductant such as (1) ammonia, either injected as ammonia or injecting urea as a precursor which decomposes to ammonia, or (2) a hydrocarbon, is added to the engine's exhaust gas as shown in Figure 8. These reductants react selectively with NO_X to form N_2 and H_2O. Ammonia-based SCR can meet the regulations being imposed, however there is currently no catalyst for hydrocarbon-based SCR to meet the efficiencies required to meet today's regulations. Ammonia SCR reactions take place in the presence of a catalyst, which is commonly a platinum catalyst when operating at low temperature, <573 K, a vanadium based catalyst at medium temperatures, <700 K, or metal-doped zeolites at higher temperatures, < 863 K. The basic stoichiometric reactions that occur in an ammonia SCR system are shown below:

$4 NH_3 + 4 NO + O_2 \rightarrow 4 N_2 + 6 H_2O$

$$4\ NH_3 + 2\ NO_2 + O_2 \rightarrow 3\ N_2 + 6\ H_2O$$
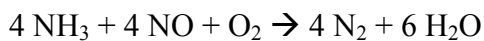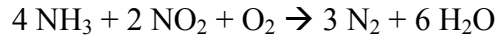
Although this technology has proven to achieve significant reductions in NO_X emissions, it has some associated problems:

- SCR catalysts with precious metals only operate well within narrow temperature bands [5] [6]. Thus, tight control and adjustment of exhaust gas temperatures are required, which is not practical for a wide range of driving conditions.

- SCR technology would require a distribution network for urea or ammonia. In addition, there are toxicity, storage and refueling problems with these reductants[7].

- Another common problem with SCR is ammonia slip and odor[8]. Consequently, it requires a very accurate injection system for urea or ammonia to assure that all the ammonia is consumed by NO_X to prevent ammonia slip.
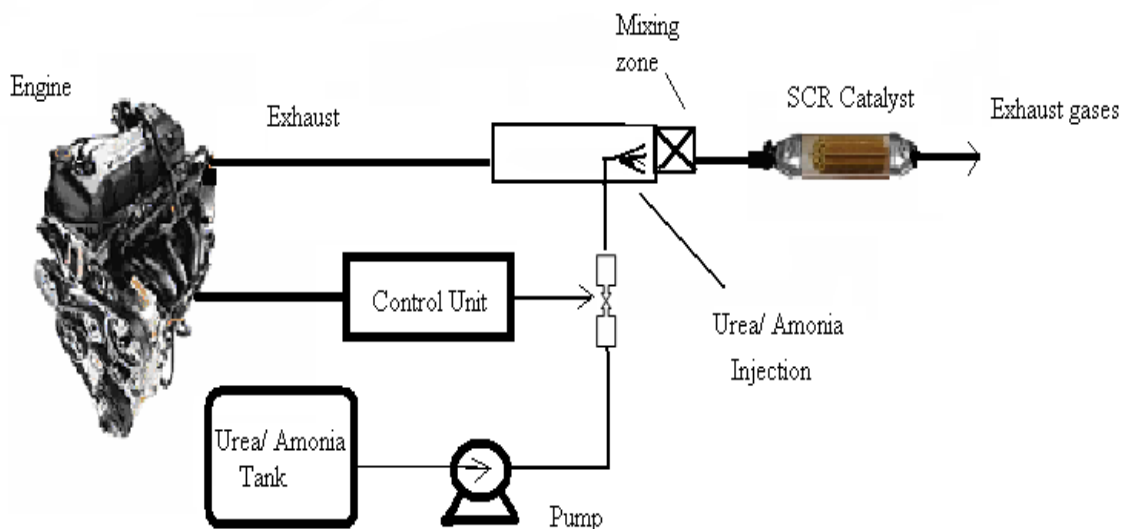
Figure 1-6 Selective Catalytic Reduction Technology

1.8.3 NSR Catalyst Technology

Nitrogen storage/reduction (NSR) catalyst technology is a new and promising technology for NO_X emission abatement from diesel engines. Reduction of NO_X to N_2 over a NSR catalyst, as described in Figure 9, is accomplished in five sequential reaction steps [9]:

1. Oxidation of NO to NO_2,

2. Adsorption of NO_2 onto alkali and/or alkaline earth components in the form of nitrate or nitrite species,

3. Reductant evolution,

4. NO_X release from nitrate or nitrite sites, and

5. Reduction of NO_X to N_2.
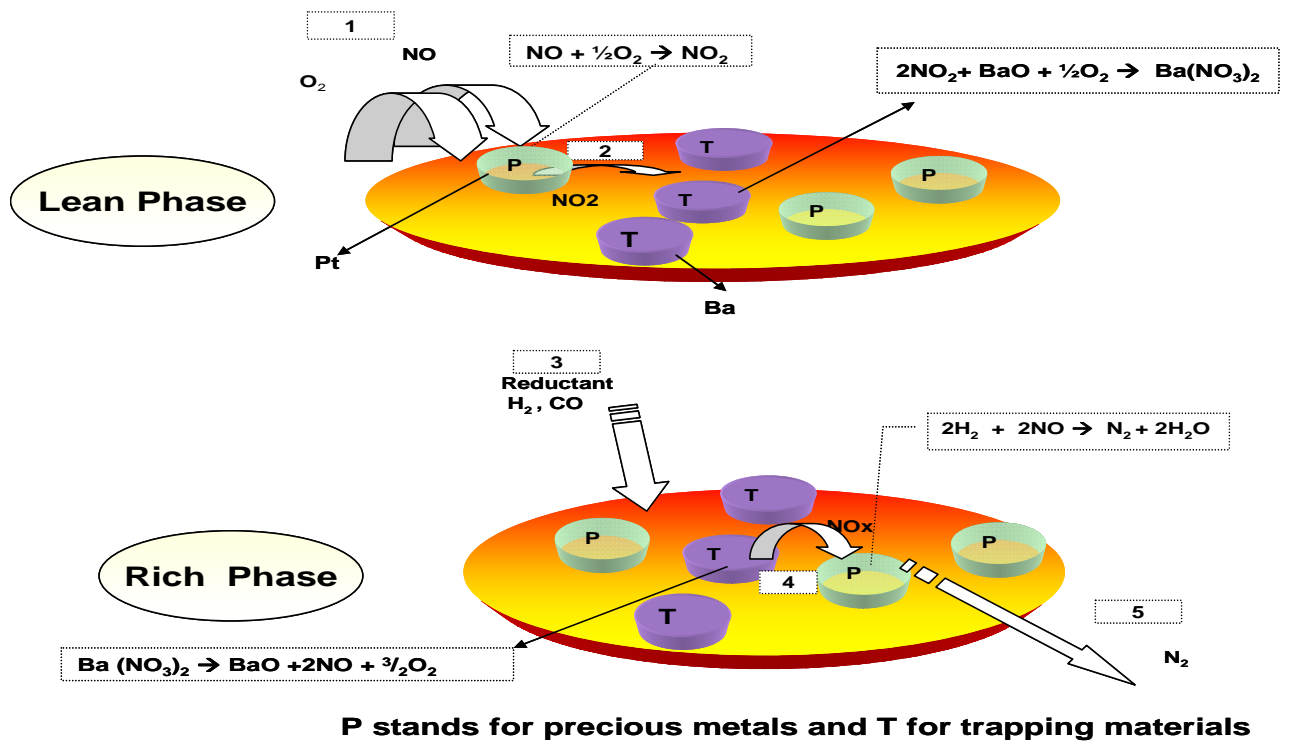
Figure 1-7 Overall Nitrogen Storage/ Reduction reactions

This technology operates in two phases; called lean and rich. The lean phase is normal engine operation and the exhaust gas in this phase includes CO_2, H_2O, O_2, N_2 and NO_X species, as shown in Table 1-3. The NSR catalyst contains alkali and alkaline metal earth components, such as BaO, as NO_X storage materials. These have the ability to store the entering NO_X species in the form of a nitrate, Ba $(NO_3)_2$ and/or nitrite, $Ba(NO_2)_2$, during lean conditions. With time, the storage materials become saturated with NO_X species.

Table 1-3 Diesel engine exhaust for both lean and rich phase

Phase	*Gases*
Lean	**H_2O, CO_2, NO_X , O_2, and N_2**
Rich	**H_2O, CO_2, reductants (for example H_2 and CO), and N_2**

Thus, the rich phase is needed to clean the storage materials from adsorbed NO_X and complete the cycle, thereby beginning a new cycle where the storage species are nitrate-free and are able to adsorb entering NO_X species again. This rich phase is also described in Table 1- 3, where a key factor is the presence of reductants.

In NSR, reductants have the ability to react with NO_X and convert it to N_2. The most commonly used reductants in NSR catalyst testing are H_2, CO, and propylene. These reductants are present in gasoline and diesel engine exhaust as a result of combustion of extra fuel and air. H_2 is the most effective reductant at low temperature, while all other reductants are comparable at high temperature[10]. When the engine switches to the rich

phase, NO_X species release from the storage materials, migrating to adjacent precious metal sites, such as Pt. On metallic Pt, NO_X can be reduced to N_2. Proposed reactions that occur between NO_X and reductants are listed below:

$2H_2 + 2NO \rightarrow N_2 + 2H_2O$

$2CO + 2NO \rightarrow N_2 + 2CO_2$

$C_3H_6 + 9NO \rightarrow 4.5 N_2 + 3CO_2 + 3H_2O$
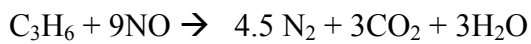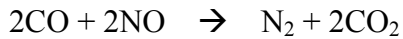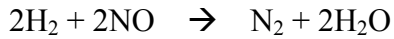
In NSR, one cycle takes approximately ½ to 2 minutes, with 1 to 5 seconds for the rich phase. Overall, NSR catalysts contain both NO_X storage materials, such as alkali and alkaline earth components, and precious metals, such as Pt, which account for oxidation of NO to NO_2 and reduction of NO_X to N_2. All these materials are supported on alumina (Al_2O_3).
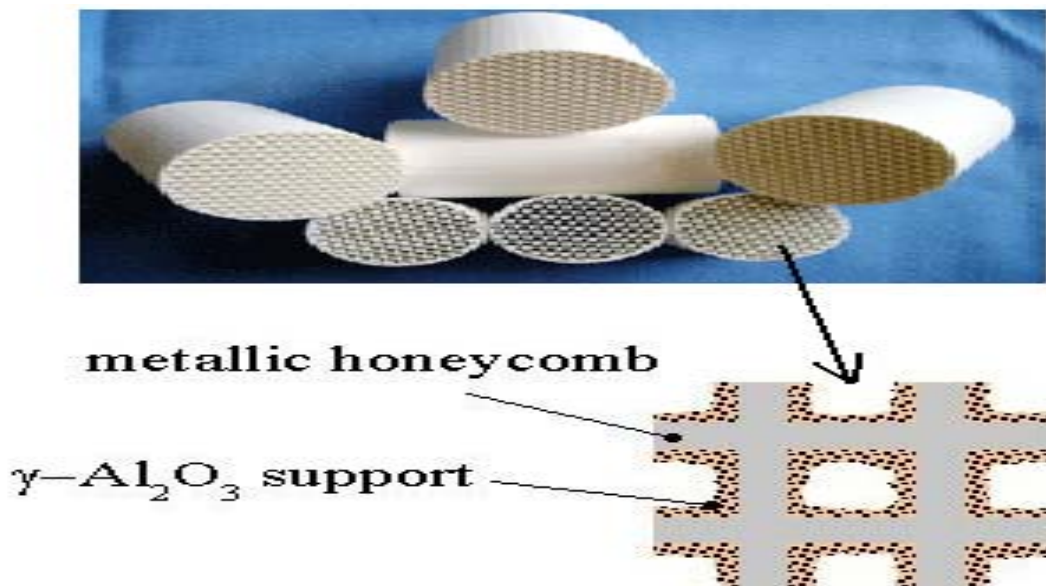
Figure 1-8 Structure of a NSR catalyst

An NSR catalyst, like the TWC, is supported on a ceramic honeycomb structure to expose the maximum surface area of catalyst to the exhaust stream while minimizing the back pressure and amount of catalyst required. Figure 10 illustrates the structure of a honeycomb catalyst.

1.8.3.1 Deactivation of NSR Catalysts

Catalyst deactivation is a generic term used to describe a decrease in the activity of a catalyst. Catalyst deactivation is typical in most catalytic processes, but hopefully a slow phenomenon. A catalyst can be deactivated via five standard mechanisms. Each one is defined briefly in Table 1-4. These mechanisms are classically categorized into three main types: chemical, thermal and mechanical[11].

Thermal aging and sulfur poisoning are the two major mechanisms for deactivation of NSR catalysts [9]. SO_2 is always found in the exhaust of diesel engines. Sulfates can then form on the alkali or alkaline-earth species just as nitrates do from NO_X. These sulfates are more stable than the nitrates and therefore they result in less NO_X storage sites available on the catalyst.

Therefore, it is critical to keep the surface sulfate concentration low, or to periodically remove sulfate build-up. The latter is called desulfation and is the accepted solution as complete S removal from fuel is not currently practical. Desulfation can be achieved by introducing a reductant such as hydrogen, but at much higher temperatures than that required to reduce the surface nitrates. The sulfur is removed via the reaction of hydrogen

15

with sulfur to form hydrogen sulfide (H_2S). However, the requirement of high temperature ultimately results in thermal degradation of the catalyst.

Table 1-4 Mechanisms of catalyst deactivation

Mechanism	Type	Problem	Cause
Fouling	**Mechanical**	**Loss of catalytic surface sites due to formation of carbon or coke films**	**Physical deposition of species from fluid phase onto the catalyst surface and pores**
Poisoning	**Chemical**	**Loss of catalytic surface sites**	**Blockage of sites by strong adsorption of Impurity**
Thermal degradation	**Thermal**	**Loss of catalytic surface area, supported area, and transformation of catalytic phases to noncatalytic phases**	**Migration of metal particle, crystallization and/or structural modification or collapse, and active phase-support reaction**
Vapor Formation	**Chemical**	**Loss of catalytic phases**	**Reaction of gas with catalyst phase to form volatile compound**
Attrition	**Mechanical**	**Loss of catalytic materials**	**Loss of catalyst surface area due to mechanical crashing of catalyst particle**

Thermal degradation of NSR catalysts is inevitable at the temperatures required for desulfation (T>650ºC)[12]. Thermal degradation of NSR catalysts occur via the loss of precious metal dispersion (sintering), the loss of surface area of the NO_X storing components, and the loss of surface area of oxygen storage capacity (OSC) components. Pt and Rh, and sometimes Pd, are commonly used in NSR catalysts. They are known to

sinter easily in an oxidizing atmosphere (O_2, H_2O, in N_2) and in reducing atmospheres (H_2, H_2O, in N_2) at high temperatures [13].

Overall, a decrease in NO_X storage capacity upon exposure to high temperature can be attributed to the following reasons. First, the storing materials, the most common example being Ba, can react with the washcoat ingredients, such as alumina resulting in a loss of trapping sites. A second reason is the loss of interface contact area between the precious metals and adsorbents because of particle growth of both [14]. Simple agglomeration of the trapping site components is another reason.

The OSC of the catalyst can be decreased as a result of particle size growth of OSC components such as ceria (Ce)[15]. These losses are on top of the loss in activity due to precious metal sintering.

1.9 Research objectives

In the research to be described, the goals were to:

1. Evaluate the effect of amount, and ratio of H_2 and CO reductants on the trapping and reduction performance of a commercial NSR catalyst.

2. Investigate the effect of thermal degradation on the performance of a commercial NSR catalyst.

Chapter 2: Literature Review

As stated, the research project had two main goals:

1. Evaluating the effect of amount and ratio of H_2 and CO reductants on the trapping and reduction performance of a commercial NSR catalyst.

2. Investigating the effect of thermal degradation on the performance of a commercial NSR catalyst.

In this section, a literature review focused on the five sequential reaction steps for NSR catalysis and the effect of thermal degradation on the performance of a commercial NSR catalyst is presented.

2.1 Overview of the NSR cycle

The NSR process cycles through two phases; a lean phase and a rich phase. In one step of the lean phase NO is oxidized to NO_2. Subsequently, NO_2 can be adsorbed by trapping materials such as Ba, in the form of $Ba(NO_3)_2$ and/or $Ba(NO_2)_2$. In operation, the lean phase continues until NO_X starts to slip, which is an indication that the trapping materials are becoming saturated. At this point, the second phase of the cycle is typically started. In the rich phase, reductants are introduced to reduce the NO_X species to N_2. The entire process takes approximately ½ to 2 minutes. Overall, the reduction of NO_X to N_2 over an NSR catalyst can be described, as shown in Figure 2-1, with five sequential reaction steps.
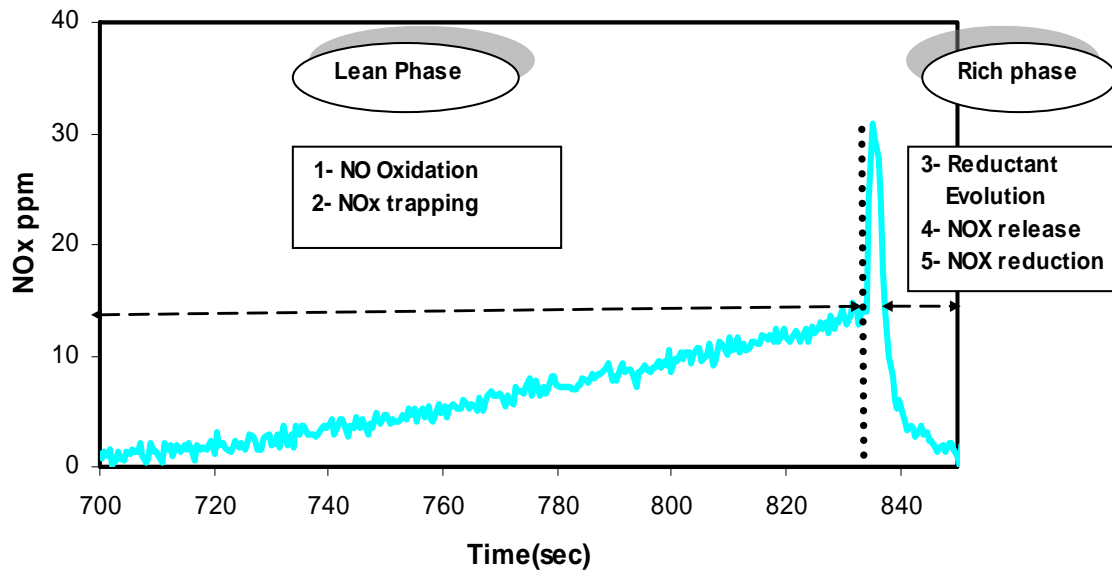
Figure 2-1 Overall NO_X cycle

2.1.1 Oxidation of NO to NO_2 over the noble metal component

The majority of NO_X emitted in diesel engine exhaust is NO, usually around 90%, with the rest NO_2. The NO oxidation reaction to NO_2 is the first step in the NSR process. Since NO_2 is trapped more readily than NO, this step is important.

$$NO + \tfrac{1}{2}\,O_2 \rightarrow NO_2$$
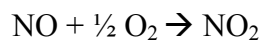
NO oxidation occurs on the surface of the catalyst precious metal species. Typically Pt, Pd, and/or Rh are used. Pt is the most common used due to its high red-ox activity. A comparative study [16] showed that when using Pt, the maximum conversion to NO_2 was 20% while no conversion was detected when using a Pd based catalyst under the conditions of the test. Although Pd and Rh have less NO oxidation activity, they have a

19

significant impact on NO_X reduction, thus their addition [17]. Not only can the type of precious metal affect NO oxidation, but also their particle size. It has been demonstrated that as the particle size of Pt increases, NO oxidation surprisingly increases, demonstrating structure dependence. For example, as a model catalyst was exposed to high temperature treatment, to approximately 750°C, NO oxidation increased [9]. As shown in Figure 2-2, NO oxidation is a function of temperature. At low temperature, the NO oxidation rate increases as the temperature increases. The conversion under the conditions of the test described reached its maximum at approximately 350°C and then started to decrease.
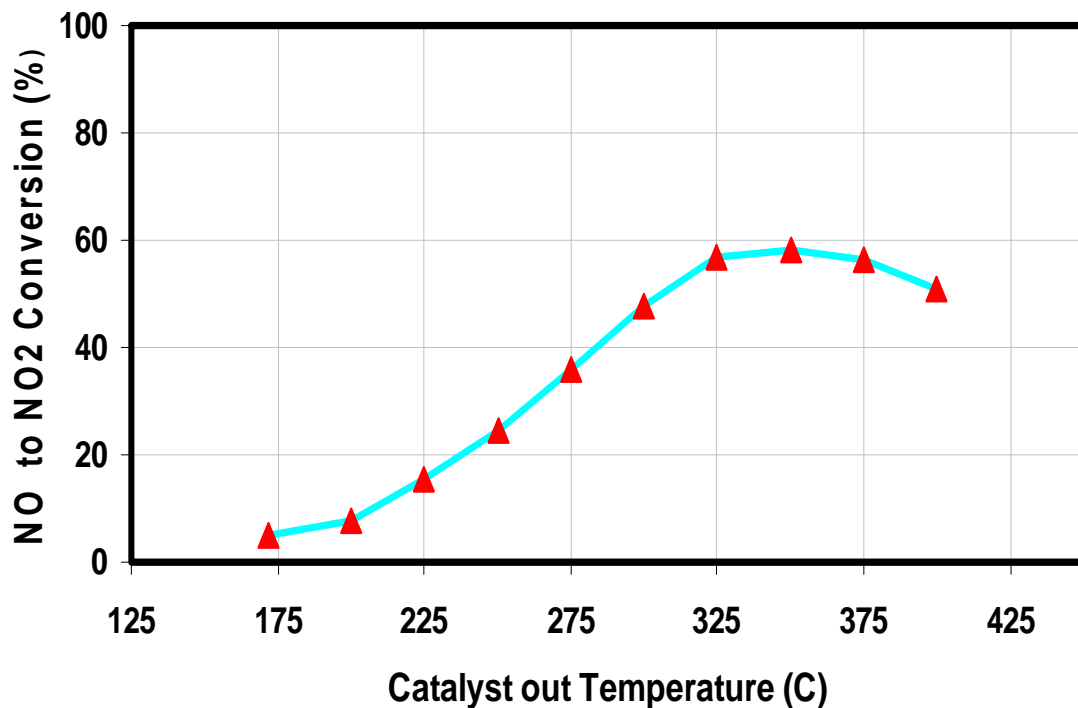
Figure 2-2 Effect of Temperature on NO oxidation. The inlet gas contained 10% O_2, 330 ppm NO, 5% H_2O, 5% CO_2 and a balance of N_2 and the experiment was run with a commercial NSR sample at a space velocity of 30,000 hr^{-1}

The decrease at high temperature is due to thermodynamic limitation; the equilibrium conversion was reached. The storage component can also hinder NO oxidation over Pt. Its presence can decrease Pt activity by covering some portion of the Pt particles[18].

2.1.2 Adsorption of NO/NO$_2$ on the trapping sites

After NO is oxidized to NO$_2$, the NO$_2$ is adsorbed by the storage materials, which are usually alkali and alkaline earth components, such as BaO. Numerous studies [19][21] have suggested that NO$_2$ is a precursor for adsorption and nitrate formation. However, NO can also be adsorbed by trapping materials in the presence of oxygen (O$_2$), although to a lesser extent and at slower rates. Overall, NO$_X$ is adsorbed in the form of nitrate (NO$_3$) and /or nitrite (NO$_2$) species on the alkali and alkaline earth components. Nitrate species, for example, have been detected when introducing NO$_2$ to Pt/Ba/Al$_2$O$_3$ [21] while nitrites and nitrates have been detected when NO + O$_2$ was introduced at low temperature [22].

The selection of trapping materials is obviously an important factor and several have been tested, such as mixed oxides, perovskites, and inorganic oxides [20]. However, alkali and alkaline earth components show better trapping capacity due to their higher basicity. BaO for instance, is the most commonly used in NSR catalyst testing as a storage material.

Although NO$_2$ is adsorbed by trapping materials, it can also be adsorbed by the catalyst support, which is typically Al$_2$O$_3$. A Fourier Transform Infrared (FTIR) study [23] has shown that NO$_2$ sorbed on Al$_2$O$_3$ when Pt/Al$_2$O$_3$, BaO/Al$_2$O$_3$, and Pt/BaO/Al$_2$O$_3$ catalysts

were used. However, the amount of NO_2 adsorbed is small; approximately 1% of the NO_X trapped by Ba [24].

Temperature also impacts NO_X sorption. With increasing temperature, the thermal stability of nitrate and/or nitrite species decrease, and therefore, at temperatures greater than ~350°C, typically NO_X storage capacity decreases. For example, in thermogravimetric analyzer (TGA) experiments, where the weight change measured represents an amount of NO_X trapped, at 200 ºC the total change in catalyst weight was 0.431 g while, at 450°C the total change in catalyst weight was 0.135 g**[9]**. But, as shown in Figure 2-3, NO_X sorption increases with temperature, until reaching approximately 350ºC where it then starts to decrease. One reason for the low temperature increase is NO oxidation. As mentioned, as the amount of NO_2 increases, storage increases. NO conversion to NO_2 typically reaches a maximum at around 350ºC, helping to increase storage rates to this temperature as well. The increase in capacity as the temperature increases, at low test temperatures, also coincides with improved regeneration as temperature increases. Thus, at low temperatures, the amount of NO_X trapped is limited by NO oxidation and efficiency in removing nitrate or nitrite species during regeneration. At high temperatures, the trapping capacity is limited by nitrate or nitrite stability.

Another factor that influences NO_X trapping capacity is the gas composition, including components like CO_2, H_2O, and O_2, since the storage capacity is affected by the sorbate surface state. A common assumption is that BaO is the easiest to form nitrates, relative to hydroxides or carbonates[9]. The presence of CO_2 in the gas stream can produce $BaCO_3$ which is more stable than BaO. This increased stability can hinder nitrate and/or nitrite

22

species formation, which in turn will affect the trapping capacity. In one example with a Pt/K/Al$_2$O$_3$ catalyst, the trapping capacity decreased by 45 % when CO$_2$ was added to the gas mixture[25].

Similarly, the presence of H$_2$O can cause decreased trapping capacity by Ba(OH)$_2$ formation. In the same study described above, the addition of 5 % H$_2$O to a dry mixture caused a 16% loss in trapping capacity[9]. However, when both CO$_2$ and H$_2$O are added, the H$_2$O had a positive impact on NO$_X$ storage capacity, via the equilibrium reaction BaCO$_3$ + H$_2$O → Ba(OH)$_2$ + CO$_2$. The carbonate is more stable than the hydroxide, so additional hydroxide relative to carbonate resulted in better trapping performance.

The presence of O$_2$ also can influence the trapping capacity via oxidation of NO to NO$_2$ as well as oxidation of surface NO$_X$ to nitrates. It has been shown [26] that as O$_2$ concentration increases, the NO$_X$ storage capacity increases.

Several mechanisms have been suggested for NO$_X$ adsorption. In the below listed mechanisms, Ba has been taken as an example for alkali and alkaline earth components. It does not necessarily mean that Ba is the only component that can adsorb NO$_X$; but is used as a representative trapping component. Hydroxide and carbonates are also present, but the oxide is selected as an example.

- NO reacts with Ba oxide to form nitrate [24]

  BaO + 2NO + 3O → Ba(NO$_3$)$_2$
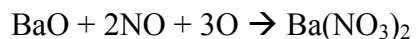
- NO$_2$ reacts with barium peroxide to form nitrate [27]

  BaO$_2$ + 2NO$_2$ → Ba(NO$_3$)$_2$
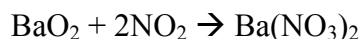
- NO$_2$ reacts with BaO to form nitrate and nitrite species [28]

   $2BaO + 4NO_2 \rightarrow Ba(NO_2)_2 + Ba(NO_3)_2$

- NO$_2$ reacts with BaO to form nitrate and NO [9]

   $BaO + 3NO_2 \rightarrow Ba(NO_3)_2 + NO$
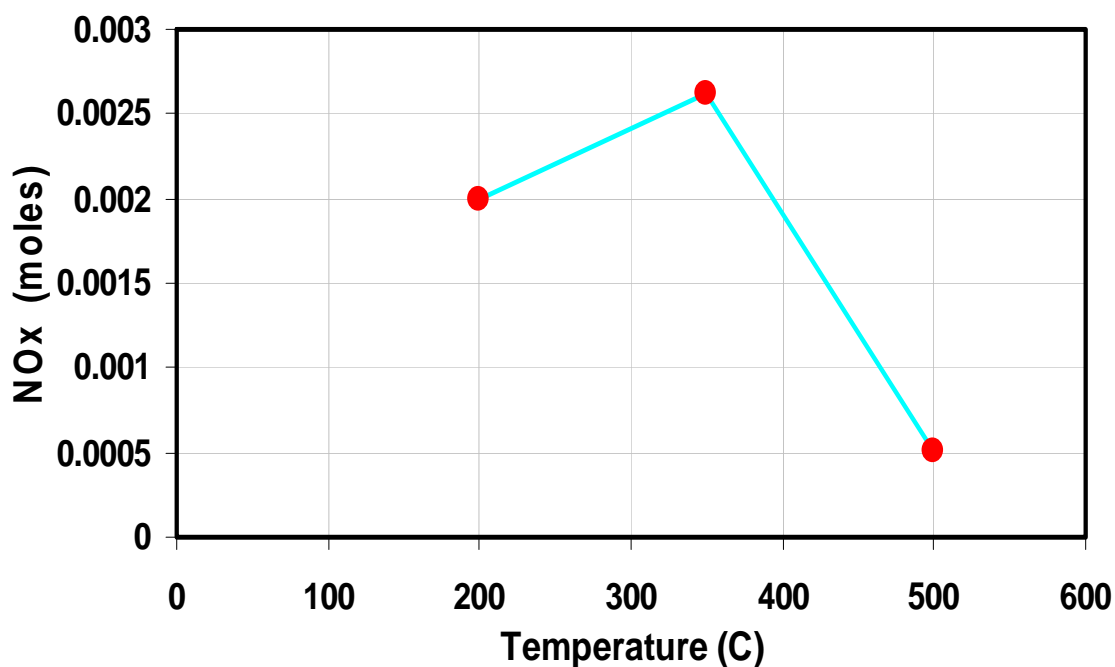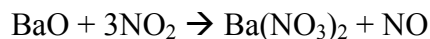
Figure 2-3 NO$_X$ Storage Capacity. The reactant gas was composed of 10% O$_2$, 330 ppm NO, 5% H$_2$O, 5% CO$_2$ and a balance of N$_2$ at a space velocity of 30,000 hr^{-1} using a commercial NSR catalyst.

2.1.3 Reductant evolution

Trapping decreases with time as the trapping sites become saturated as nitrate and/or nitrite species. Consequently, the catalyst needs to undergo periodic regeneration to remove the adsorbed NO$_X$, and hopefully reduce these to N$_2$. This can be achieved by

introducing reductants and removing the O_2, resulting in a net-reducing environment. The reductants can be introduced in a few ways. One is via adjusting combustion so that they exit with the rest of the exhaust. Thus, for the rich phase, more fuel is injected into the engine, which in turn increases the amount of reductant. Enough fuel must be added so that more reductant exits than O_2, thus the stream is reductant rich. The most widely used reductants in NSR catalyst testing are hydrogen, carbon monoxide, and propylene, the former two observed in rich engine exhaust and the last representing hydrocarbons, also observed. Hydrogen is superior for NO_X reduction with NSR catalysts at lower temperatures compared to carbon monoxide and propylene; however, they are all comparable at higher temperature.

Carbon monoxide has been tested as a reductant for NO_X due to its presence in diesel engine exhaust when the engine is run rich[29]. Carbon monoxide can reduce NO_X directly or indirectly. It can be used directly via reaction with NO_X: $2\ CO + NO \rightarrow N_2 + CO_2$. While indirectly it can participate in the water gas shift (WGS) reaction; $CO + H_2O \rightarrow CO_2 + H_2$. The produced H_2 then reacts with the NO_X. It has been demonstrated [11],[30] that the WGS reaction occurs over precious metals and is therefore expected to occur over NSR catalysts as well [31].

Although CO is a reductant for NO_X at higher temperatures, it can poison Pt at lower temperatures. Therefore, NO oxidation and NO_X reduction steps can be affected at low temperature when CO is present.

Propylene can break down to smaller components that in turn can act as reductants. Propylene is comparable with hydrogen and carbon monoxide at higher temperature in NSR regeneration.

The effect of reductant mixtures on the overall performance of a NO_X trap catalyst has been investigated by Szailer and coworkers[32]. They found that when mixtures of CO and H_2 were used at low temperature (~147ºC), low NO_X reduction was achieved in comparison with using only H_2. They attributed the poor NO_X reduction when using the mixture to reductant competition for adsorption sites on Pt particles. With stronger CO bonding, the surface H_2 concentration would be lower in the presence of CO and if conditions favor reduction with H_2 instead of CO, the NO_X reduction rate would be lowered. They also showed that NO_X conversion was higher with mixtures of H_2 and CO in comparison to just CO as the reductant under otherwise identical conditions. With only CO as the reductant, NCO and CO_2 species were formed. And in the presence of H_2, the resultant H_2O hydrolyzed the NCO to form the intermediate that ultimately decomposed to N_2 and H_2O. Overall, as would be expected, literature evidence suggests that the reduction efficiency of the different reductants depends on its activation on the surface.

The amount of reductant also of course has an impact on NO_X reduction. Furthermore, reductants are not only required to reduce the trapped NO_X, but they are also consumed by stored oxygen as will be discussed in further detail in the results section. Consequently, the amount of reductant needed is dependent on surface oxygen, the more stored oxygen, the more reductant required.

2.1.4 NO$_X$ release

Release of NO$_X$ from the catalyst surface occurs via two paths [9]. The first is due to heat caused by the exothermic reaction between the entering reductant and any surface oxygen. The more oxygen on the surface, the more heat will be generated. The associated temperature rise may be enough to decrease the stability of the surface nitrate or nitrite species. The second reason for NO$_X$ release is the change in gas composition with the switch to the rich phase. With an absence of NO and O$_2$, the stability of nitrate and/or nitrite species are reduced.

NO$_X$ release is a function of temperature. For example, at lower temperatures, the release of NO$_X$ is strongly dependent on the degree that the catalyst can activate the reductants **[9].** As the temperature increases, the capability of reductants to reduce NO$_X$ to N$_2$ should increase and the release of observed NO$_X$ in the outlet gas should decrease. While, at higher temperatures, around 350°C and above, where the activation of reductant is not an issue, the weak stability of nitrate species is the main cause for observed NO$_X$ release [9]. Realize that for reduction to occur, release must occur first. So, observed NO$_X$ in the outlet during regeneration is actually released and unreduced NO$_X$, whereas even if none is observed being released in the outlet gas, a substantial amount might have been released but most reduced.

As mentioned above, another factor that can affect the release of NOx is the exhaust gas composition. Via thermodynamic-based calculations, it has been predicted [33] that there is a direct correlation between the amount of carbon dioxide and the stability of NO$_X$ species. The more carbon dioxide present, the more NO$_X$ released from trapping sites

under otherwise identical conditions. This could be due to the competition between carbonate and nitrate formation/stability.

Oxygen also has an impact on the release of NO_X. It was demonstrated by Liu and Anderson [34] that oxygen enhances the stability of nitrate and/or nitrite species. Therefore, upon switching to the rich phase, where little or no oxygen is introduced, the nitrate and/or nitrite species will destabilize. This leads to nitrate and/or nitrite species decomposition and NO_X release to hopefully be reduced on adjacent precious metal sites or find their way out of the catalyst without being reduced. If O_2 remains present, then some nitrate species may remain stable enough to not decompose and not result in NO_X release.

Water also has a significant influence on NO_X release [33][35]. Epling et al [35] have investigated the influence of the presence and absence of H_2O in the gas stream. They found that the presence of H_2O in the gas stream lowered the magnitude of NO_X release in the outlet gas. This could be related to displacement of carbonate groups by hydroxyl groups.

Impacting the overall conversion of NO_X is the release of any unconverted NOx. Overall, the observed unconverted NO_X is due to slower reduction at precious metal sites, compared to Ba nitrite/nitrate decomposition[36]. This is more significant at higher temperatures due to nitrate stability.

Contributing to this is the proximity of Pt sites to the alkali and alkaline earth components [8]. It is speculated that it is easier to reduce NO_X molecules that are released

from trapping sites near to the Pt. For trapping sites further from Pt, NO_X can readsorb after release or will exit with the gas stream.

2.1.5 Reduction of NOx to N_2

Reduction of NO_X to N_2 is the last step in the overall NSR cycle description. In this step, the NO_X stored during the lean phase and then released at the onset of the rich phase is reduced to N_2 over the precious metals. Two main mechanisms have been proposed for reduction of NO_X to N_2 on the precious metal sites of NSR catalysts. The first mechanism postulates that the reductant reduces the precious metal site. Afterward, the reduced precious metal site participates in NO decomposition. As part of this mechanism, James et al [37] suggested that Pt size can plays an important role in NO_X reduction. They postulated that small Pt particles are unable to dissociate NO effectively because they form the oxide species more readily. The second mechanism, supported by Olsson et al [38], proposes that the reductant is activated on the precious metal and reacts directly with NO_X:

C_3H_6 (g) + Pt → Pt-C_3H_6

Pt –C_3H_6 +2Pt → 3 Pt- CH_2

Pt-CH_2 + 3Pt-NO → 4 Pt + CO_2 (g) + H_2O (g) + 1.5 N_2 (g)
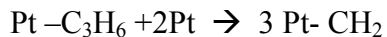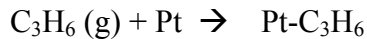
Reductant type and amount, temperature, and lean/rich time ratio are known to affect NO_X reduction. Abdulhamid et al [39] did a comparative study between H_2, CO, C_3H_6, and C_3H_8 for reduction of NO_X over BaO/Al_2O_3 samples containing Pt, Pd, or Rh. The results of this study showed that H_2 and CO are superior for NO_X reduction in comparison

to hydrocarbons, C_3H_6, and C_3H_8, especially when $Pt/BaO/Al_2O_3$ was used. Another comparative study between H_2, CO, and a mixture of H_2 and CO as a reductant source over Pt/Al_2O_3 and $Pt/BaO/Al_2O_3$ catalysts was performed by Szailer et al [30]using FT-IR and X-ray Diffraction (XRD) measurements. The results showed that H_2 was more efficient than CO and a mixture of H_2 and CO on NO_X reduction, especially at a temperature of 150°C. Furthermore, as mentioned above, CO is inefficient at lower temperature likely due to Pt site poisoning, hindering the release and reduction of NO_X. Experiments have been performed to investigate the effect of combining CO with H_2 [40]. In their first experiment, where 2.25% CO was introduced with 0.75% H_2 as a reductant source at 200°C, the overall conversion attained was approximately 40% while in the second experiment when only 3% CO was used, the overall conversion was achieved was 22%. Furthermore, it has been shown that [41] combining CO with H_2 at lower temperatures also hampers the effect of H_2 on NO_X reduction over a Pt-Rh/Ba-based NSR catalyst.

The amount of reductant of course has an effect on NO_X reduction. Bailey et al [42] demonstrated that increasing the amount of CO during the regeneration phase resulted in an improvement in overall NO_X reduction under the conditions tested.

2.2 Effect of thermal degradation

NSR is a promising technology to mitigate NO_X emissions. However, a significant challenge that questions their long-term durability is poisoning by sulfur compounds present in the exhaust[43]-[49]. The problem is that sulfur will lead to sulphates on the

catalyst surface, with these sulphates forming where nitrates should form during trapping/storage. Furthermore, these sulphates are thermodynamically more stable than nitrates[50][51].

Several studies have evaluated the influence of sulfur on the performance of NSR catalysts. For Ba-based NSR catalysts, it has been shown that the presence of SO_2 and O_2 in the lean phase forms surface sulfates on storage components, which later migrate into the bulk phase[52]. These sulphates hinder the adsorption of NO_X species on the surface of Ba [53] and hence NO_X storage capacity decreases during subsequent cycles. H_2S and COS that are present in the rich phase are also harmful and under certain conditions are even worse for decreasing the performance of trapping materials [43]. H_2S and COS will be oxidized to SO_2 in the lean phase where the oxygen is in excess, but they reside on the precious metal sites during the rich phase. With their oxidation, they poison sites next to the Pt, which is proposed as more efficient in trapping than sites further away [54]. Sulfur was also found to interact strongly with alumina on alumina-based NSR catalysts to form $Al_2(SO_4)_3$ [55]. SO_2 can react with other catalyst components, such as ceria, and has a negative effect on water gas shift and steam reforming reactions[56].

Beyond forming sulphates, via interaction with the trapping materials, sulfur influences precious metal activity as well. For example; sulfur characterization studies have shown that during rich conditions, Pt can interact with sulfur forming a layer of sulfur on Pt [44]. With sulfur in the gas feed in testing a Pt-based NSR catalyst, the NO oxidation and reduction were activity decreased after a few cycles at 350ºC [56]. The authors attributed the drop in the oxidation and reduction activity to poisoning of Pt by

31

SO$_2$ and SO$_2$ derived species. Such site blocking had been previously proposed [57]. NO oxidation is more severely affected by sulfur at lower temperatures than higher temperatures. This has been attributed to two possible reasons [9]. First, the rate of Pt-S decomposition increases as the temperature increases, so the impact of S on NO oxidation will diminish since there is less Pt-S interaction. Second, between 350 and 400ºC, the stability of S species on the alumina support decreases, such that S desorption would take place. But, S species could be readsorbed, forming stronger bonds on Pt or Ba.

To maintain performance, sulfur compounds need to be removed from the catalyst in order to regain its activity. To remove sulfur compounds, NSR catalysts require an intermittent high-temperature exposure to a reducing environment[48][51]. This desulfation protocol ultimately, however, results in thermal degradation of the catalyst. The thermal degradation can include the loss of precious metal dispersion (sintering), the loss of surface area of NO$_X$ storing components, and the loss of surface area of oxygen storage capacity (OSC) components.

Desulfation temperatures can reach 700°C [12], resulting in deactivation by sintering of the noble metals that are present in NSR catalyst formulations for oxidation and reduction of NO$_X$. For example, Graham and coworkers [58] investigated the effect of temperature and exposure to oxidizing versus reducing conditions on Pt particle size changes with a Pt/BaO/Al$_2$O$_3$ catalyst. The authors found that Pt agglomeration occurred when the sample was exposed to an oxidizing atmosphere for three hours at temperatures as low as 600°C. On the other hand, no significant change in Pt size was observed even when the catalyst was exposed to high temperature at 950°C but in a reducing

atmosphere. Another study also investigated the effect of reducing versus oxidizing conditions on Pt/Al_2O_3 and $Pt/Ba/Al_2O_3$ model catalysts [59]. A Pt/Al_2O_3 catalyst was exposed to both reducing and oxidizing conditions at temperatures between 670 and 1041ºC. The increase in the Pt particle size was observed after exposure to oxidizing conditions beginning at 763ºC and increased with temperature, while less change in particle size was observed under reducing conditions in comparison with oxidizing environment. On the $Pt/Ba/Al_2O_3$ model catalyst, the sample was exposed to both reducing and oxidizing conditions at 900ºC for 7 hours. Again, little change in Pt size was observed with reducing conditions while growth in Pt size was readily observed with oxidizing conditions. Furthermore, a Pt/Rh based NSR catalyst was evaluated after aging at 800 and 900ºC with 10% H_2O and 90% air [60]. The authors found severe sintering of Pt. The above discussion shows that Pt particle size is affected by high temperature exposures; however, oxidizing environments seems to have more effect on Pt size than reducing environment.

Another reason for the degradation in the performance of NSR catalysts with high temperature exposure is the loss of surface area of the NO_X storage components. Studies with a $Pt/Ba/Al_2O_3$ catalyst have shown that when the catalyst was thermally aged at 750°C for 24 hrs, the NO_X conversion dropped from 86% to 55% due to a decrease in the storage capacity. They reported that the decrease in the storage capacity could occur via two possible pathways. The first is due to the reaction of the trapping component with the washcoat material[61][62]. For example, in testing four catalysts types, Pt/Al_2O_3, Ba/Al_2O_3, $Pt–Ba/Al_2O_3$, and a physical mixture of Pt/Al_2O_3 + Ba/Al_2O_3, Jang et al [63] found that the deterioration in the catalyst NSC capacity arising from thermal aging in all

Ba-based catalysts was attributed to a phase transition of BaO into a Ba–Al solid alloy. That transition occurred above 600°C and ultimately became more stable $BaAl_2O_4$ at above 950°C. Another study investigated the effect of lean/rich thermal cycling on a Pt / "Ba+K" based NSR catalyst at 700, 800, 900 and 1000°C [64]. It was found that as the thermal aging temperature increased, the catalyst performance decreased. The drop in the catalyst performance after each incremental increase in aging temperature was attributed to several reasons. For example, at 700 and 800°C, the transition of γ-Al_2O_3 to δ-Al_2O_3, which has lower specific area, as well as agglomeration of both K and Ba, were observed. At 830°C, a significant amount of K migrated toward the cordierite substrate. As the temperature increased to 1000°C, even more severe deterioration in catalyst performance was observed. The authors attributed this final effect to the reaction of $BaCO_3$ with the catalyst washcoat to form $BaAl_2O_4$. Such a transformation to $BaAl_2O_4$ has actually been reported as low as 800ºC [65]. The second reason for decrease in the storage capacity is a loss in interface contact between the precious metals and trapping components because of particle size growth of both[51][63]. Toops et al [51] investigated the thermal aging of a Pt/Rh/Ba/γ-Al_2O_3 catalyst under lean/rich cycling at 600, 700, and 800°C. They reported that the catalyst capacity to store NOx decreased when the catalyst was exposed to 800°C due to agglomeration of adsorbent materials such as Ba. Thermal aging can also induce a decrease in the catalyst OSC**[66]**, likely due to a loss in the surface area of the OSC components. Ceria, for example, is a well-known OSC component that is present in three-way catalysts (TWC) and has been shown to promote NSR catalyst performance[67]. The loss in OSC via thermal aging can occur via growth of OSC component crystallites [15] when they are exposed to high temperature, which would lead to less oxygen stored on

34

the ceria[65]. Another possibility is again the reaction of OSC components with the catalyst support. For example [68]in characterizing CeO_2/Al_2O_3 samples, the formation of $CeAlO_3$ upon reduction in H_2 at temperatures higher than 600˚C has been observed.

Chapter 3: Experimental work

3.1   Experiment Description

3.1.1   Feed and delivery system

For the research done, the typical operating conditions and gas compositions of diesel engine exhaust have been simulated, excluding particulate matter and sulfur compounds. The gas compositions were obtained by mixing gases from gas cylinders supplied by Praxair. The experiments were carried out with a total flow of 14.32 L/min or a space velocity of 30000 h^{-1}. The typical compositions of the lean and rich flows are listed in Tables 3-1 and 2.

As mentioned in the previous two sections, this technology cycles through two phases; a lean and a rich phase. The lean phase is the normal diesel engine operation where the NO_X is trapped while the rich phase is the regeneration phase where the reductant is introduced to reduce stored NO_X to N_2. Each of the two gas compositions was set using Bronkhorst mass flow controllers controlled via a LabVIEW program.

The gas mixtures entered a four-way solenoid valve that was also controlled by the LabVIEW program. Simply, this valve allows either the lean or the rich mixture to flow to the reactor while the other is vented to an exhaust. The mixture directed to the reactor is mixed with water vapor downstream of the 4-way valve. The water was introduced as steam using a Bronkhorst vaporizing system. After water introduction the gas mixture is directed through an insulated line, which is also wrapped by a heating cord to compensate

for heat loses to the environment. A pre-heater section after the water introduction is used to heat the gas to the target test temperature, prior to entering the reactor itself.

3.1.2 Reactor

The experiments were performed in a bench-scale reactor. The catalyst was wrapped with high-temperature Zetex insulation and inserted into a quartz tube. The insulation was used to cover the gap between the catalyst and the wall of the tube to ensure that no gas slipped around the sample. The quartz tube was then inserted into a horizontal tube furnace. Two K-type thermocouples were placed at the radial center of the catalyst; one just inside the inlet face of the catalyst and one just inside the outlet face of the catalyst. Another two were placed ~ ½ inch upstream and downstream of the sample. A picture of the reactor and the catalyst is shown in Figure 3-1. The gases exiting the reactor were maintained at >190°C to avoid condensation and NH_3 hold-up. The outlet gas mixture concentrations were constantly detected with an FT-IR analyzer described below.

Figure 3-1 Reactor and catalyst section

3.1.3 Gas analysis:

Fourier Transform Infrared (FT-IR) spectroscopy was used to measure outlet gas concentrations. The instrument used is a MKS MultiGas™ 2030. It has four main components; a fourier transform infrared spectrometer, a gas cell an optics box containing an infrared detector, and associated transfer optics, and supporting electronics. In our experiments, CO, CO_2, NO, NO_2, N_2O, NH_3, and H_2O gas concentrations were measured.

Principle of Operation

When the gas sample passes through the gas cell, some of infrared radiation is absorbed by the gas molecules. For each gas in the sample, molecular bonds vibrate at various frequencies based on the type of chemical bond and the strength of that bond. The absorption spectrum is different for each infra-red-active gas. The MultiGas analyzer converts these absorption spectrums to concentrations using its analysis algorithms and pre-loaded calibrations.

3.1.4 Catalyst

A commercial NO_X storage/reduction catalyst was used in these experiments, supplied by a catalyst vendor who requested their name not be used yet in public communications. The catalyst was supported on a ceramic honeycomb cordierite structure. The sample was removed from a larger monolith block which had a cell density of 300 cpsi. The sample used was 0.912" in diameter with a length of about 3".

3.2 Process Flow Schematic
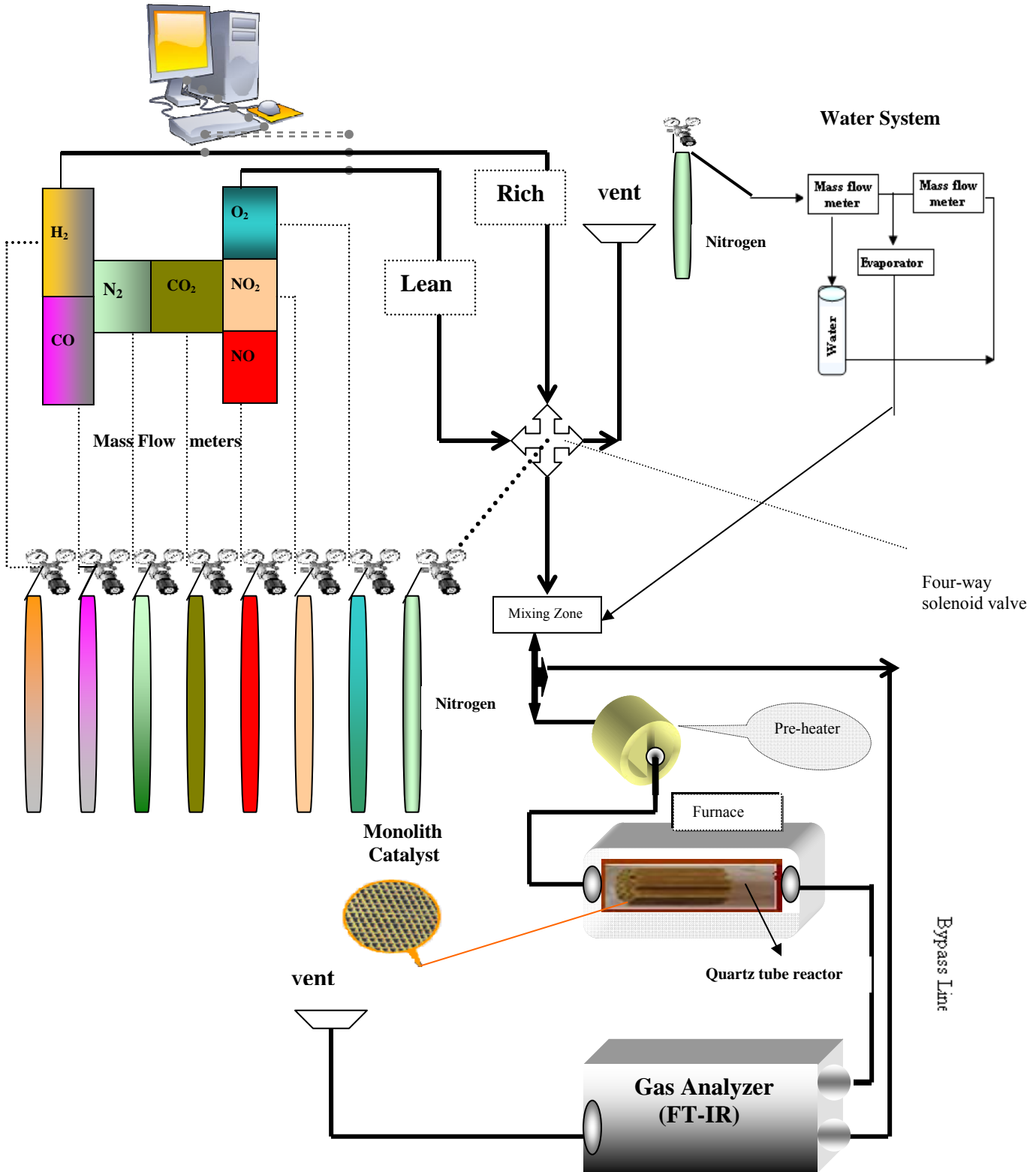
Figure 3-2 Process Flow schematic

3.3 Experiments Types:

3.3.1 Influence of reductant type and amount on the performance of a commercial NSR catalyst

The objective of this set of experiments was to evaluate the effect of amount and ratio of CO and H_2 on the trapping and reduction of NO_X at different temperatures; 200 to 500°C. The compositions of the lean and rich flows for these experiments are listed in Tables 3-1and 2.

Table 3-1 Typical composition of the lean and rich flows

Flow conditions	Sorption (lean)	Regeneration (rich)
Space velocity	30,000/h	30,000/h
NO	330 ppm	0 ppm
O_2	10%	0%
CO_2	5%	5%
H_2O	5%	5%
H_2	0%	see table 5
CO	0%	see table 5
N_2	Balance	Balance
Temperature (˙C)		
200	60 sec	5 sec
300	150 sec	5 sec
400	180 sec	5 sec
500	120 sec	5 sec

Table 3-2 Hydrogen and carbon monoxide concentrations and ratios

Hydrogen (H_2) %	Carbon monoxide (CO) %
0	0
1.5	0
3	0
5	0
0	1.5
0	3
0	5
1.25	1.75
1.75	1.25
1	2
2	1

Before each experiment, the sample temperature was ramped to 500°C with 5% H_2O, 5% CO_2, and a balance of N_2 and then the catalyst was cleaned with a regeneration mixture consisting of 5% H_2O, 5% CO_2, 1% H_2, and a balance of N_2 for 15 min. The reactor was then cooled to the target test temperature. Experiments were performed at 200, 300, 400 and 500°C with a space velocity, at standard conditions, of 30,000 hr^{-1}.

3.3.2 Effect of thermal degradation on the performance of a commercial NSR catalyst

The aim of this set of experiments was to investigate the effect of thermal degradation on the performance of a commercial NSR catalyst. The performance changes were evaluated

after exposing the sample to air with 2% H_2O at 600, 650, 700 and 750°C. Performance change measures include NO_X storage capacity, water-gas-shift reaction extent, NO oxidation, oxygen storage capacity, and NO_X conversion under cycling conditions.

3.3.2.1 NO_X storage capacity

After the sample was cleaned at 500°C and then cooled to the test temperature, the sample was exposed to the same conditions as those of the lean phase in the cycling experiments. This was ended once a steady value of 330 ppm NO + NO_2 was measured at the outlet. The number of moles of NO_X stored in the catalyst at each temperature can then be calculated:

- **Stored NO_X (ccm) = Total NOx in – Total NO_X out**

3.3.2.2 Water-gas-shift reaction

In this set of experiments, 10 to 15 cycles were repeated at the 4 standard test temperatures. A lean period of 60 seconds and a rich period of 30 seconds were used, with the lean composition containing 10% O_2, 5% CO_2, 5% H_2O and a balance of N_2 and the rich phase containing 1% CO, 5% CO_2, 5% H_2O and a balance of N_2. The water-gas-shift reaction extent values were calculated after steady-state CO and CO_2 values were reached:

$$\textbf{CO Conversion} = \frac{Inlet\ CO - Outlet\ CO}{Inlet\ CO} \times 100$$

3.3.2.3 NO oxidation to NO_2

The objective of this set of experiments was to evaluate NO to NO_2 oxidation as a function of temperature. The experiments were carried under the same lean phase conditions as those used in the cycling experiments. The temperature was stepped upward in 25°C increments from 150 to a temperature where equilibrium limitations were reached. This occurred approximately between 375 and 425°C. The NO_2 conversion was calculated after a steady value of 330 ppm $NO + NO_2$ was reached:

$$NO_2 \text{ conversion} = \frac{NO}{NO + NO2} \times 100$$

3.3.2.4 Oxygen storage capacity

The objective of this set of experiments was to evaluate the oxygen storage capacity (OSC) of the catalyst. In this set of experiments, 10 to 15 cycles were repeated at the 4 standard test temperatures. A lean period of 60 seconds and a rich period of 30 seconds were used, with the lean composition containing 10% O_2, 5% CO_2 and a balance of N_2 and the rich phase containing 1% CO, 5% CO_2 and a balance of N_2. To remove the effect of the water-gas-shift reaction on the oxygen storage capacity, water was not used in these experiments. Oxygen storage capacity was calculated from the amount of CO converted:

- **CO (moles) =** $\dfrac{CO \; pulse \; (ccm.\sec) \times 143200 ccm \times 1\min \times 1\,mole}{1000,000 \; ccm \times \min \times 60\sec \times 22400 \; ccm}$

- **CO Converted (moles) =** Inlet CO − Outlet CO

- **O_2 Stored (moles) =** CO Converted (moles) / 2

Chapter 4: The Effects of Regeneration-Phase CO and/or H_2 Amount on the   Performance of a NO_X Storage/Reduction Catalyst

4.1 Effect of regeneration phase H_2 concentration on the storage and reduction of NO_X

Outlet NO_X (the sum of $NO + NO_2$) concentrations obtained using different H_2 concentrations with an inlet temperature of 200°C are shown in Figure 4-1. For this set of experiments, the lean, or trapping, time was 60 seconds and the rich, or regeneration, time was 5 seconds. The conversions and amounts of NO_X trapped and released for these experiments are listed in Table 4-1. All reported values and plotted data were obtained once steady cycle-to-cycle performance was observed. With no reductant added, and after a steady cycle-to-cycle trend was attained, the calculated conversion was 0.25%, close to the expected nil conversion with no reductant at such a low temperature. With the addition of reductant, 1.5% H_2 in the first step, the overall NO_X conversion reached 77% and with 3% H_2, the NO_X conversion increased to 85%. With further H_2 addition, little change in performance was observed; the conversion increased from 85 to 86.5% with the increase from 3 to 5% H_2. With each increase in H_2 concentration in the regeneration phase, the amount of NO_X trapped increased. This is due to increased catalyst regeneration with additional H_2. Thus, since the catalyst is being more deeply regenerated, more NO_X can be trapped in the subsequent lean phase, resulting in the increased trapping observed once steady performance was obtained. And although more NO_X was trapped in the lean phase, with additional H_2, the amounts released during the regeneration also decreased, to an extent that with 5% H_2, 99% of the NO_X trapped in the

44

previous lean phase was reduced. This is explained by the excess amount of H_2 relative to inlet NO_X. The total inlet NO_X was 0.21 mmole. With 5% H_2, 2.66 mmoles of H_2 were introduced to the catalyst during the 5 second regeneration period. The reduction equation is assumed as follows; $Ba(NO_3)_2 + 5H_2 \rightarrow N_2 + BaO + 5H_2O$. Therefore for 2 moles of NO_X trapped, 5 moles of H_2 are required for reduction to N_2, or 0.53 mmoles to reduce all the entering NO_X. However, at 200°C, 0.99 mmoles of H_2 are also needed to consume surface oxygen on this sample, which is considered associated with oxygen storage capacity (OSC). The OSC values in the range of 200 and 500°C are listed in Table 4-2, as O_2 equivalent. As a result, 1.67 mmoles of H_2 remain for nitrate reduction, still in excess amount relative to the inlet NO_X. However, 1.5% H_2 is insufficient to account for both the OSC and entering NO_X, one factor contributing to the lower efficiency observed.
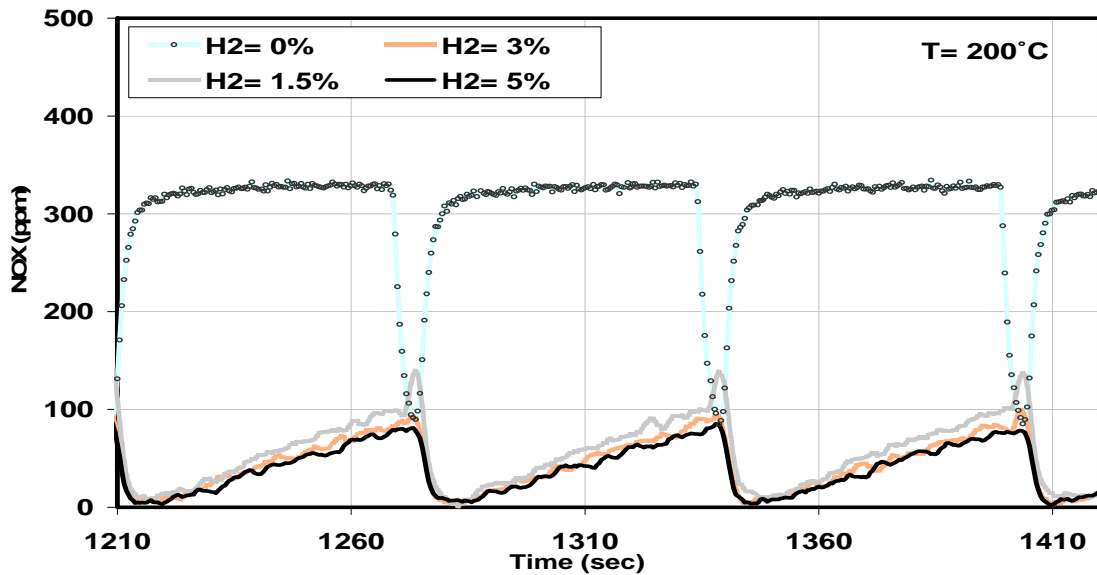
Figure 4-1 NO_X outlet concentrations obtained when testing the sample at 200°C with 0, 1.5, 3 and 5% H_2 in the regeneration phase.

Similar experiments were carried out at 300°C and 500°C to investigate the influence of temperature on the storage and reduction of NO_X as a function of reductant level. The outlet NO_X concentration profile for a set of 150 second storage and 5 second regeneration periods at 300°C are shown in Figure 4-2. The changes in overall NO_X performance, trapping and reduction as a function of H_2 concentration are also listed in Table 4-1.

In the absence of reductant, and after steady cycle-to-cycle performance, the calculated conversion was 1%, again close to the expected value of 0. With the addition of 1.5% H_2, the NO_X conversion attained was 50.5%. The calculated inlet NO_X during the 150 second lean period was 0.53 mmoles and the required H_2 to reduce this amount if all was trapped, assuming nitrate formation, should be 1.33 mmole. Therefore, 1.5 % H_2, or about 0.8 mmoles input during 5 seconds, is insufficient amount to reduce inlet NO_X. This also does not account for that needed to consume the OSC.

Some conversion is observed though, due to the integral nature of such a catalyst system. The entering H_2 does likely first interact with the OSC at the inlet of the sample. Once that OSC is consumed, the entering reductant can reduce nitrates at the inlet portion, where no remaining reactive surface oxygen exists. With the addition of 3% H_2, the NO_X conversion increased to 98%. When the H_2 concentration was increased from 3% to 5%, little overall performance change was observed. The NO_X conversion, trapping and release were all similar.
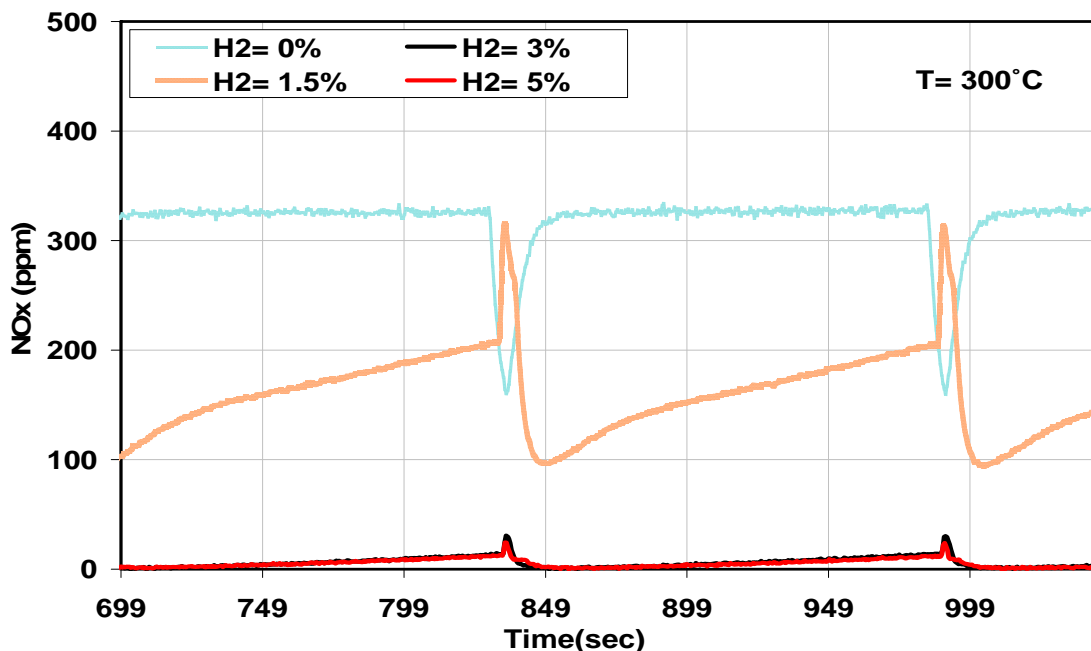
Figure 4-2 NO_X outlet concentrations obtained when testing the sample at 300°C with 0, 1.5, 3 and 5% H_2 in the regeneration phase.

The outlet NO_X concentration profiles obtained at 500°C are shown in Figure 4-3. In the absence of reductant, the NO_X reduction efficiency was calculated to be 2.5%, slightly higher than our typical error and therefore may be due to NO decomposition on the surface at the onset of the lean phase when Pt is reduced. When the H_2 concentration was increased to 1.5%, the overall performance of the catalyst increased to 32% and was further improved to 52% and 66.5% with 3% and 5% H_2, respectively. It is apparent from the data in Figure 4-3 that the primary differences in observed outlet NO_X concentration occur during the early stages of trapping for the three tests that included H_2. At the end of the storage period, upon switching to the regeneration period, the difference in outlet NO_X concentrations are small, as all the available trapping material, for 500°C trapping, has become saturated and the outlet concentration has approached the inlet value. In addition, at the beginning of the trapping phase, the NO_X level did not reach 0 ppm for

the 1.5 and 3% H_2 levels. This indicates that although the rates of reaction are rapid due to the elevated catalyst temperature, the reductant amount is apparently still critical for the trapping performance. Previous work has demonstrated that Ba nitrates on Ba/Al_2O_3 samples decompose between approximately 350 and 475°C [69]. Furthermore, Pt catalyzes the decomposition of nitrate species [70], at least those in close proximity to the precious metal site, suggesting that even lower temperatures would be needed to release surface NO_X. However, the catalyst maintained some performance at 500°C, indicating that the catalyst being tested has some high-temperature performance built into the formulation. The rate of decomposition is still rapid however, and therefore the rate of reductant delivery should be critical. Indeed, NO_X release decreased when the H_2 concentration increased indicating that delivery rate was important.
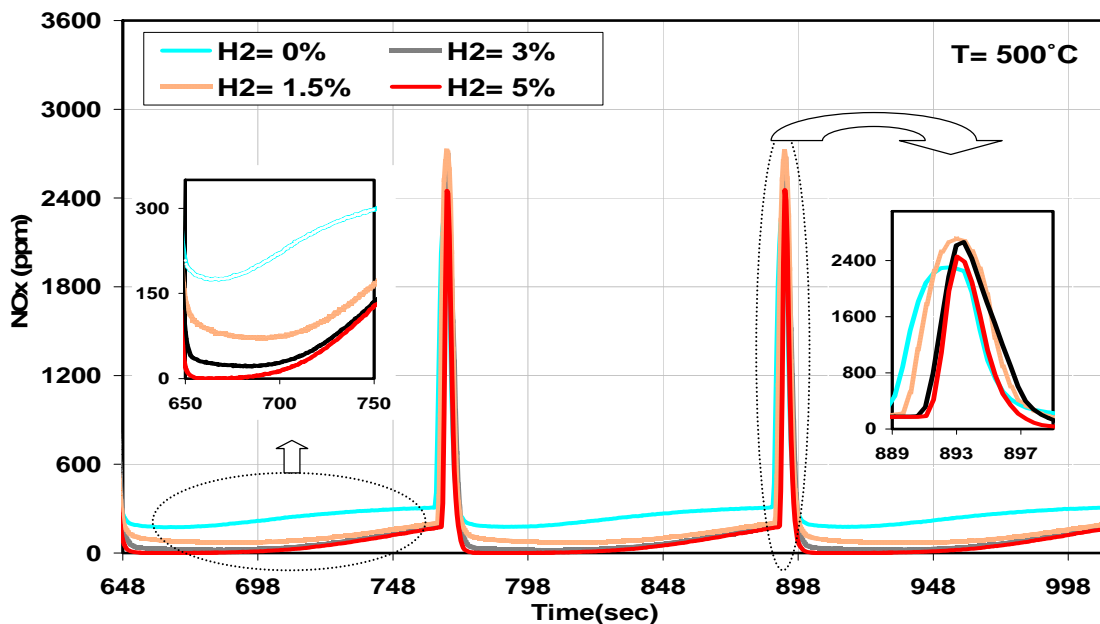
Figure 4-3 NO_X outlet concentrations obtained when testing the sample at 500°C with 0, 1.5, 3 and 5% H_2 in the regeneration phase.

Table 4-1 calculated performance characteristics as a function of temperature, and amount of CO and/or H_2

Temperature (°C)	Reductant (%) CO	H₂	NO$_X$ Conversion (%)	NO$_X$ Trapped (μmoles)	NO$_X$ Released (μmoles)	NH$_3$ Released (μmoles)
200	0	0	0.25	9	8.4	0
	0	1.5	77	169	6	52.1
	0	3	85	182	2	78.6
	0	5	86.5	185	2.3	100.9
	1.5	0	23	79	30.8	3.2
	3	0	14.8	63	31.4	1.6
	5	0	10	59	37.5	1.2
	1	2	22	83	36.0	34.5
	1.25	1.75	36	103	27.6	26.4
	1.75	1.25	41	106	19.8	19.4
	2	1	47	117	18.6	15.4
300	0	0	1	17	11.6	0
	0	1.5	50.5	272	5.5	0
	0	3	98	518	0.1	10
	0	5	98.3	519	0.5	63.9
	1.5	0	52	281	6.2	0
	3	0	96	507	2	10.8
	5	0	97	514	0.9	103
	1	2	97.7	516	1.2	16.6
	1.25	1.75	96.6	511	1.5	15.9
	1.75	1.25	97.1	513	1.5	13.6
	2	1	97.6	516	1.2	8.9
400	1.25	1.75	91	464	17	0
	1.75	1.25	92	467	16.3	0
	3	0	88	450	19	0
	0	3	87	455	25.9	0
500	0	0	2.5	88	77.7	0
	0	1.5	32	241	105.3	0
	0	3	52	319	98.7	0.32
	0	5	66.5	357	76.6	2.43
	1.5	0	35	258	109	0
	3	0	53	327	104	0.4
	5	0	64	350	81	4.1
	1	2	54	324	97	0.85
	1.25	1.75	56	329	95	0.78
	1.75	1.25	57	333	93	0.73
	2	1	57	329	87	0.67

When the H_2 concentration was increased from 3% to 5% at 200 and 300°C, little difference in NO_X trapping was observed, while at 500°C a significant difference was noted.

At 500°C, the weaker stability of nitrate species and higher OSC contribute to the observation that increasing the reductant amount from 3 to 5% still has a pronounced effect. For example, at 500°C, the OSC was 1.10 mmoles and the amount of NO_X trapped was 0.36 mmoles during 5% H_2 tests. With 5% H_2, 2.66 mmoles of H_2 were introduced to the catalyst during the 5 second regeneration period. 0.72 mmoles of H_2 are needed for reduction of the nitrate and 2.2 mmoles are needed to consume surface oxygen. Using 3% H_2 obviously leads to even less sufficient reductant delivery.

The NO_X trapping and reduction performance at 500°C was poor in comparison with 200 and 300°C. As observed in Figure 4-3, NO_X breakthrough increased sharply after just 50 seconds of trapping time. The poorer performance of the catalyst at 500°C can be primarily attributed to the thermal stability of nitrate and/or nitrite species[71]. Although NO oxidation is also thermodynamically limited at this high test temperature, NO_2 was observed in the outlet, indicating this should not limit trapping. Similar to adsorption/desorption rates, the formation and decomposition rates of the nitrates have different dependencies on temperature, and as the temperature is increased the decomposition rate gains significance. Therefore, although there is no inhibition to nitrate formation at such high temperatures, less of the trapping material is used due to the rapid establishment of surface nitrate/gas-phase NO_X equilibrium. At lower temperatures the decomposition rate is not as significant, shifting equilibrium between the surface and gas-

phase species, thus allowing more availability of the trapping material. Therefore, at lower temperatures an equilibrium would also eventually be achieved, but at higher usage than that observed at 500°C.

At 500°C, a significantly higher amount of NO_X was released in comparison to 200 and 300°C. For example, with 3% H_2, 2 μmoles were released at 200°C, 0.1 μmoles at 300°C and 98.7 μmoles at 500°C. Nitrate instability, or rapid nitrate decomposition at the elevated temperature, caused this performance loss[72]. Furthermore, upon switching from the lean to rich phase, the partial pressure of oxygen drops to zero in these experiments, decreasing the stability of the nitrates further[34].

Compounding this loss in performance, via a loss in stability, heat is generated via the exothermic reaction between the reductants entering and stored oxygen on the catalyst surface upon the switch from lean to rich. This generated heat raises the surface temperature, further affecting the thermal stability of the nitrate species. Release of the NO_X, or decomposition of the nitrates to an intermediate NO_X species, is ideally accompanied by reduction on adjacent noble metal sites.

The rate of NO_X reduction also increases with temperature, but there is competition for the reductant between OSC consumption and the NO_X reduction reaction and therefore the actual delivery rate of the reductant to the NO_X reduction sites are not high enough. Therefore, the rapid decomposition of the nitrates at the higher operating temperature results in the observed, large release in Figure 4-3, because enough reductant is not immediately available coincident with the large and rapid release from the surface.

The increase in temperature from 200 to 300°C did result in increased NO_X conversion. This has been attributed to several reasons. First, from a kinetics perspective, NO oxidation to NO_2 increases with temperature [73]. In general, a maximum in NO oxidation is attained between 300 and 400°C over these catalyst types, being ultimately limited by thermodynamics. As a result, going from 200 to 300°C, the NO_2 amount will be increased at the catalyst surface resulting in higher adsorption rates, as NO_2 has been demonstrated as more favorable for trapping by the alkali and alkaline earth species. A second reason for the higher NO_X storage and reduction performance at 300°C is the decreased thermal stability of nitrate species. When the nitrate species are too stable, NO_X may not be released upon switching from the lean to rich phase. Without release from the trapping sites, reduction and regeneration is not as easy.

Also, the activity for not only oxidation by precious metals is higher, but reduction rates are also higher; therefore, the rate of reduction might be faster than or as fast as NO_X release. Another possible contributing factor is increased activity toward the water-gas-shift reaction as the temperature is increased. Finally, another reason that has been proposed is increased surface diffusion rates with temperature. The nitrates formed around the precious metal sites can act as a barrier toward further trapping, but if these species can diffuse to sites further from the oxidation or precious metal sites, then more trapping availability is realized. Individually, or in parallel, these explain the increased performance between 200 and 300°C.

Table 4-2 Oxygen storage capacities

Temperature (°C)	OSC (mmole)
200	0.496
300	0.628
400	0.901
500	1.10

4.2 Effect of regeneration phase CO concentration on the storage and reduction of NO_X

Figure 4-4 compares the NO_X storage and reduction performance as a function of CO concentration at 200°C under otherwise the same conditions as described in Figure 4-1. The conversions and amounts of NO_X trapped and released for these experiments are also listed in Table 4-1. It is clear from these data that increasing the CO concentration in the regeneration period at 200°C, beyond the first addition of 1.5%, actually results in a decrease in the overall NSR catalyst performance. With 1.5% CO in the regeneration phase, the overall NO_X conversion was 23%. However, when the CO concentration was increased from 1.5% to 3%, the NO_X conversion decreased to 14.8% and decreased further to 10% with 5% CO. With the increase from 1.5 to 5% CO, the amount trapped decreased from 79 to 59 μmoles, while the amount released increased from 30.8 to 37.5 μmoles demonstrating that these drops in conversion are related to both decreased trapping and increased released NO_X. A likely explanation is that when CO is added at low temperature, it poisons the precious metal sites[74]. This will directly affect the NO oxidation and NO_X reduction reaction steps, as they are dependent on the precious metal activity. However, the additional CO impacts the amount released as well. This conclusion is based on the lower amounts trapped in subsequent trapping phases when

53

additional CO was used. Previous research has indicated that the precious metals catalyze not only NO_X reduction, but also nitrate decomposition [70], and apparently CO poisoning affects this reaction process as well.

Figure 4-4 NO_X outlet concentrations obtained when testing the sample at 200°C with 0, 1.5, 3 and 5% CO in the regeneration phase.

The little NO_X storage and reduction performance observed may have actually originated from the water-gas-shift (WGS) reaction. The H_2 formed may have been the ultimate reducing agent or may have led to NH_3 formation, where NH_3 has been termed a hydrogen carrier or the reductant itself [8][75]. WGS reaction experiments were performed, and at 200°C, the maximum conversion attained was only ~10%, but enough to possibly account for some of the observed conversion. During the NO_X cycling experiments, upon switching from the lean to rich phase when CO was being used, there was a slight increase in the CO_2 outlet concentration and a simultaneous decrease in the

H$_2$O concentration. This is also an indication that some H$_2$O was consumed to form H$_2$ during the regeneration period.

The data obtained at 300°C with CO as the reductant are shown in Figure 4-5. The cycle time was again 150 seconds for storage and 5 seconds for regeneration, as in Figure 4-2. The conversion and trapped and released amounts are listed in Table 4-1. It is obvious that the increased temperature results in very different trends than those observed at 200°C. When 1.5% CO was used in the regeneration, the NO$_X$ conversion was 52%, with 3% CO it was 96% and with 5% CO 97% conversion was attained. The NO$_X$ release decreased from 6.2 to 2 to 0.9 μmoles with 1.5, 3 and 5% CO, respectively. Although the amounts released decreased, it was primarily the trapping performance that increased when the CO concentration was increased. The trapping efficiency increased from 54% to 98% between 1.5 and 5% CO. The slight improvement in the performance of the catalyst when the CO concentration was increased from 3% to 5% was not observed when the H$_2$ concentration was increased from 3% to 5%. This indicates, as does the actual calculated values, that even at 300°C, CO may not be quite as effective as H$_2$ in regenerating the catalyst or reducing the trapped NO$_X$ before ultimate release, however, this is difficult to conclude with such a small change. Equivalent performance was observed with 1.5% of either reductant, but this can be interpreted as the easier, or more efficient, sites being regenerated first, and not enough reductant available to regenerate more distant or more difficult to regenerate sites.

Another possibility is that CO is still having to go through the water-gas-shift reaction and at higher levels of CO; the reaction is not driven to completion, thereby

limiting the amount of H_2 available. This however, should not fully explain the trend since at 1.5% reductant, both performed similarly. It is apparent from these data that the catalyst performance using CO was overall similar to that when H_2 was used at 300°C. There are slight differences, such as the overall conversion mentioned above, where both slightly improved trapping and decreased NO_X released was observed when H_2 was used in regeneration period.

The improvement in the catalyst performance at 300°C versus 200°C was again observed but obviously much more significant than the improvement observed when using H_2. Several reasons for the improvement were discussed above in conjunction with the H_2 reductant data. Most importantly, when CO is used, decreased CO poisoning occurred as the temperature was increased above 200°C, which caused the significant improvement observed.
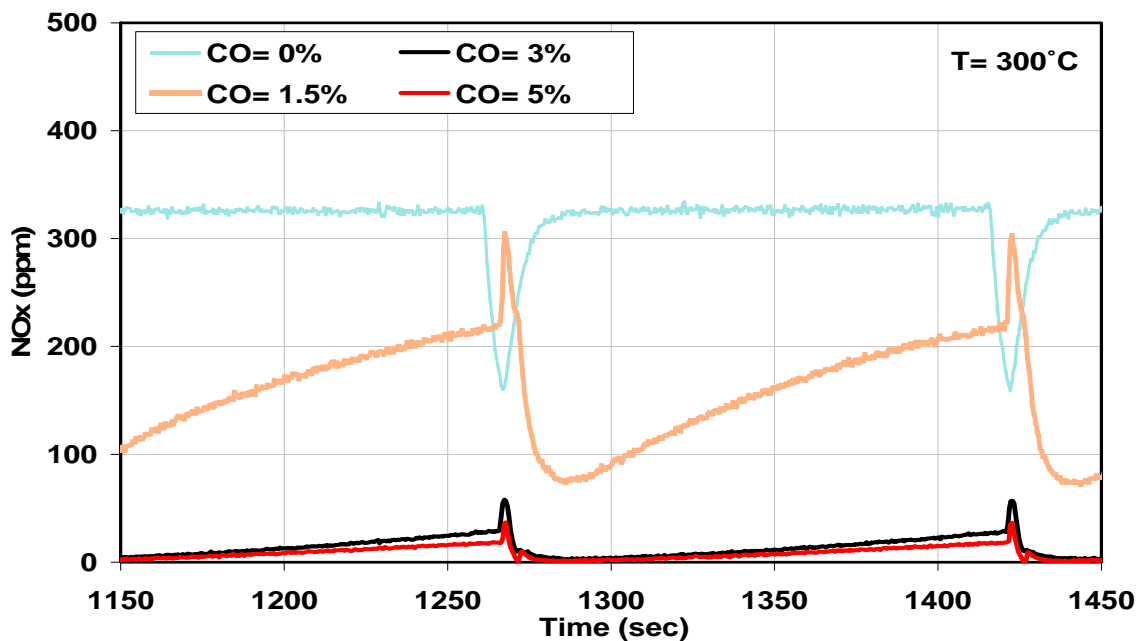
Figure 4-5 NO_X outlet concentrations obtained when testing the sample at 300°C with 0, 1.5, 3 and 5% CO in the regeneration phase.

The data obtained at 500°C when using CO as the reductant are shown in Figure 4-6. The test conditions are the same as those used for the data shown Figure 4-3. Catalyst performance increased monotonically with each increase in the CO concentration. With the addition of 1.5 % CO, the NO_X conversion was 35%, with 3% CO it was 53%, and with 5% it was 64%. The increase between 1.5 and 3% was attained via improved NO_X trapping, as shown in Figure 4-6. There was some change in release with the increase from 1.5 to 3%, but only 5 µmoles. The improved performance with the change from 3 to 5% CO was again not observed at the 200 and 300°C test points. This is again evidence that the NO_X release rate and OSC consumed increased faster than the reduction rate as a function of temperature.
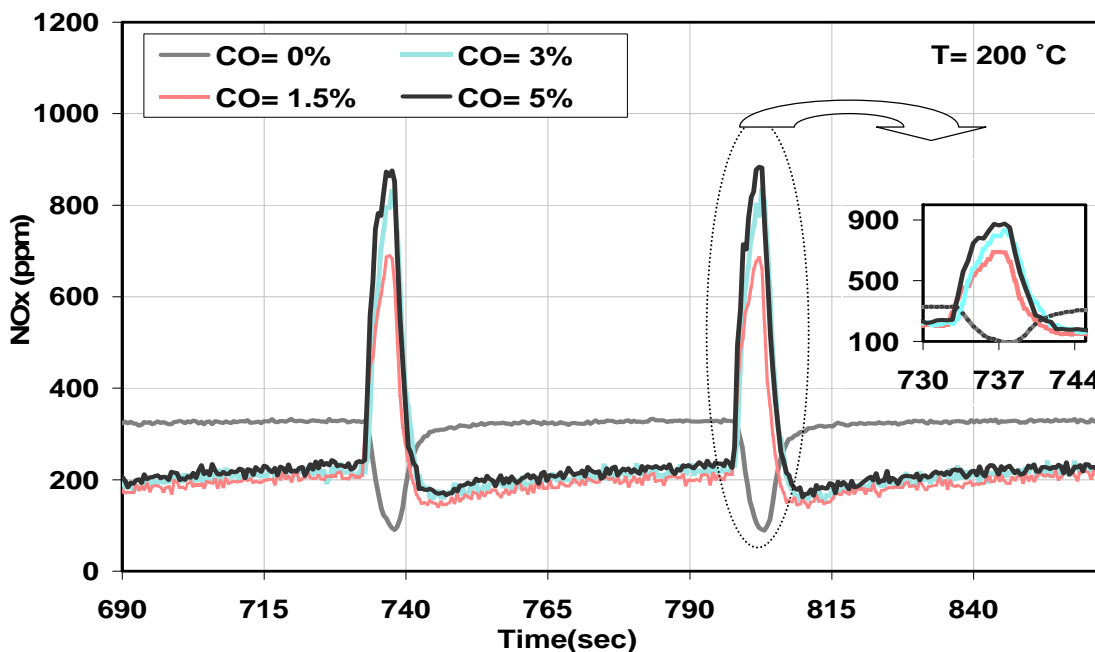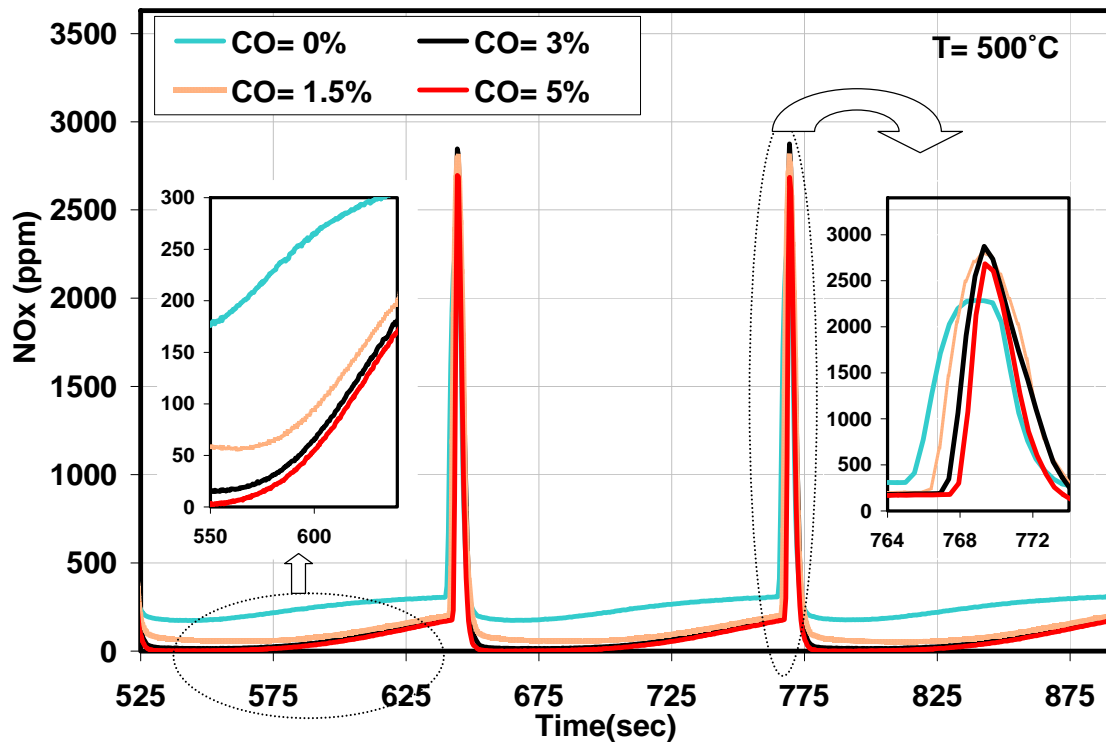

Figure 4-6 NO_X outlet concentrations obtained when testing the sample at 500°C with 0, 1.5, 3 and 5% CO in the regeneration phase.

The slightly higher amount of unconverted NO_X observed when CO was used as the reducing agent at 500°C can be attributed to a few factors. One possibility is the increased amounts of CO_2 leading to increased competition between nitrate species and carbonate on the trapping materials. As barium carbonate is more stable than barium nitrate [33], the presence of CO_2 should, and has been observed to[35], lead to the decomposition of nitrates at lower temperatures than in its absence. This would in turn lead to even more rapid NO_X release. H_2O, leading to hydroxyls, could have a similar effect, but its impact has been reportedly less significant [33], [35], [76].

Another possibility is the slightly higher exothermic nature of CO oxidation compared to H_2 oxidation, leading to higher surface temperatures when using CO upon the switch from lean to rich. Due to the very sensitive stability as a function of temperature at these higher temperatures, even a small increase would lead to measureable differences in release. Lastly, any limitation in WGS activity could also result in less reduction, without much if any difference in subsequent trapping. Overall however, the performance of the catalyst was primarily affected by the reductant concentrations rather than type of the reductant at 500°C.

4.3 Effect of H_2 and CO mixtures (CO + H_2 = 3%) on the storage and reduction of NO_X

NSR catalyst performance was also evaluated using mixtures of CO and H_2. No significant differences were observed in the catalyst performance when either the CO or H_2 reductant amount was increased from 3 to 5% at 200 and 300°C. Therefore, when

testing with the mixtures, 3% as the total amount ($CO + H_2 = 3\%$) was chosen. Selected data obtained at 200°C with 3% total reductant, but different CO/H_2 ratios, are shown in Figure 4-7. Like the data presented in Figures 4-1 and 4-4, the lean phase was 60 seconds and the regeneration phase was 5 seconds. The calculated NO_X trapped, released and reduced are listed in Table 4-1. It is clear that H_2 was better at 200°C; however, it is also apparent that the CO poisoning effect was still significant. For example, with 1.5% H_2 and no CO, see Figure 4-1, 77% NO_X conversion was attained. However, with 1.75% H_2 and 1.25% CO, twice the total reductant amount, and at least more H_2 than was available with just 1.5% H_2, only 41% was attained. Overall however, as the amount of H_2 in the regeneration phase was increased, the conversion did increase, but not in proportion to the amount being added due to CO poisoning. This improvement occurred via both increased trapping during the lean phase and decreased release during regeneration. The addition of the H_2 to the CO-containing mixtures resulted in improved performance, but when CO was completely removed, a large jump in trapping performance was observed.

The addition of CO poisons the precious metal sites to not just reduction of released NO_X, but also toward the catalyzed decomposition of the nitrates leading to released NO_X, further supporting the mechanism that includes reductant and the precious metal both inducing decomposition of the nitrate species [77]. Some trapped NO_X was released (here released means NO_X observed as unreduced and in the outlet, as well as that released and reduced) when only CO was used, or even when CO was present, but it is less than when H_2 was included, as is demonstrated by improved trapping in subsequent lean phases when H_2 was added. The increased performance with decreasing CO addition can be attributed to a decrease in CO poisoning, via simple competition with H_2 present.

59

Figure 4 -7 NO_X outlet concentrations obtained when testing the sample at 200°C with 3% mixtures of CO and H_2 in the regeneration phase.

Selected data obtained at 300°C using two of the mixtures, and also re-plotting the data with just H_2 or CO, are shown in Figure 4-8. The cycling experiment again consisted of a 150 second storage phase and a 5 second regeneration phase. The increase in operating temperature from 200 to 300°C resulted in higher NO_X removal efficiency with the CO/H_2 mixtures as well. The reasons for such improvement are the same as those discussed above with the individual reductants.

As shown in Figure 4-8 and Table 4-1, with each incremental addition of H_2, improvement in trapping performance was observed. However, the maximum difference in the overall NO_X conversion, and trapping, among all the reductant mixtures was only in a range of 1-2%. Both reductants are similar in efficiency, with the differences

observed real, but quantitatively not very significant under the conditions of this test. Longer lean-phase times may have resulted in different conclusions. The differences in trapping are still due to better regeneration of the catalyst by the H_2 reductant in a prior regeneration phase. The amount of NO_X released during the regeneration did not follow a clear trend, although it is obvious that with H_2 less was released than in the case where just CO was the reductant source.
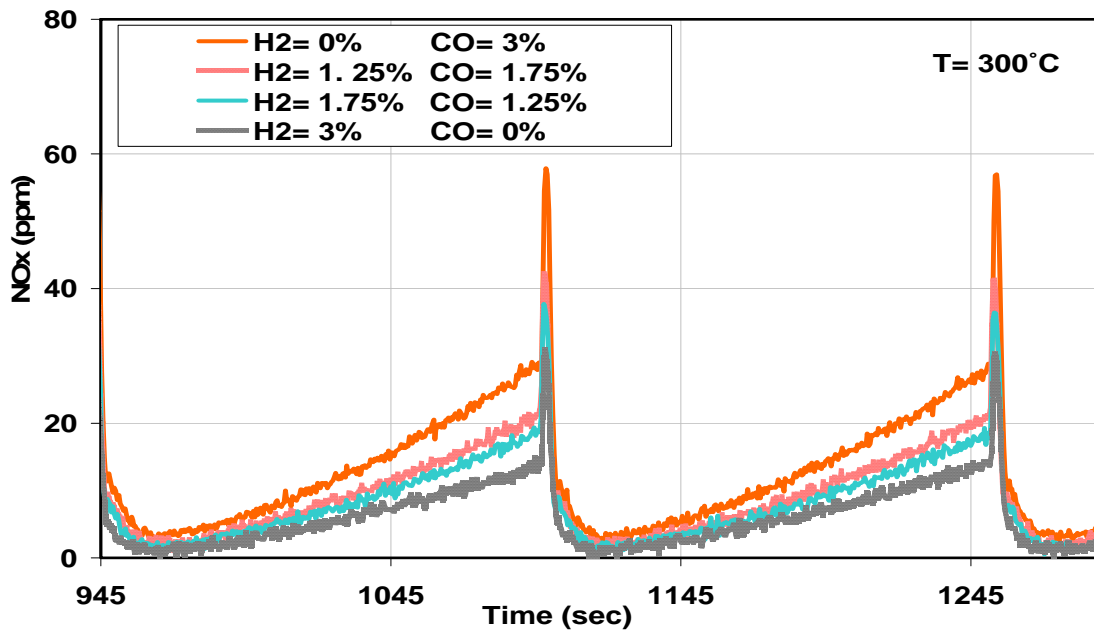
Figure 4-8 NO_X outlet concentrations obtained when testing the sample at 300 with 3% mixtures of CO and H_2 in the regeneration phase.

Selected data obtained at 400°C are shown in Figure 4-9. A complete set of data at this temperature was not obtained due to difficulty in obtaining comparable breakthrough data as a function of chosen trapping time. In other words, with shorter trapping times, 0 ppm slip was observed, and when slip was finally observed by going to longer trapping times, the outlet NO_X level would not reach 0 ppm at the beginning of the lean phase during subsequent trapping cycles. As a balance, the cycle time was 140

seconds for trapping and again 5 seconds for regeneration. Calculated conversions and amounts trapped and released are also listed in Table 4-1 for the few experiments done. There was little difference in the overall catalyst performance when either of 3% H_2 or CO was used separately; 88% with 3% H_2 and 87% with 3% CO. However, when mixtures of the two reductants were used, but still maintaining a total of 3% reductant, there was an improvement in the performance. The NO_X conversion rose to 91% when 1.25% H_2 and 1.75 % CO was used and to 92% when 1.75% H_2 and 1.25% CO was used. Although not definite, there are a couple of possibilities that could explain this observation. First, CO oxidation is more exothermic than H_2 oxidation whereas the activation of H_2 on precious metals is much easier than CO. When mixtures of the two reductants were used, it is possible that these two effects occurred simultaneously. The heat generated from the more exothermic CO oxidation reaction via its interaction with OSC resulted in more nitrate decomposition and NO_X release coupled with the presence of H_2 resulted in better regeneration. Another possible reason for the improved performance relates to the formation and reduction ability of NH_3, which will be discussed in further detail below. Briefly, however, higher concentrations of NH_3 were observed in the outlet when using the CO and H_2 mixtures at 300 and 500°C and NH_3 has been proposed as the reductant or at least as a H_2 carrier during regeneration.

The performance of the catalyst at 400°C, regardless the reductant, was lower than that with the 300°C tests. Again, this is due to the poorer thermal stability of the nitrate species on the trapping materials, as discussed above. Coupled to this is insufficient reductant to account for the trapped NO_X. The total trapped NO_X was around 0.46 mmoles and OSC was 0.90 mmoles. 1.16 mmoles of reductant are needed to reduce

the nitrate species and 1.8 mmoles of reductant are needed to consume the surface oxygen. Therefore, even with 3% or 1.6 mmoles of reductant, there is an insufficient amount of reductant. Again, shorter trapping times which would alleviate this problem, led to 0 ppm breakthrough during the trapping period.
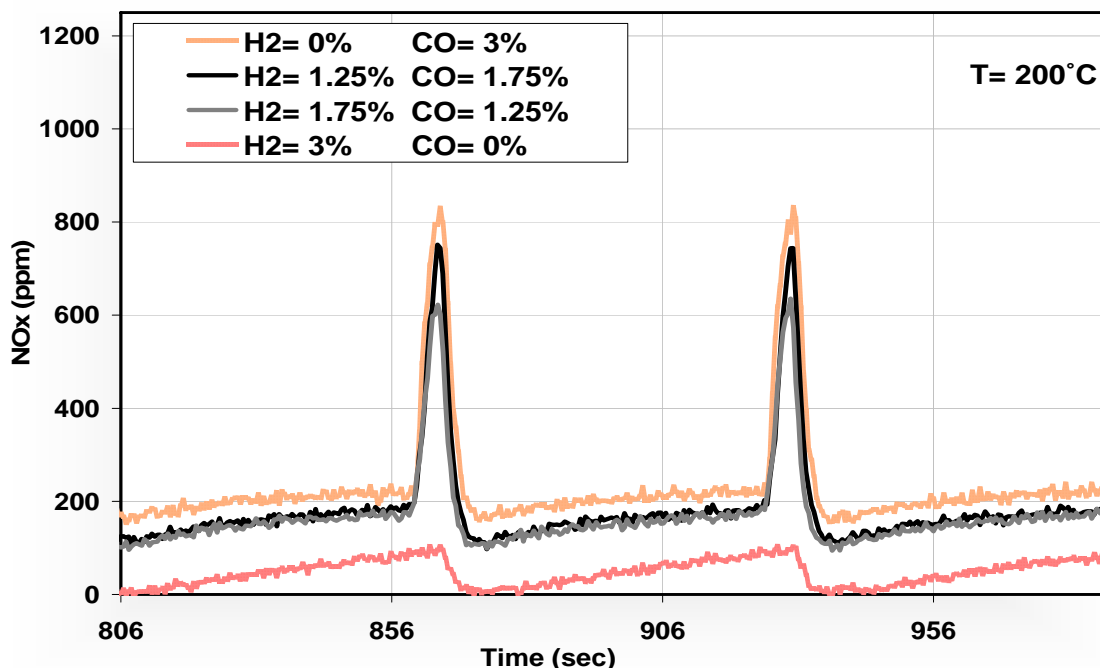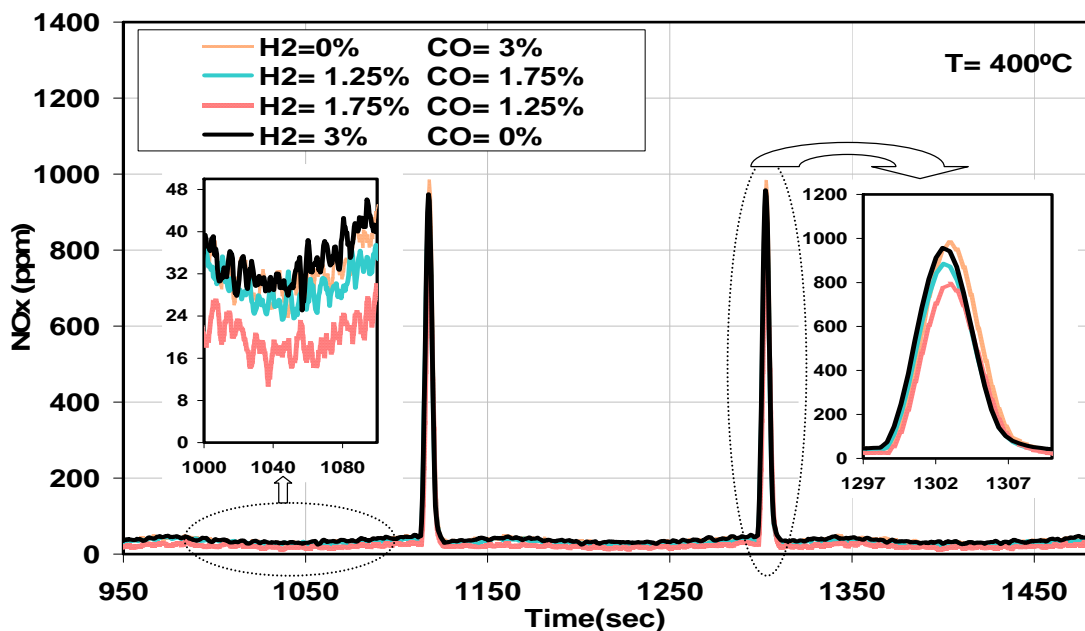

Figure 4-9 NO_X outlet concentrations obtained when testing the sample at 400°C with 3% mixtures of CO and H_2 in the regeneration phase.

The data obtained at 500°C are shown in Figure 4-10. As was discussed previously, no significant changes were observed in the overall performance of the catalyst when using H_2 or CO in the regeneration period. The NO_X conversion when 3% H_2 was used was 52% while 53% conversion was achieved with 3% CO. Again, however, when mixtures of the two reductants were used, the performance was better. For example, with 1.25% H_2 and 1.75 % CO, the NO_X conversion was 56% and 57% when 1.75% H_2 and 1.25% CO was used. In addition, the NO_X release associated with using the mixtures of the two reductants was slightly lower than using either H_2 or CO

separately. Reasons for such improvement in the catalyst performance when using mixtures of the two reductants were discussed above.
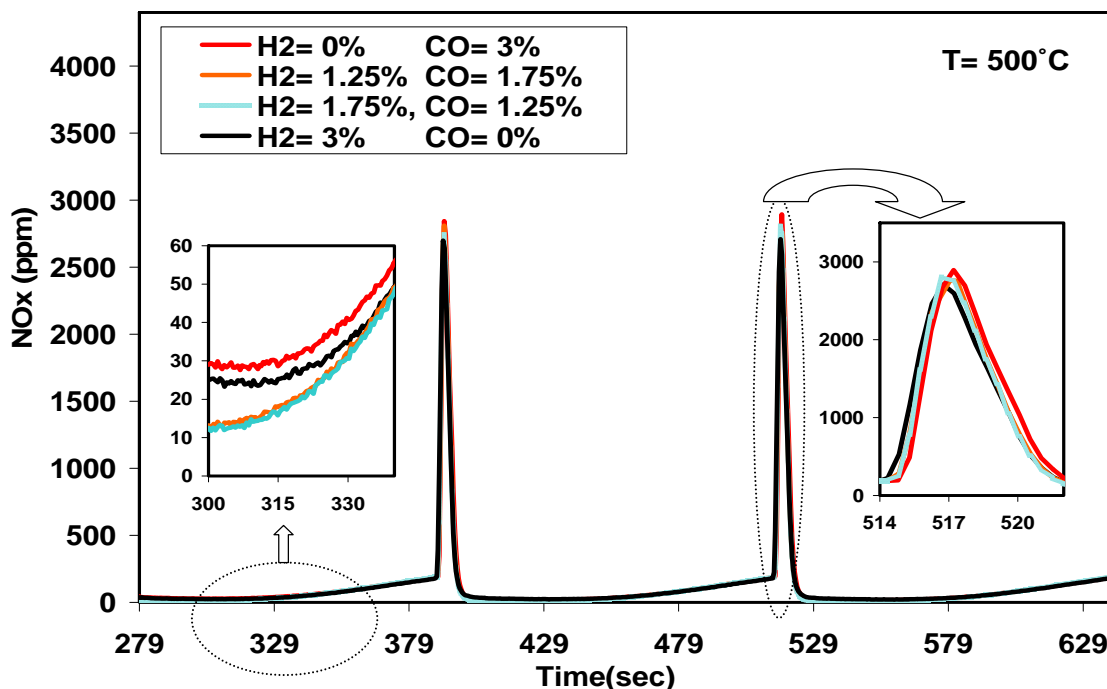
Figure 4-10 NO_X outlet concentrations obtained when testing the sample at 500°C with 3% mixtures of CO and H_2 in the regeneration phase.

4.4 NH₃ formation

Ammonia is a common byproduct in NSR experiments[76]-[81]. NH_3 formation has been observed when H_2 was used as a reducing agent in the regeneration period overPt/Ba-based catalysts [77] as well as with mixtures of H_2 and CO [79], and pure CO [80]. In this study, NH_3 was observed when H_2, CO, and the mixtures of H_2 and CO were used at all temperatures. Cumaranatunge et. al. [75] have demonstrated equivalent reduction efficiency of H_2 and NH_3 in NSR catalysis, and facile formation of NH_3 from a

feed of NO and H_2 over a Pt/Al_2O_3 catalyst. NH_3 has therefore been proposed as a hydrogen carrier or even the reductant participating in the NO_X reduction reaction.
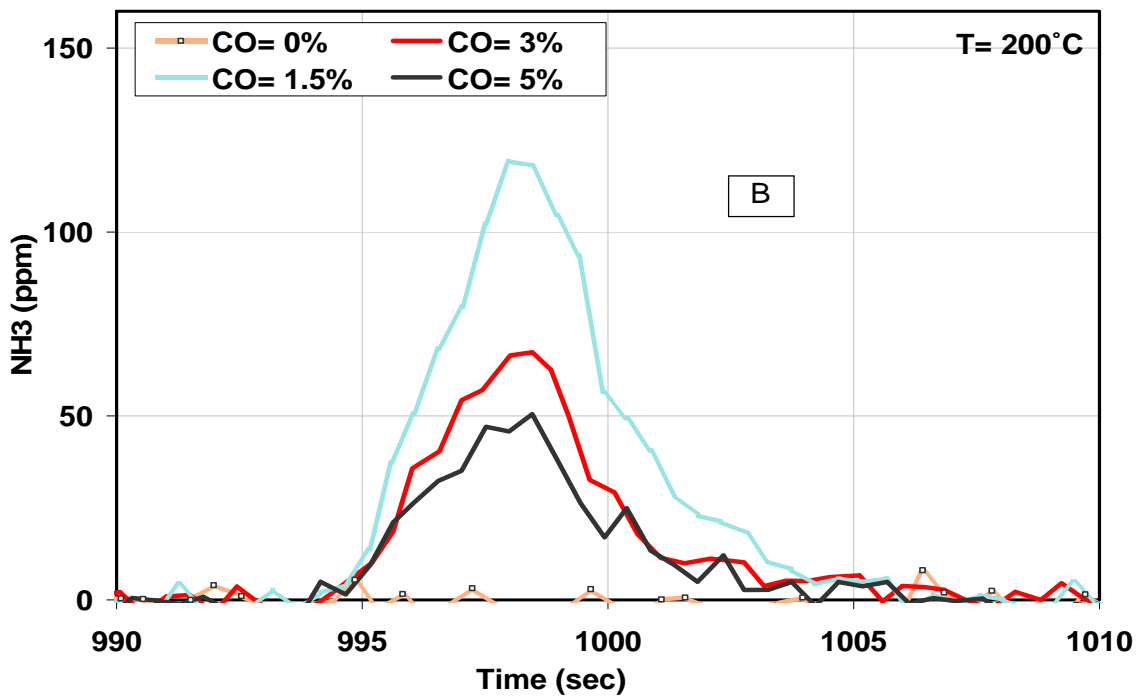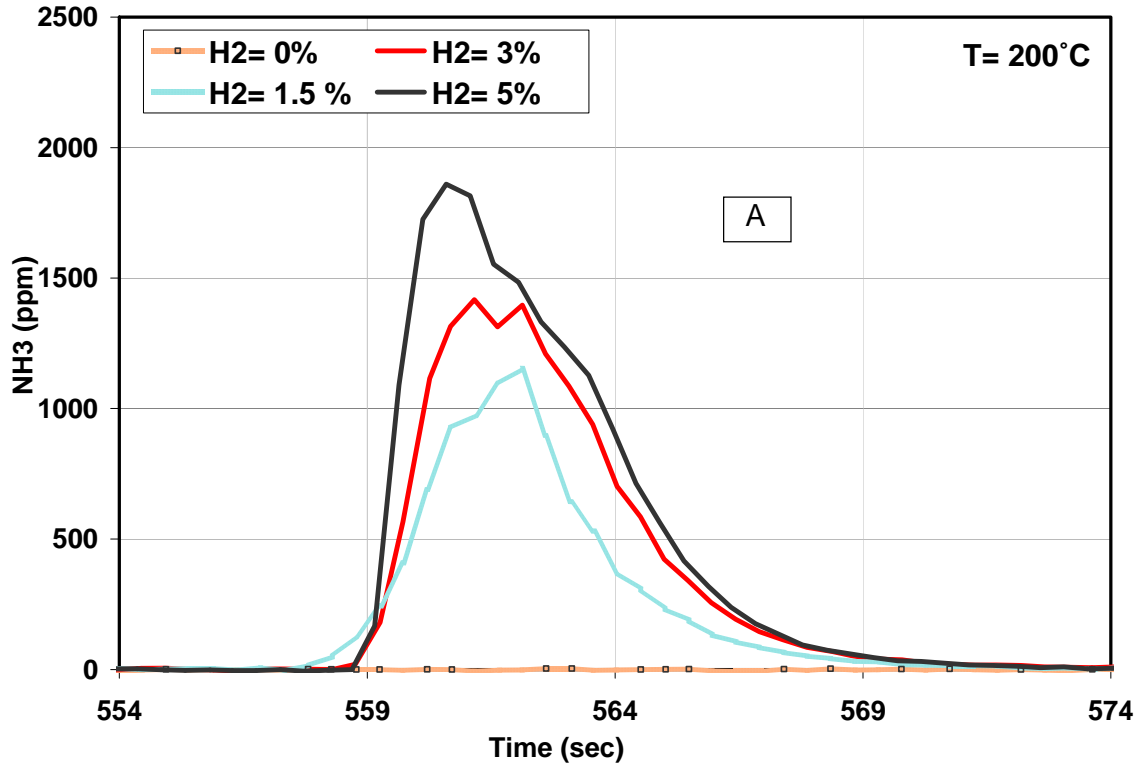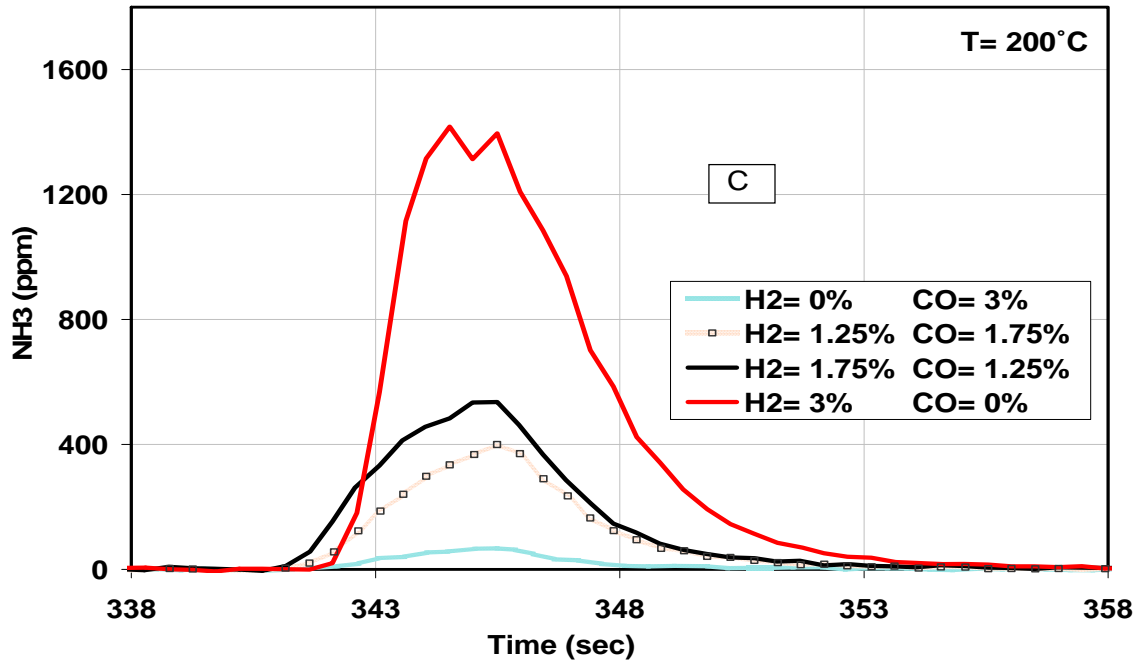
Figure 4-11 NH_3 outlet concentration data obtained when testing the sample at 200°C with regeneration-phase (A) H_2 concentrations of 0, 1.5, 3, and 5%, (B) CO concentrations of 0, 1.5, 3, and 5%, and (C) mixtures of H_2 and CO of 3%.

Ammonia can be formed directly from reaction of H_2 with NO on the catalyst, with the H_2 added to the regeneration mixture or produced from the WGS reaction when CO and H_2O are available in the regeneration mixture[9]. NO can be easily dissociated to atomic nitrogen and oxygen over precious metals at higher temperatures[82]. Subsequently, the N atom would react with dissociated H_2 to form NH_3. In comparing the data at the different test temperatures listed in Table 4-1, it is apparent that NH_3 in the outlet increased as the temperature was decreased. At 200°C, the NO_X-to-NH_3 reduction mechanism is rapid, relative to the reduction reaction that results in N_2. The NO_X-to-N_2 reduction mechanistic path increases with temperature until it is more comparable to the

NH$_3$ formation mechanism and/or surpasses it. And finally as the temperature is further increased, the weak stability of NO$_X$ species causes the release of unconverted NO$_X$ and hence NH$_3$ formation, as well as NO$_X$ reduction to N$_2$ will be limited.

The NH$_3$ outlet concentration data obtained from the 200 and 300°C experiments described above are shown in Figures 4-11 and 4-12. It is clear from these that NH$_3$ formation at 200 and 300°C, when H$_2$ was used as the reductant source, is proportional to H$_2$ concentration in the regeneration mixture; as the H$_2$ concentration increased, the NH$_3$ in the exhaust increased. Similarly, when CO was used at 300°C, NH$_3$ in the outlet increased with increasing CO concentration from 3 to 5%. This NH$_3$ must originate from H$_2$ generated via the WGS reaction. At 200°C however, NH$_3$ formation was found to decrease as the CO concentration increased, as shown in Figure 4-11b. This is again attributed to the negative impact of CO poisoning on the precious metals at 200°C. Little or no NH$_3$ was observed during the tests at 400 and 500°C. However, the small amounts that did form changed proportionally to the inlet reductant concentrations; as the reductant concentrations increased, the NH$_3$ outlet concentration increased.

At 300°C, NH$_3$ was not observed with the lower reductant concentrations, 0% and 1.5%. This is due to insufficient reductant, relative to trapped NO$_X$, delivered during regeneration. This does not suggest NH$_3$ is not formed along the catalyst, but that any NH$_3$ that is formed is used downstream in nitrate or released NO$_X$ reduction. NSR catalysts operate as integral devices and spatial resolution of the chemistry along the axial length of channel is evolving. However, there are several publications that suggest NH$_3$

formation is constantly occurring, but the NH_3 formed can easily react with downstream nitrates of surface NO_X species to form product N_2[74][76].

Figure A: NH3 (ppm) vs Time(sec), T=300°C
Legend: H2= 0%, H2= 3%, H2= 1.5%, H2= 5%

Figure B: NH3 (ppm) vs Time(sec), T=300°C
Legend: CO= 0%, CO= 3%, CO= 1.5%, CO= 5%
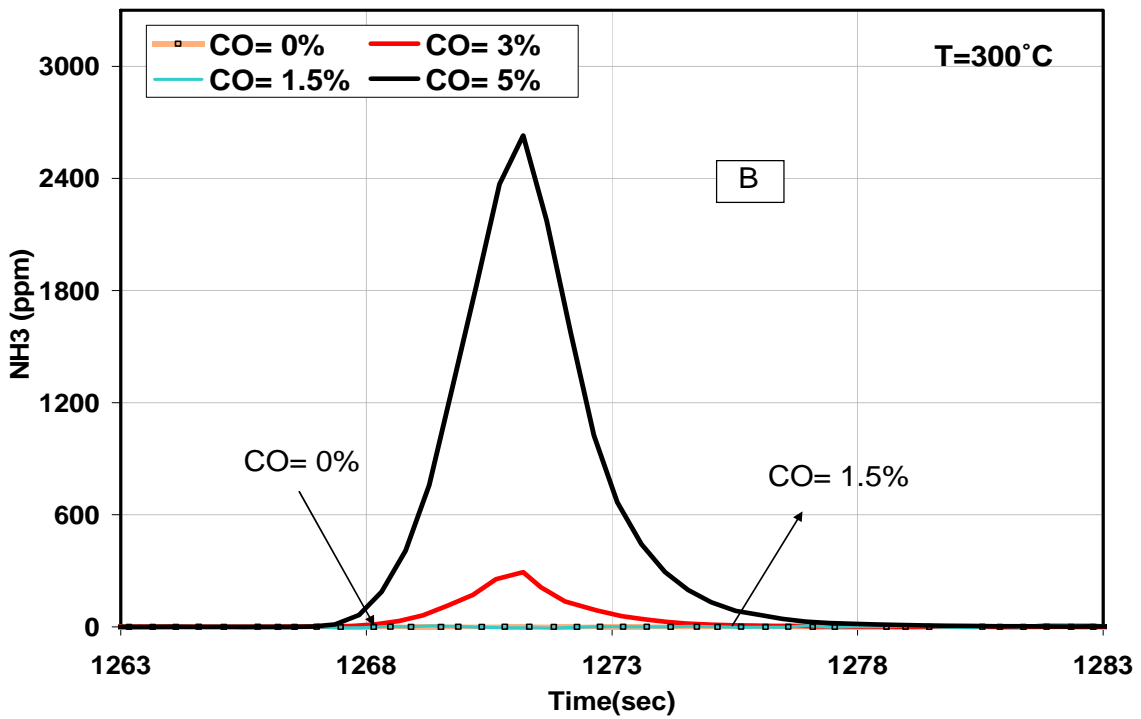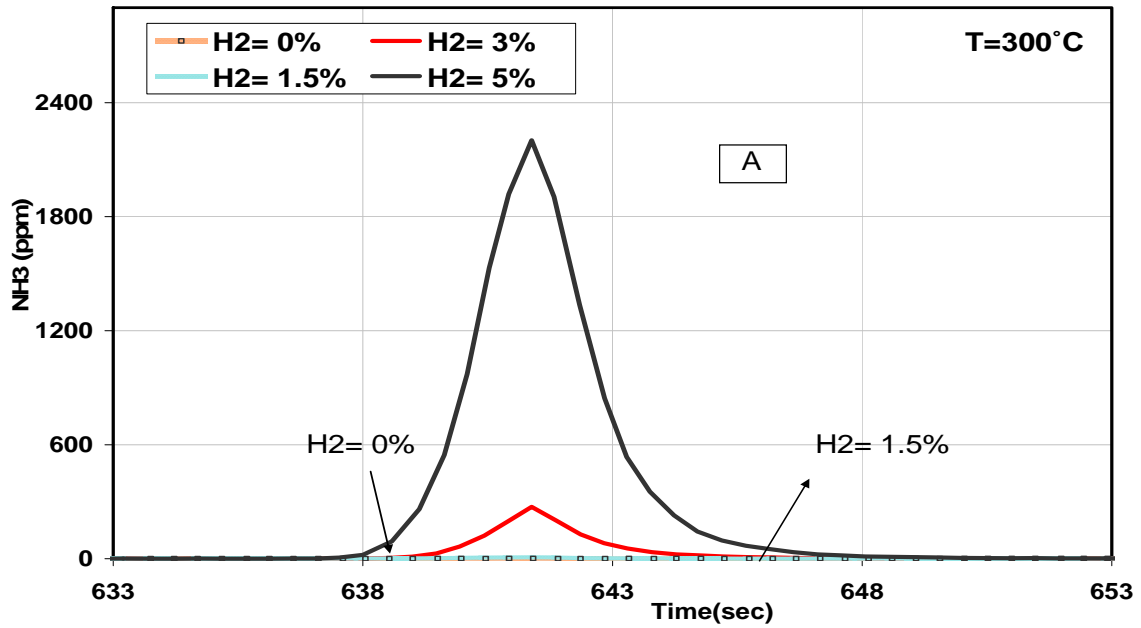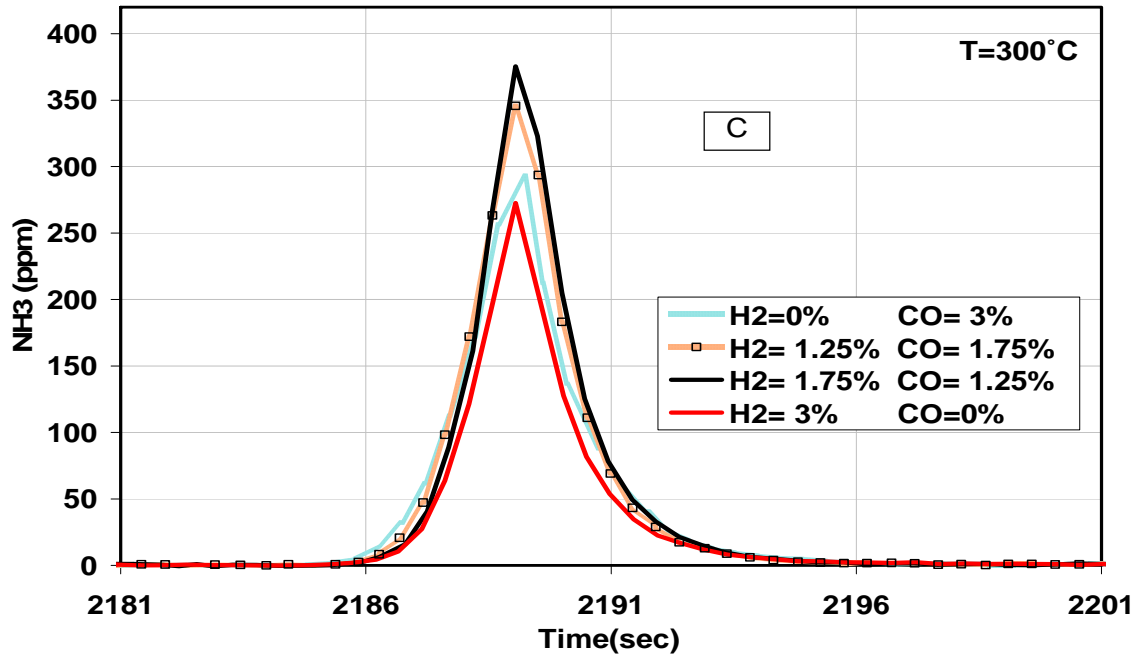
Figure 4-12 NH$_3$ outlet concentration data obtained when testing the sample at 300°C with regeneration-phase (A) H$_2$ concentrations of 0, 1.5, 3,and 5%, (B) CO concentrations of 0, 1.5, 3, and 5%, and (C) mixtures of H$_2$ and CO of 3%.

As can be seen in Figure 4-12c, at 300°C using H$_2$ surprisingly led to lower levels of NH$_3$ in the outlet gas composition in comparison to the amount evolved when using the mixtures. This coincides with the slightly higher conversion observed with the mixtures as well. It is likely that this is due to a combination of effects observed at 200°C. It is apparent that CO hinders NO$_X$ release from the surface at 200°C, and this effect may be reduced at 300°C, but still present. H$_2$, as noted, induces release. With just H$_2$, NO$_X$ release occurs and the local H$_2$: NO$_X$ ratio determines the amount of NH$_3$ made. When CO is added with the H$_2$, the CO slows the release of NO$_X$, or decomposition of the surface NO$_X$ species, relative to H$_2$ such that the local H$_2$: NO$_X$ ratio must be higher than with just H$_2$, leading to more NH$_3$ evolved. With just CO, the local amount of H$_2$

generated from the WGS reaction relative to the surface NO_X species determines the amount of NH_3 made, and although the CO would still slow NO_X release, the extent of the WGS reaction is only 62% at the catalyst outlet at 300°C, indicating less at the inlet where most trapped NO_X resides at the end of the lean phase. The CO slowing the release, combined with the presence of H_2 results in more NH_3 formed. A similar argument can be made for the 500°C operating condition, where slightly more NH_3 was also made when using the mixtures. Here, however, and likely at 400°C also although no significant NH_3 was observed in the outlet, the extra NH_3 made down the axial length of catalyst could also result in the slight improvement in NO_X conversion observed, as shown in Table 4-1 and discussed in section 4.3 above.

Chapter 5: The Effects of Thermal Degradation on the Performance of a Commercial NSR Catalyst.

To obtain a detailed understanding of the effect of chronic thermal aging on the overall performance of NO_X storage/reduction catalysts, a vendor-supplied catalyst was exposed to different temperatures in air with 2% H_2O in the range of 500 to 750°C. After each exposure temperature, the catalyst performance was evaluated at different operating temperatures in the range of 200 to 500°C. Performance measures included NO_X storage capacity, water-gas-shift reaction extent, NO oxidation, oxygen storage capacity, and NO_X conversion under cycling conditions. For cycling experiments using an unaged sample, 0-5% of either H_2, CO, or a mixture of H_2 and CO were used as a reductant source. However, no significant changes were observed in catalyst performance when either the CO or H_2 reductant amount was increased from 3 to 5% at 200 and 300°C. Therefore, in this study only 3% of either H_2, CO, or mixtures with 3% as the total amount (CO + H_2 = 3%) were chosen.

5.1 Effect of thermal degradation on NO_X reduction efficiency during cycling

5.1.1 Effect of thermal degradation on NO_X reduction efficiency with H_2

The outlet NO_X (NO + NO_2) concentrations obtained using the unaged catalyst and thermally aged catalysts during cycling experiments with 3% H_2 as the reductant in the regeneration phase at an inlet temperature of 200°C are shown in Figure 5-1. For this set of experiments, the lean, or trapping, time was 60 seconds and the rich, or regeneration, time was 5 seconds. The conversions and amounts of NO_X trapped and released for these

71

experiments are listed in Table 5-1. All reported values and plotted data were obtained once steady cycle-to-cycle performance was observed. With the unaged catalyst, the calculated NO_X conversion was 85%. With the first two degradation steps, at 600 and 650°C for 2 hours each, the NO_X conversion decreased to 81 and 71%, respectively. The NO_X trapped decreased from 0.182 mmoles for the unaged sample, to 0.154 mmoles after aging at 650°C. The amount released was relatively small, but increased from 0.002 mmoles with the unaged catalyst to 0.005 mmoles after the 650°C degradation step. However, when the catalyst was aged for 2 hrs at 700°C, the NO_X conversion actually increased to 88%. The trapped amount increased and the release decreased. With further exposure at 700°C, for 8 hours total, the NO_X conversion decreased to 81% and further decreased to 67% with the 750°C degradation step. The NO_X release increased from 0.002 mmoles after 2 hours at 700°C to 0.004 and 0.008 mmoles after 8 hours at 700°C and 2 hours at 750°C, respectively.

To obtain further understanding about the improvement that occurred after the sample was aged at 700°C for 2 hours; a new sample was aged with different exposure times at 700°C. Exposure times of ½, 2, 5, 8 and 15 hours were tested. This was done with one sample, with the times being the cumulative time spent at 700°C. The data obtained are listed in Table 5-2 and shown in Figure 5-2. It is apparent from Figure 5-2 that the catalyst performance or NO_X conversion improved after exposure to $^1/_2$ and 2 hrs at 700˚C. However, after exposure for 5 hours, the NO_X conversion decreased. No further changes in the catalyst performance were observed when the catalyst was aged for 8 and 15 hours.

Figure 5-1 NO$_X$ outlet concentrations as a function of thermal degradation obtained when testing the sample at 200°C with 3 % H$_2$ in the regeneration phase.
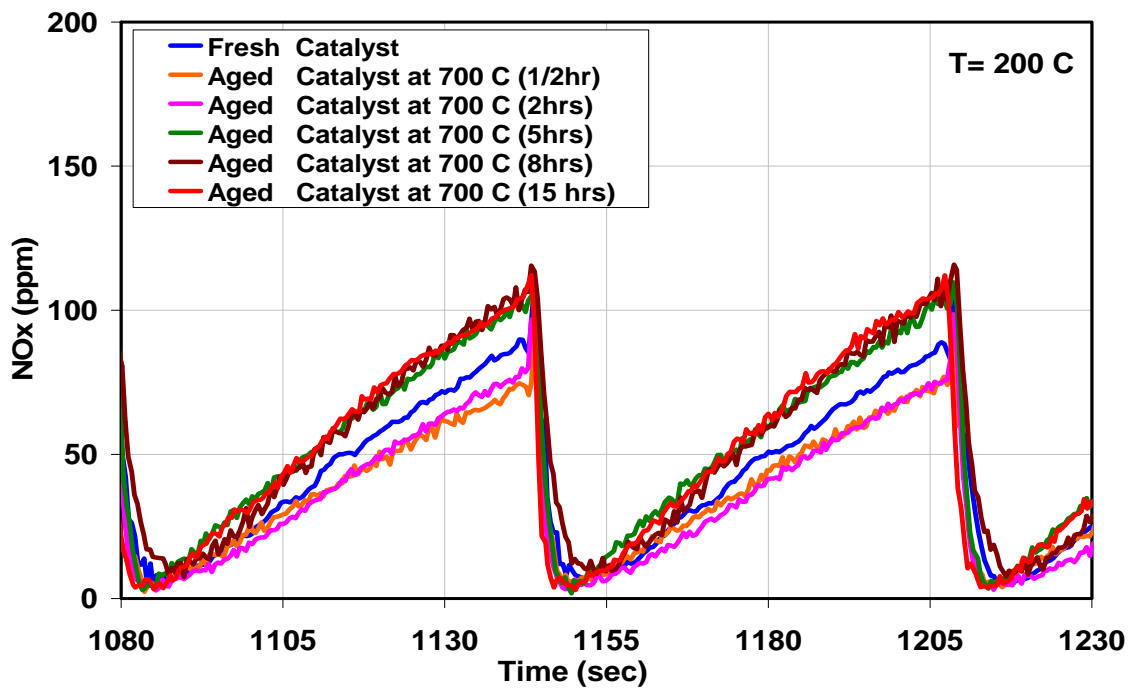
Figure 5-2 NO$_X$ outlet concentrations after different aging times at 700°C obtained when testing the sample at 200°C with 3 % H$_2$ in the regeneration phase.

Table 5-1 calculated performance characteristics as a function of temperature, thermal aging, and type of reductant, CO and/or H$_2$.

Temperature (°C)	Reducing Agent H$_2$	CO	Unaged Catalyst	Aged at 600°C	Aged at 650°C	Aged at 700°C (2hrs)	Aged at 700°C (8 hrs)	Aged at 750°C
					NO$_X$ Conversion (%)			
200	3	0	85	81	71	88	81	67
	0	3	15	12	15	24	17	13
	1.25	1.75	36	12	9	53	50	6
300	3	0	98	90	88	88	90	87
	0	3	96	89	91	90	88	82
	1.25	1.75	97	94	94	95	92	87
400	3	0	81	78	83	70	75	70
	0	3	80	76	82	64	75	45
	1.25	1.75	82	80	86	78	82	80
500	3	0	52	54	46	42	46	42
	0	3	53	56	47	42	53	37
	1.25	1.75	55	57	40	42	41	33
					NO$_X$ Trapping (mmoles)			
200	3	0	0.182	0.173	0.154	0.186	0.175	0.150
	0	3	0.063	0.048	0.053	0.095	0.062	0.050
	1.25	1.75	0.103	0.050	0.043	0.131	0.120	0.035
300	3	0	0.518	0.477	0.466	0.464	0.476	0.462
	0	3	0.507	0.474	0.481	0.478	0.467	0.436
	1.25	1.75	0.511	0.496	0.500	0.501	0.486	0.462
400	3	0	0.544	0.513	0.562	0.490	0.503	0.479
	0	3	0.547	0.525	0.566	0.474	0.507	0.326
	1.25	1.75	0.552	0.554	0.577	0.550	0.556	0.540
500	3	0	0.319	0.295	0.285	0.265	0.266	0.246
	0	3	0.327	0.304	0.289	0.256	0.287	0.220
	1.25	1.75	0.330	0.310	0.253	0.250	0.236	0.211
					NO$_X$ Release (mmoles)			
200	3	0	0.002	0.001	0.005	0.002	0.004	0.008
	0	3	0.031	0.023	0.022	0.046	0.025	0.021
	1.25	1.75	0.027	0.025	0.023	0.020	0.015	0.023
300	3	0	0.001	0.003	0.003	0.003	0.004	0.003
	0	3	0.002	0.003	0.004	0.004	0.004	0.005
	1.25	1.75	0.001	0.002	0.002	0.003	0.003	0.004
400	3	0	0.033	0.018	0.040	0.046	0.031	0.037
	0	3	0.038	0.042	0.050	0.067	0.035	0.044
	1.25	1.75	0.031	0.046	0.034	0.061	0.034	0.035
500	3	0	0.098	0.070	0.091	0.090	0.070	0.068
	0	3	0.104	0.070	0.090	0.080	0.064	0.064
	1.25	1.75	0.095	0.070	0.086	0.071	0.061	0.071

Table 5-2 NO$_X$ conversions at 200°C after different aging times at 700°C

Test	Reducing Agent		½ hr	2hrs	5hrs	8 hrs	15 hrs
	H$_2$	**CO**					
NO$_X$ conversion (%)	3	0	86	88	81.78	81.30	81.95
	0	3	85	24	50	17	29
	1.25	1.75	63	53	40	50	55

Similar experiments were carried out at 300, 400 and 500°C to investigate the effects of thermal aging on NO$_X$ storage and reduction at different operating temperatures. Figure 5-3 shows the outlet NO$_X$ concentration profile for a set of 150 second storage and 5 second regeneration periods at 300°C. Summary data are listed in Table 5-1. With the unaged catalyst, and after steady cycle-to-cycle performance was reached, the calculated conversion was 98%. This high conversion is due to a combination of factors, including nitrate stability, decent NO oxidation kinetics, and sufficient regeneration/cleaning during the rich phase due to sufficient reductant delivered, coincident with lower OSC at 200 and 300°C as shown in Table 5-3. However, as shown in Table 5-1 and Figure 5-3, the performance drops after just the 600°C degradation temperature. The amount of NO$_X$ trapped decreased from 0.518 to 0.477 mmoles while the NO$_X$ release also increased from 0.001 to 0.003 mmoles as a result of this thermal aging step. With exposure at 650°C and higher, little if any change in performance occurred.
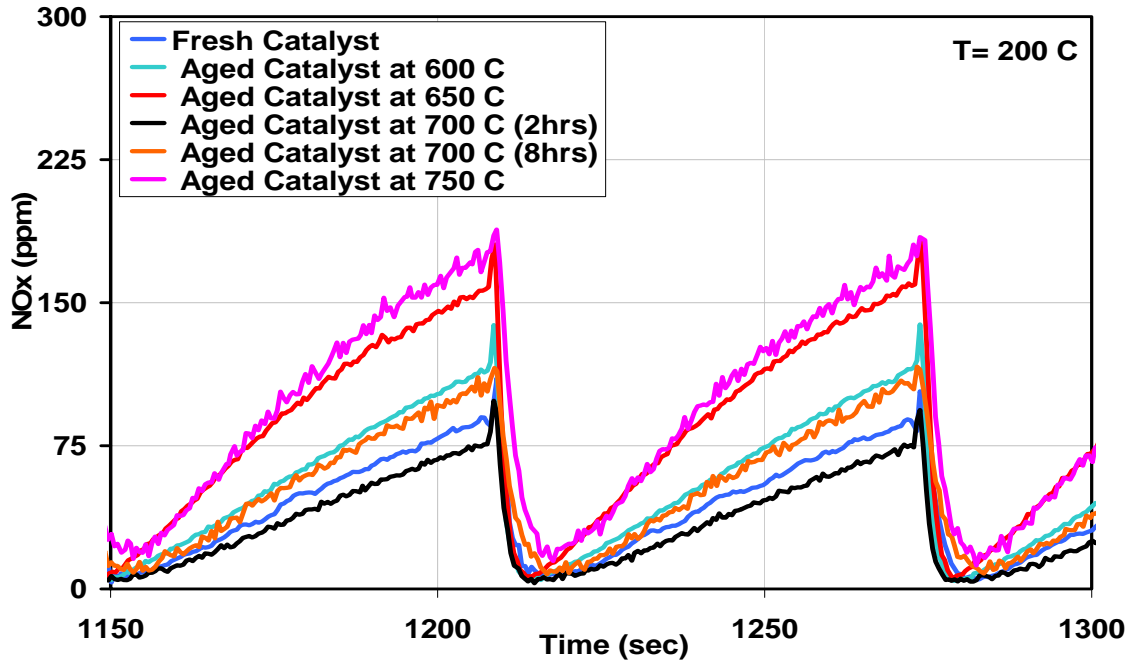
Figure 5-3 NO_X outlet concentrations as a function of thermal degradation obtained when testing the sample at 300°C with 3 % H_2 in the regeneration phase.

The outlet NO_X concentration profiles obtained at 400°C are shown in Figure 5-4. For this set of experiments, the trapping time was 180 seconds and the regeneration time was 5 seconds. The conversions and amounts of NO_X trapped and released for these experiments are listed in Table 5-1. With the unaged catalyst, the calculated NO_X conversion was 81%. Although the NO_X conversion at 400°C was less than that at 200 and 300°C, a longer NO_X trapping period was used, convoluting the comparison. It is of course possible to improve the NO_X reduction ability or conversion by using shorter trapping times; for example with a 140 second trapping period, the conversion attained was 88%. Decreased nitrate thermal stability, combined with higher OSC, and insufficient reductant amounts are the main reasons for this lower conversion.

The NO$_X$ observed in the outlet reached a minimum value of about 25 ppm 11 seconds after the rich-phase ended and the trapping phase began. Then, the NO$_X$ slip increased to a maximum value of about 45 ppm, 42 seconds after the minimum value was reached, and then again decreased until the regeneration phase began. This NO$_X$ slip profile can be explained by the heat being generated via the exothermic reactions during the regeneration phase, as shown in Figure 5-5. NO$_X$ trapping is a function of catalyst temperature and hence changes in the temperature will affect the trapping ability. With the increase in catalyst temperature as result of the exothermic regeneration reactions, nitrate stability decreased, and as the catalyst cooled, taking many seconds, the trapping ability increased. This increase becomes apparent with the decrease in NO$_X$ slip noted 42 seconds after the minimum was reached. Previous work has discussed this trend, specifically in the 400 to 475°C range **[71]**[83]**.**

Figure 5-4 NO$_X$ outlet concentrations as a function of thermal degradation obtained when testing the sample at 400°C with 3 % H$_2$ in the regeneration phase.
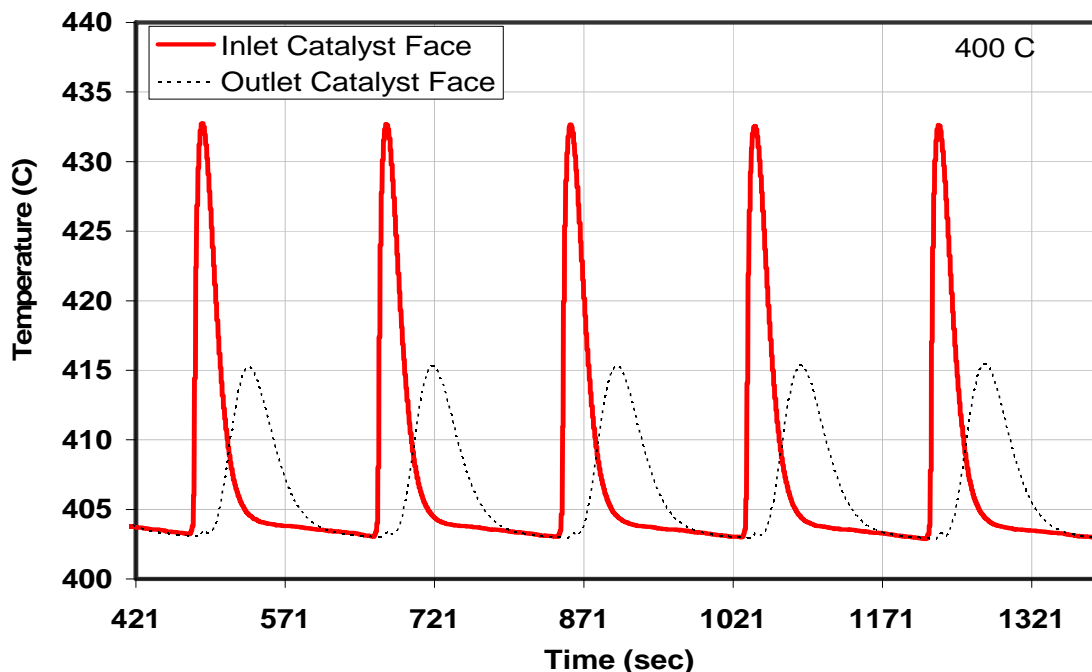
Figure 5-5 Temperature data obtained in the radial center, just inside the inlet and outlet
faces of the catalyst. These data were obtained when testing the sample at
400°C with 3 % H_2 in the regeneration phase.

It is clear from Figure 5-4 and Table 5-1 that no significant changes were observed
with the first two thermal degradation temperatures; 600 and 650°C. A significant change
was however observed when the catalyst was aged for 2 hours at 700°C. The NO_X
conversion decreased sharply from 83% after aging at 650°C to 70% after aging at
700°C. The NO_X trapped decreased from 0.562 to 04.9 mmoles at 650 and 700°C
respectively. With the longer exposure at 700°C, the catalyst slightly improved in
performance relative to performance observed after the 700°C degradation for two hours.
After degradation at 750°C, the observed conversion was less than that at observed after
the aging at 700°C for 8 hours.

The data obtained at 500°C with H_2 as the reductant are shown in Figure 5-6. The cycle time was 120 seconds for storage and 5 seconds for regeneration. The conversion and trapped and released amounts are listed in Table 5-1. With the unaged catalyst, the calculated NO_X conversion was 52%. It is apparent from Figure 5-6 and Table 5-1 that the performance at 500°C was less than 200, 300, and 400°C tests. The weak stability of nitrate species, insufficient reductant amount with 3% H_2, and higher OSC at 500°C are the reasons for this low performance, which was also observed in the data discussion presented in the previous chapter.

With 500°C performance, the first degradation temperature resulted in no significant change observed. Degradation was observed with the degradation step at 650°C. The NO_X conversion decreased from 53.5% to 46% at 600 and 650°C, respectively. Again, there was a slight drop in the NO_X conversion after first exposure at 700°C, but with longer exposure, there was a slight increase in the performance of the catalyst. With the exposure at 750°C, no significant conversion changes were relative to the performance observed after degradation at 700°C, although both trapping and release amounts changed. It is noticeable from the data in Figure 5-6 that there were changes in observed outlet NO_X concentration after the different degradation steps, apparent during the early stages of trapping. However, the amount of NO_X released changed as well and balanced the effect of thermal degradation on the trapping phase catalyst. Therefore, little change was observed in the overall NO_X conversion. The improvement observed with the longer 700°C exposure originates from differences at the very early lean-phase times. The amount of NO_X slip was actually higher at the end of the lean time after the 700°C 8-hour exposure in comparison to after the 2-hour exposure. This indicates that if the lean-phase

79

time were to have been increased, the observed performances may have been more similar ,or even led to the conclusion of a different trend.
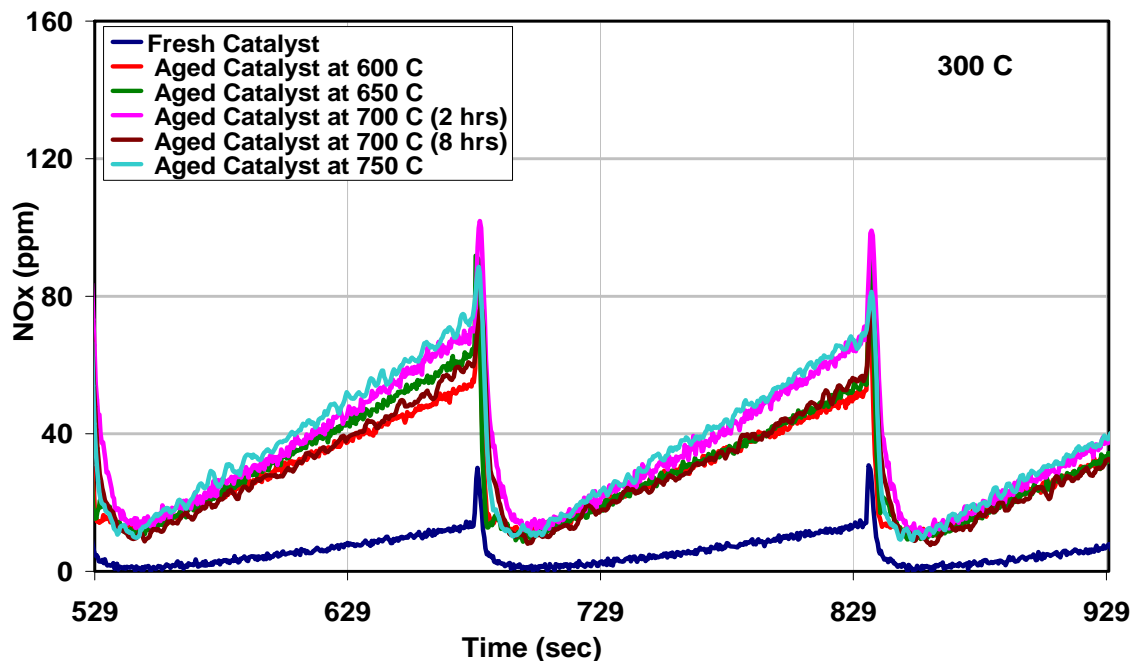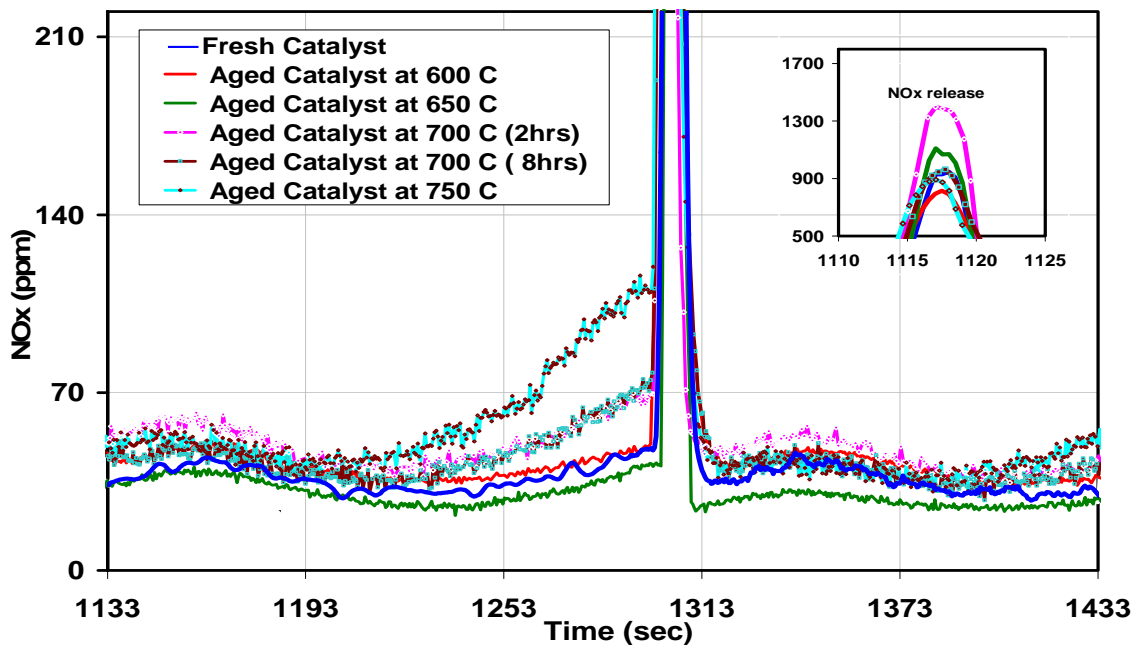

Figure 5-6 NO_X outlet concentrations as a function of thermal degradation obtained when testing the sample at 500°C with 3 % H_2 in the regeneration phase.

The data shown demonstrate an overall negative effect of thermal aging on catalyst performance. This degradation can be attributed to several mechanisms. The first is a loss in precious metal dispersion via sintering and/or pore closure. Upon exposure to high temperature (at least 600°C), sintering of precious metals on TWC and NSR catalysts is considered typical [9], [84]-[86] For example, a change in Pt particle size after aging in air, for 4 hrs in the range of 600 and 900°C has been reported on a Pt/Ba-based catalyst and a Pt/γ-Al$_2$O$_3$ catalyst [62]. The calculated Pt particles sizes the Ba-containing catalyst were 2.6, 21.3, 37.2, and 48.4 nm after aging at 600, 700, 800, and 900°C, respectively. Similar observations were also seen on the Pt/γ-Al$_2$O$_3$ catalyst where the calculated Pt particles sizes are 3.4, 17.1, 26.1, and 39.5 nm after the same aging

temperatures. In this study, the aging temperatures were in the range of 600 and 750°C, therefore, some growth in precious metal particle sizes is expected based on the literature data discussed. The growth in precious metal particle sizes could have a negative effect on NSR activity by limiting oxidation and reduction reactions. Precious metal sintering also leads to a reduction in precious metal to storage component contact surface area, which is thought important in NSR performance[54].

Another possible reason for NSR performance loss with high-temperature exposure is reaction of the storage components with the support or other washcoat components to form mixed oxides, such as $BaAl_2O_4$ and $BaCeO_3$ if Ba, Al_2O_3 and CeO_2 are present. Jang et. al. reported the interaction between Ba and Al to form a Ba-Al solid alloy during aging above 600°C, and subsequently the transformation into stable $BaAl_2O_4$. Casapu et. al. [87] have also reported formation of both $BaAl_2O_4$ and $BaCeO_3$ when Ba/CeO_2 and Ba/Al_2O_3 based NSR catalysts were tested, however, the aging was done above 850°C. Such a transformation would lead to a reduced number of available trapping sites and hence would lower the storage capacity. Still other possibilities include the loss in surface area or dispersion of NO_X and oxygen storage components. This will be discussed in more detail below.

The data above suggest redistribution and/or redispersion of one or more trapping materials when the catalyst was aged at 700°C, resulting in more available trapping sites during subsequent NSR cycling tests. Furthermore, it appears that some of the "activated" trapping materials are more active at low temperatures whereas others are more active at higher temperatures. With the first exposure at 700°C for 2 hours, the trapping materials

81

that are active at low temperatures were redistributed/redispersed. Hence, an improvement in the catalyst performance was observed during low temperature tests. While the trapping materials that are more active at high temperatures, were redistributed/redispersed with the longer exposure, 8 hours, at 700°C.

5.1.2 Effect of thermal degradation on NO_X reduction efficiency with CO

NO_X breakthrough and release profiles for a 60 second trapping and 5 second regeneration cycle using 3% CO as a reductant source at 200ºC are shown in Figure 5-7. The conversions and amounts of NO_X trapped and released for these experiments are also listed in Table 5-1. It is apparent from these data that using CO as a reductant source at 200°C results in poorer overall NSR catalyst performance compared to H_2. With the unaged catalyst, and after steady cycle-to-cycle performance, the calculated conversion was only 15%. The drop in NO_X conversion in comparison with using H_2 as a reductant source under the same conditions is related to both decreased trapping and increased NO_X release. The total inlet NO_X was 0.21 mmole and the amount trapped when H_2 was used as reductant source was 0.181 mmoles while only 0.0624 mmoles were trapped with CO. The amount released, on the other hand, with CO was 0.0314 mmoles whereas 0.0025 mmoles were released with H_2. The drop in NO_X conversion is likely related to precious metal site poisoning by CO at these low operating temperatures[88]. As a result, this will affect the oxidation and reduction steps since both are reliant on precious metal activity. When the catalyst was aged at 600 and 650°C, there was a decrease in trapping performance. The NO_X release during regeneration also decreased, as expected since less was trapped. Thus, no significant change was observed on the overall NO_X conversion.

When the catalyst was further aged at 700°C for $^1/_2$ hour, a similar trend as that with H_2 was observed. The NO_X conversion increased from 15% to 85%. Beyond the first ½ hour of aging, however, no consistent trend was observed. A further drop in catalyst performance was observed with the degradation step at 750°C.
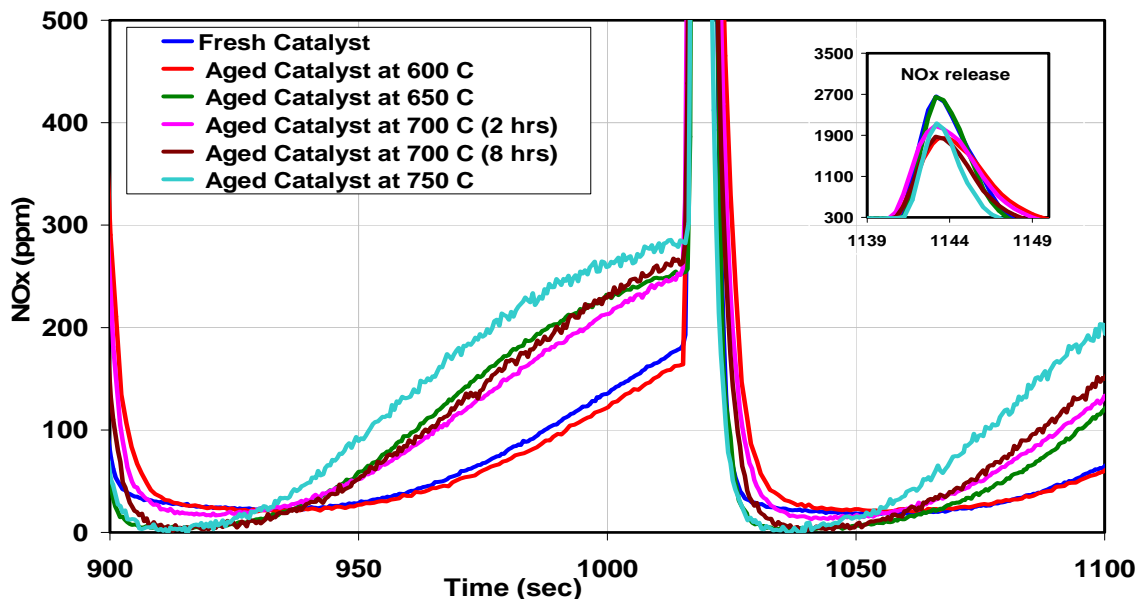

Figure 5-7 NO_X outlet concentrations as a function of thermal degradation obtained when testing the sample at 200°C with 3 % CO in the regeneration phase.

The data obtained at 300°C with CO as the reductant are shown in Figure 5-8. Like the data presented in Figure 5-3, the lean phase was 150 seconds and the regeneration phase was 5 seconds. The conversion and trapped and released amounts are listed in Table 5-1. The NO_X conversion with the fresh catalyst was 96%. It is apparent that there is a significant improvement in the catalyst performance at 300°C versus 200°C. There are several reasons for the improvement in catalyst performance at 300°C versus 200°C

as discussed above, but the most important reason is that the impact of CO poisoning on precious metal activity decreased as the temperature was increased to 300°C.

After the degradation step at 600ºC, there was a drop in catalyst performance, as the NO_X conversion decreased from 96% to 89%. The trapping amount decreased from 0.507 to 0.474 mmoles and the NO_X release slightly increased from 0.002 mmoles to 0.003 mmoles. With further degradation, through 700ºC, no significant change was observed in the catalyst performance. With the degradation step at 750°C, there was another drop in the performance of the catalyst. The NO_X conversion decreased from 88% after the aging at 700ºC to 82% after the aging at 750°C.

Figure 5-8 NO_X outlet concentrations as a function of thermal degradation obtained when testing the sample at 300°C with 3 % CO in the regeneration phase.

Several reasons for the deactivation of the catalyst were discussed above in conjunction with the H_2 data. The trends observed with using CO were similar to those with H_2. There

were differences, such as the overall conversion, especially at 200ºC, as mentioned above. The NO_X released when using CO was always higher than with H_2 for both the unaged and aged catalysts. But, the NO_X release, when CO was used as the reductant source, did decrease after each thermal degradation step.

The data obtained at 400°C when using CO as the reductant source are shown in Figure 5-9. The conditions are otherwise the same as those used for the data shown in Figure 5-4. The conversions and amounts of NO_X trapped and released for these experiments are listed in Table 5-1. It is apparent that both CO and H_2 are comparable as reductants at 400°C. The NO_X slip pattern upon switching from rich to lean at approximately t = 1909 seconds was discussed above in conjunction with H_2 data at 400°C.

With the first two thermal degradation temperatures, 600 and 650°C, there was little if no change observed. However, when the catalyst was aged at 700°C for 2 hours, there was a sharp drop in conversion, decreasing from 86% to 64%. The NO_X release increased from 0.050 to 0.067 mmoles after aging at 650 and 700°C for 2 hours. With further exposure at 700°C, the catalyst performance improved, with the NO_X conversion increasing from 64% to 75%. Such data again suggest redistribution and/or redispersion of trapping materials. A similar trend was observed with the H_2 data. However, there was again a sharp decrease in catalyst performance with degradation at 750°C, where the NO_X conversion decreased to 45%. The reasons for this drop were discussed above.
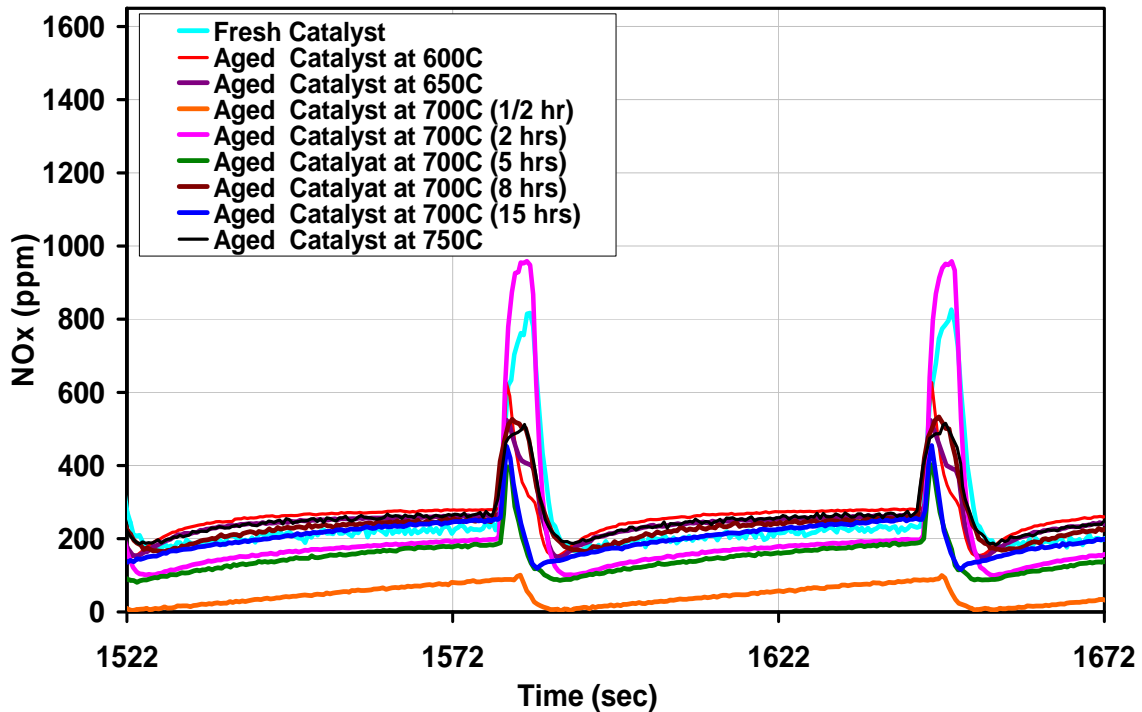
Figure 5-9 NO_X outlet concentrations as a function of thermal degradation obtained
when testing the sample at 400°C with 3 % CO in the regeneration phase.

The outlet NO_X concentration profiles obtained at 500°C are shown in Figure 5-10. For this set of experiments, the trapping and the regeneration times were the same as those used in Figure 5-6. The conversion and trapped and released amounts are again listed in Table 5-1. At this high operating temperature, it is clear that the performance with CO is comparable when H_2 was used in regeneration phase. The calculated NO_X conversion with the unaged catalyst was 53%. With the degradation exposure at 600°C no significant change in conversion was observed. With the degradation at 650°C, the NO_X conversion decreased from 56% to 47%. No significant change was observed with the next thermal degradation step. With the longer exposure at 700°C, the catalyst performance again improved, with the NO_X conversion increasing to 53%. Such an

improvement was also seen with the H_2 reductant data. This consistent trend with both CO and H_2 further supports the idea of a redistribution/redispersion of a trapping material, in this case trapping components with activity at higher temperature. The catalyst performance decreased after the final degradation step at 750°C, for the reasons discussed above.
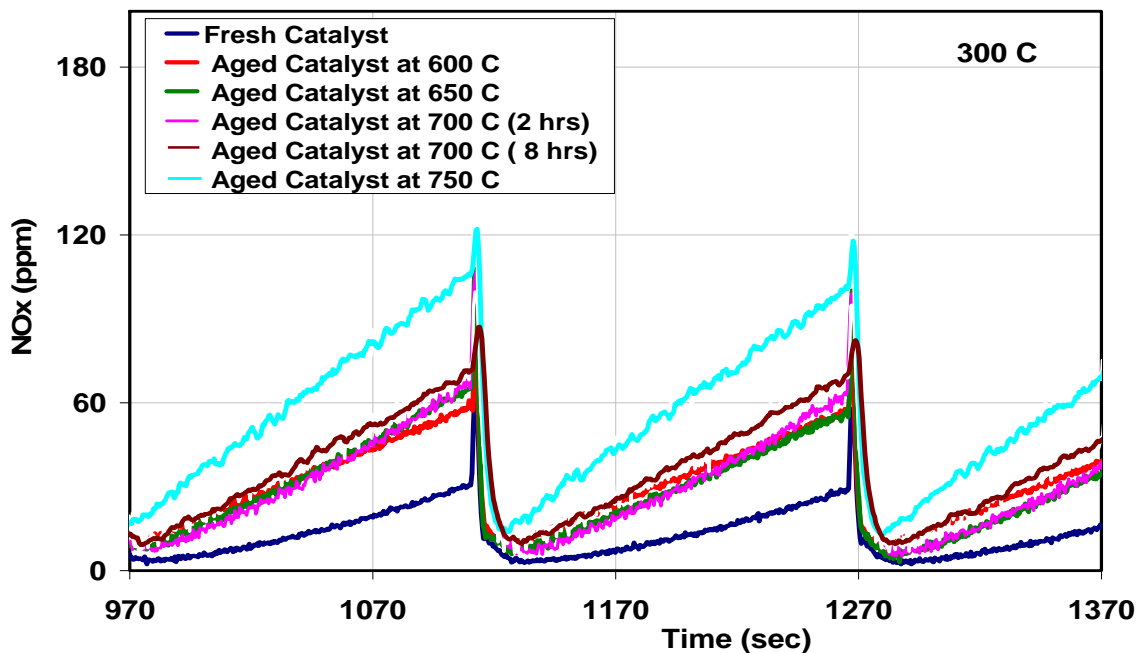

Figure 5-10 NO_X outlet concentrations as a function of thermal degradation obtained when testing the sample at 500°C with 3 % CO in the regeneration phase

5.1.3 Effect of thermal degradation on NO_X reduction efficiency with mixtures of CO and H_2

The outlet NO_X concentrations obtained when using the unaged and aged catalysts while using 1.75% CO and 1.25% H_2 at 200°C are shown in Figure 5-11. The cycling experiment again consisted of a 60 second storage phase and a 5 second regeneration

phase. The calculated conversion of NO_X and the amounts trapped and released are listed in Table 5-1. It is apparent that the CO poisoning effect is still significant and using only H_2 results in better performance at 200°C. For example, with 3% CO and no H_2, the calculated NO_X conversion was 15% while with just 1.75% CO and 1.25% H_2, 36% was attained. The increased performance can be attributed to the decrease in CO poisoning, via simple competition with H_2 present. With the first two degradation exposures, at 600 and 650°C, the NO_X conversion decreased to 12 and 9%, respectively. The decrease in the catalyst performance was mostly observed in the trapping period, since there was little released. With the first exposure at 700°C for $^1/_2$ hr, the NO_X conversion increased from 9% at 650°C degradation step to 63%. The NO_X trapped also increased from 0.043 to 0.139 mmoles. This was coincident with a significant decrease in NO_X release. Subsequently, there was a decrease in the catalyst performance with the two intermediate 700°C degradation times of 2 and 5 hours. However, again after exposure for 8 and 15 hours, the NO_X conversion increased. This trend is inconsistent with the pure H_2 or CO data, but can be explained by the high release coincident with CO and fast reduction by H_2. When the exposure time increased from 5 to 8 hours at 700°C, the NO_X release in conjunction when only CO was used increased from 0.013 to 0.025 mmoles respectively. A similar trend could also occur when using 1.75% CO but the presence of H_2 in the mixture resulted in fast reduction of the released NO_X. As a result, an increase in the catalyst performance was observed. With 15 hours exposure at 700°C, the increased performance was coincident with an increase that was observed with CO data with similar exposure time. The overall trends with either H_2, CO, or mixture of H_2 and CO are overall relatively similar.

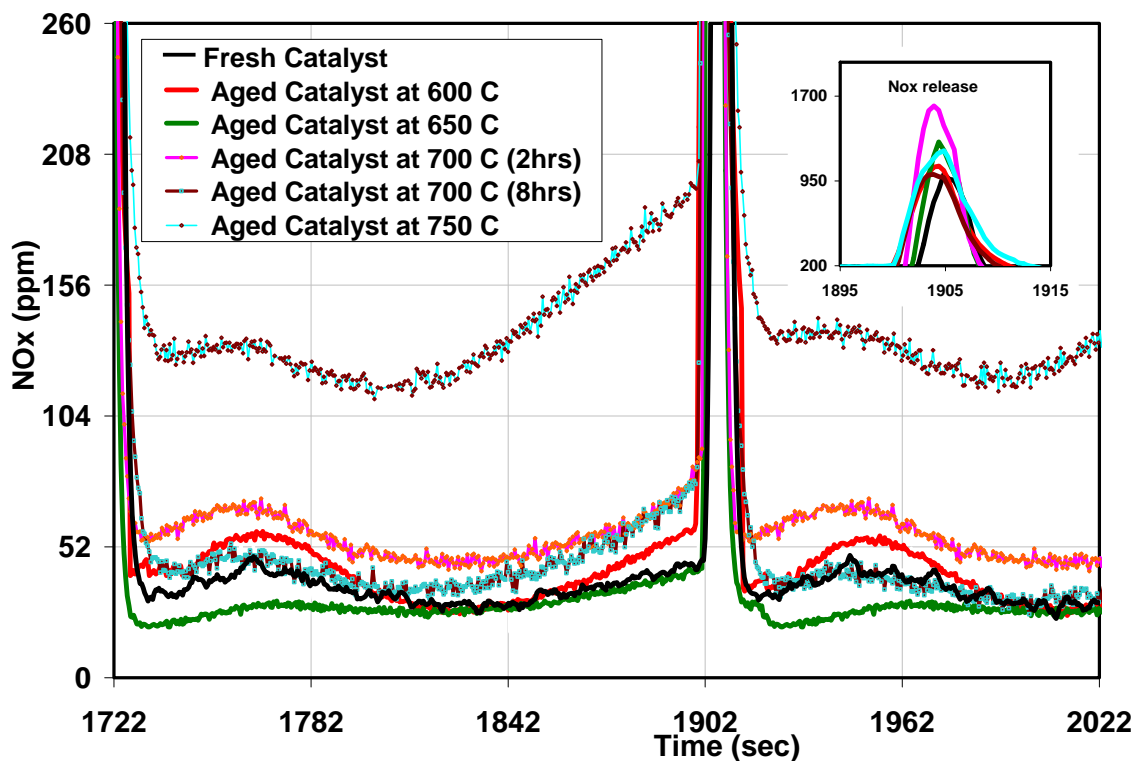**Figure 5-11** NO_X outlet concentrations as a function of thermal degradation obtained when testing the sample at 200°C with mixture of 1.75 % CO and 1.25% H_2 in the regeneration phase

Selected data obtained at 300°C with a mixture of CO and H_2 are shown in Figure 5-12. Like the data presented in Figures 5-3 and 5-8, the lean phase was 150 seconds and the regeneration phase was 5 seconds. The conversion and trapped and released amounts are listed in Table 5-1. With the unaged catalyst the calculated conversion was 97%. The NO_X conversion slightly deceased to 94% after just the first degradation step at 600°C. With higher temperature exposure, little if any change in performance occurred until the last exposure step at 750°C where the conversion decreased to 87%.
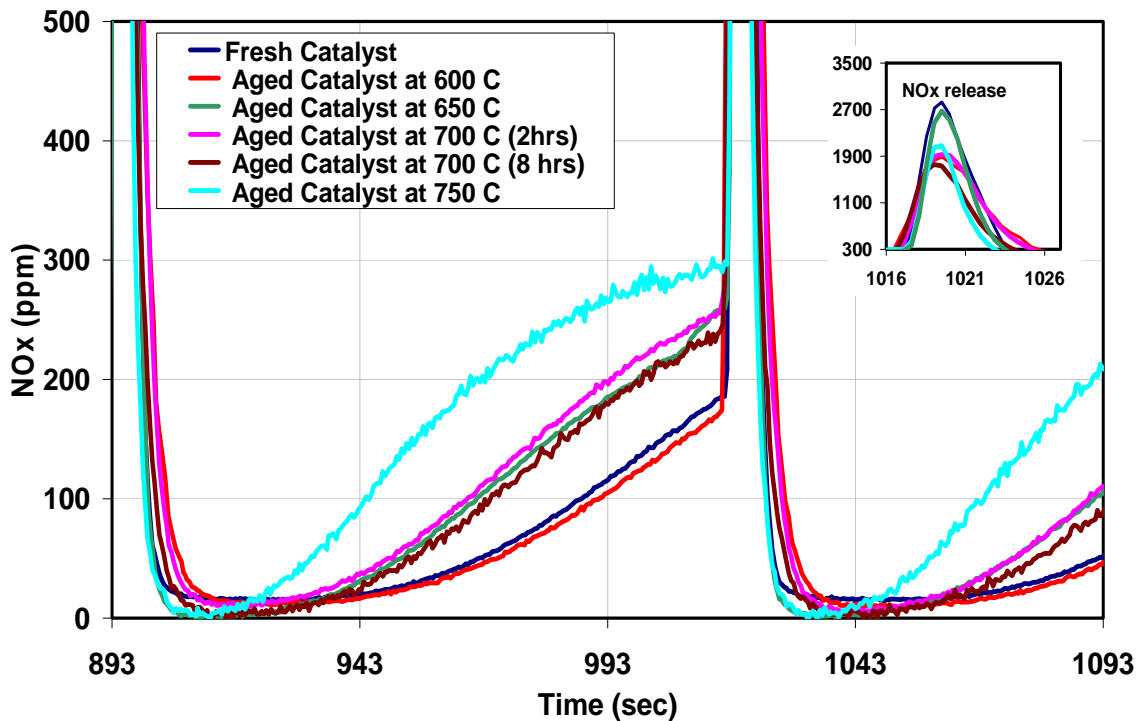
Figure 5-12 NO_X outlet concentrations as a function of thermal degradation obtained when testing the sample at 300°C with mixture of 1.75 % CO and 1.25% H_2 in the regeneration phase

As the aging temperature increased, the NO_X release increased. Interestingly, the amount of NO_X released during the regeneration, when a mixture of CO and H_2 was used, was always lower than that with either H_2 or CO. Overall, the conversions as a function of thermal degradation temperature with using the mixture of CO and H_2 were always higher than with using either H_2 or CO alone. This might be attributed to a larger release with CO but faster reduction with H_2.

The data obtained from the experiments carried out at 400°C using the mixture during regeneration are shown in Figure 5-13. The NO_X conversion performance, trapping and released amounts are also listed in Table 5-1. After exposure to the high temperatures, the observed trends were similar to those with H_2 and CO. But again, with the mixture, the trapping and reduction performance was always better than with either

H$_2$ or CO alone. Again from the data shown in Figure 5-13 and results listed in Table 5-1, there was an improvement in performance after longer exposure time at 700°C. This supports the idea of a redistribution and/or redispersion of trapping materials, in this case those active at high temperatures.
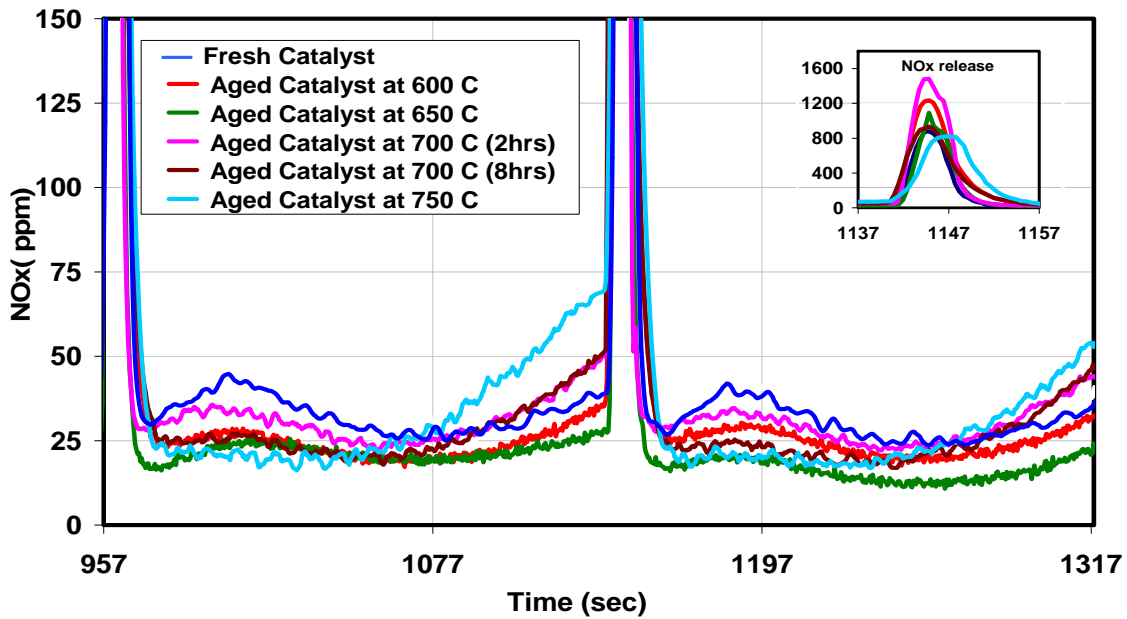
Figure 5-13 NO$_X$ outlet concentrations as a function of thermal degradation obtained
when testing the sample at 400°C with mixture of 1.75 % CO and 1.25% H$_2$
in the regeneration phase

Figure 5-14 compares the NO$_X$ storage and reduction performance as a function of thermal degradation at 500°C using the mixture of 1.75% CO and 1.25% H$_2$ under otherwise the same conditions as described in Figures 5-6 and 5-10. The conversions and amounts of NO$_X$ trapped and released for these experiments are also listed in Table 5-1. Again, the performance with a mixture was better than the performance with either H$_2$ or CO alone. With the degradation step at 600°C, a small change in performance was observed. However, a big drop in the catalyst performance was observed after the

degradation step at 650°C with the NO_X conversion decreasing from 57% to 40%. The NO_X release also increased from 0.070 to 0.086 mmoles. No significant changes were observed with the exposures at 700°C. With the exposure at 750°C, there was another drop in catalyst performance, to 33%.
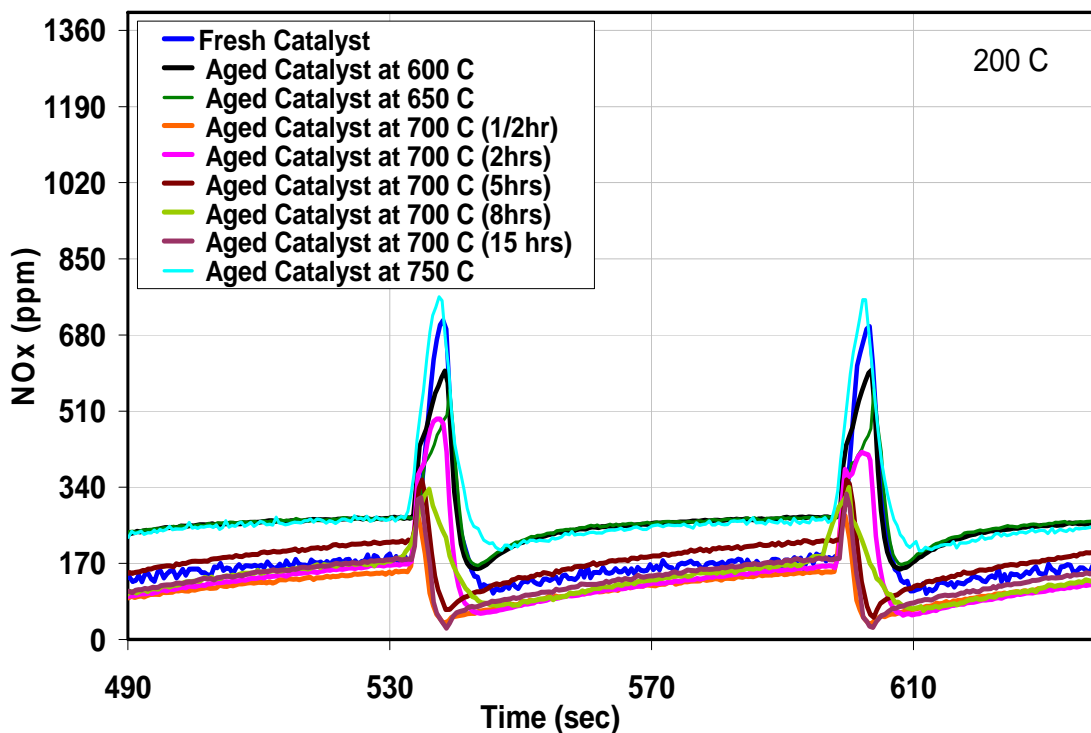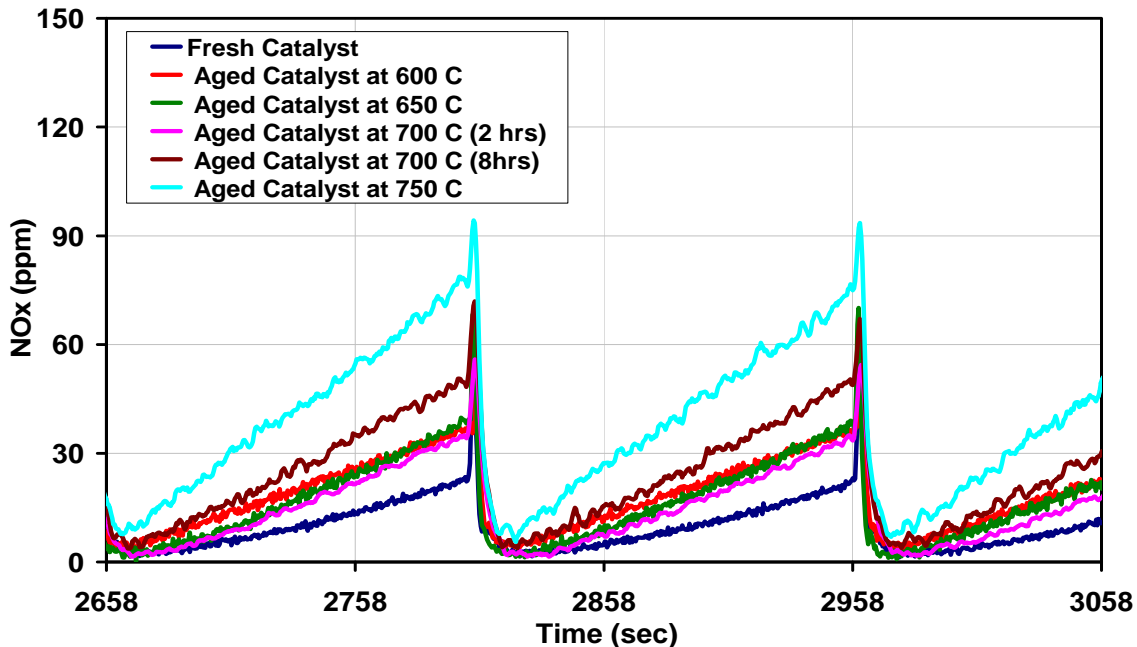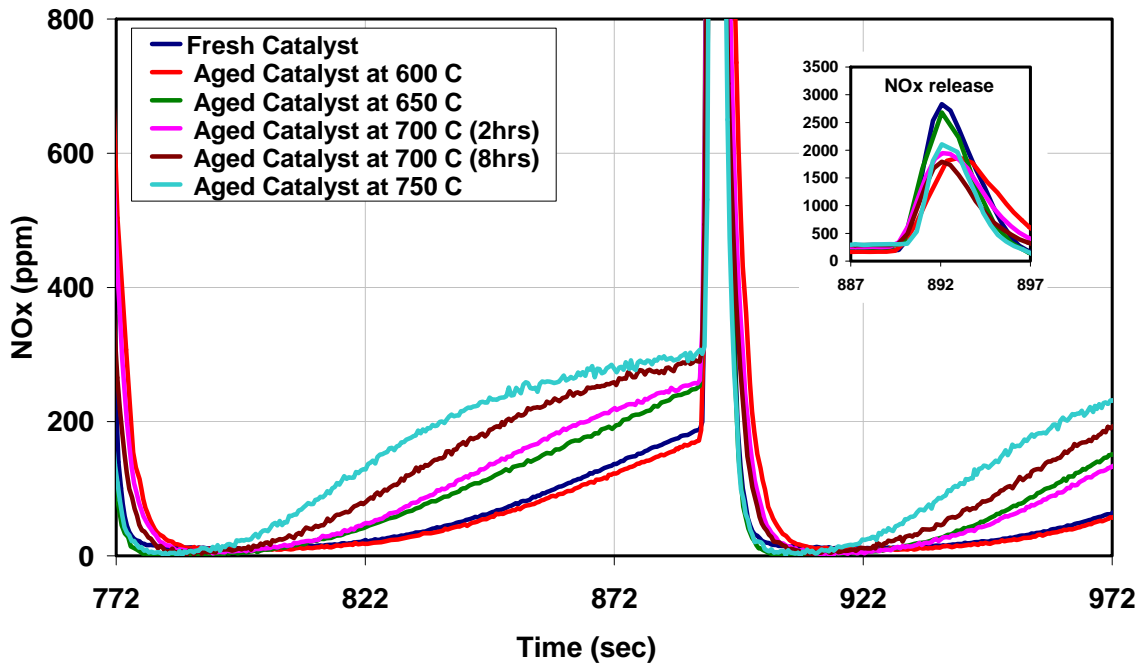

Figure 5-14 NO_X outlet concentrations as a function of thermal degradation obtained when testing the sample at 500°C with mixture of 1.75 % CO and 1.25% H_2 in the regeneration phase.

5.2 Effect of thermal degradation on NO oxidation to NO_2

The objective of this set of experiments was to evaluate NO to NO_2 oxidation as a function of temperature and thermal degradation. These experiments were carried out under the same lean phase conditions as those used in the cycling experiments, and as described in Table 3-1. The temperature was stepped upward in 25°C increments from 150°C to a temperature where equilibrium limitations were observed. This occurred

between 375 and 425°C. The data listed in Table 5-3 were obtained after a steady value of 330 ppm NO + NO_2 was measured at the outlet. It is clear from Table 5-3 that no significant effect was observed with the 600 and 650°C degradation temperatures. After exposing the sample to 700°C for two hours, the conversions across the whole temperature range dropped. This is inconsistent with the trend observed with the cycling data at 200°C. After the first exposure at 700°C there was an increase in NO_X conversion, while a decrease in the NO oxidation across the whole temperature range was observed. It therefore seems that the improved cycling performance is not due to increased NO oxidation. With further exposure at 700°C, the NO oxidation performance increased across the entire range. With the 750°C exposure, low temperature NO oxidation slightly increased but decreased above 275°C.

It is important to point out that Pt particle size has an influence NO oxidation [89]. It has been shown that as Pt particle sizes increase on a Pt/Al_2O_3 and a $Pt/Ba/Al_2O_3$ catalyst, with a coincident decrease in dispersion, the NO oxidation rate increased [90]. Although an increase in NO oxidation was observed with one high temperature treatment, the overall trend discussed in the literature was not observed here. However, the catalyst used in this research is not a model sample, but commercial and likely made differently than that used in literature studies. Overall, NO oxidation decreased as the thermal degradation temperature was increased. But there were no consistent trends with each increase in thermal degradation.

Table 5-3 performance changes as a function of thermal degradation.

Test	Temperature (°C)	Unaged Catalyst	Aged at 600°C	Aged at 650°C	Aged at 700°C (2hrs)	Aged at 700°C (8 hrs)	Aged at 750°C
NO Oxidation (%)	175	4.9	5.5	6.9	3.4	3.9	6.9
	200	7.7	11.4	10.9	5.3	8.1	9.8
	250	24.8	26.3	29.5	12.1	18.3	21.7
	300	47.8	42.7	50.7	24.6	33.4	27.2
	350	58.1	53.2	54.3	44.0	48.1	37.5
	400	50.7	51.5	53.3	48.8	48.4	50.3
OSC (mmoles)	200	0.50	0.17	0.061	0.22	0.091	0.023
	300	0.63	0.32	0.13	0.30	0.27	0.18
	400	0.90	0.55	0.34	0.44	0.45	0.27
	500	1.1	0.74	0.62	0.59	0.70	0.43
WGS (%CO) conversion	200	10	6.3	0.80	4.3	3.5	1.9
	300	62.4	58.4	58.2	45.2	44.3	32.2
	400	90.9	89.0	88.6	89.6	88.7	86.6
	500	81.1	81.3	79.9	80.6	80.4	81.6
NO_X Storage Capacity (mmoles)	200	2.1	2.28	2.0	2.6	2.2	1.7
	350	2.6	2.5	2.3	2.2	2.1	1.9
	500	0.51	0.51	0.51	0.52	0.49	0.32

5.3 Effect of thermal degradation on water-gas-shift reaction (WGS) extent

In this set of experiments, a lean period of 60 seconds and a rich period of 30 seconds were used, with the lean composition containing 10% O_2, 5% CO_2, 5% H_2O and a balance of N_2 and the rich phase containing 1% CO, 5% CO_2, 5% H_2O and a balance of N_2. The cycles were repeated 10 to 15 times to ensure steady performance. The data

shown in Figure 5-15 and results listed in Table 5-3 were obtained and calculated after a steady-state CO and CO_2 value were reached.

Again, the lower thermal degradation temperature steps resulted in negative changes for the low temperature performance. At 200°C, the WGS reaction extent dropped from 10% to near-zero after the 650°C exposure. However, at the higher test temperatures, little change was observed. As a matter of fact, no significant change in the extent of WGS was observed at 400 and 500°C after any of these thermal degradation steps. For 300°C, there is a steady decrease in WGS performance with each increased degradation temperature, dropping from 62.4% for the fresh sample to 32.2% after being aged at 750°C.
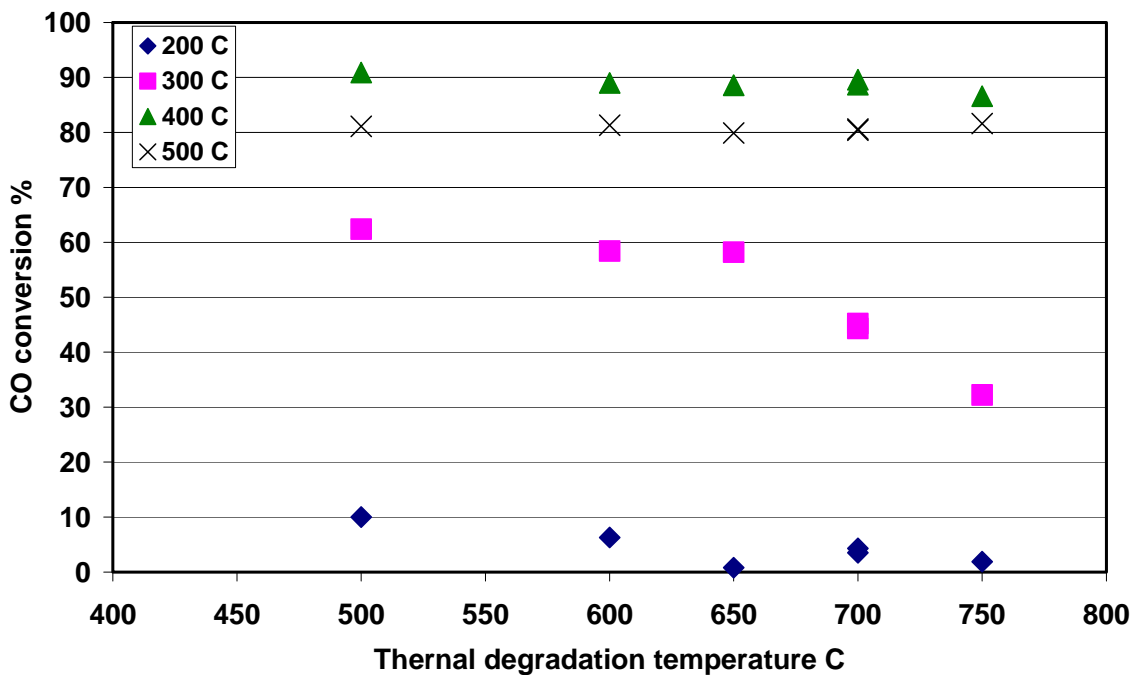
Figure 5-15 CO conversion via the WGS reaction as a function of temperature and thermal degradation

However, at 200°C there appears to be an improvement with the 700°C degradation mode, at least it is not nil. This could be, or is likely, related to the "activation" of ceria or some other OSC related component, as the WGS reaction is definitely promoted by such OSC-type components.

5.4 Effect of thermal degradation on NO_X storage capacity (NSC)

The total NO_X storage capacity was also evaluated as a function of thermal degradation. The experiment consisted of cleaning the sample at 500°C and then reducing the temperature to the target temperature, and exposing the sample to the same conditions as those of the lean phase in the cycling experiments. The lean phase was ended once a steady value of 330 ppm $NO + NO_2$ was measured at the outlet rather than at some set time. The data are listed in Table 5-3 and plotted in Figure 5-16.

As shown there is little change in total capacity when trapping at 500°C until the thermal degradation temperature exceeds 700°C. This is not coincident with the cycling data at 500°C. This inconsistency stems from better earlier trapping rates but constant total available sites. As the catalyst was thermally aged, the rates of trapping decreased, especially when aged between 600 and 650°C, but the total number of active trapping sites remained unchanged.

Operating at 350°C, the trapping capacity decreased with high temperature exposure, and the loss in trapping capacity accelerated as the temperature was increased. At 200°C, the capacity actually increased with the 700°C thermal degradation step. This was earlier attributed to redispersion of some trapping component. With further exposure

at 700 and exposure at 750°C, the capacity decreased, following the cycling performance

trend.
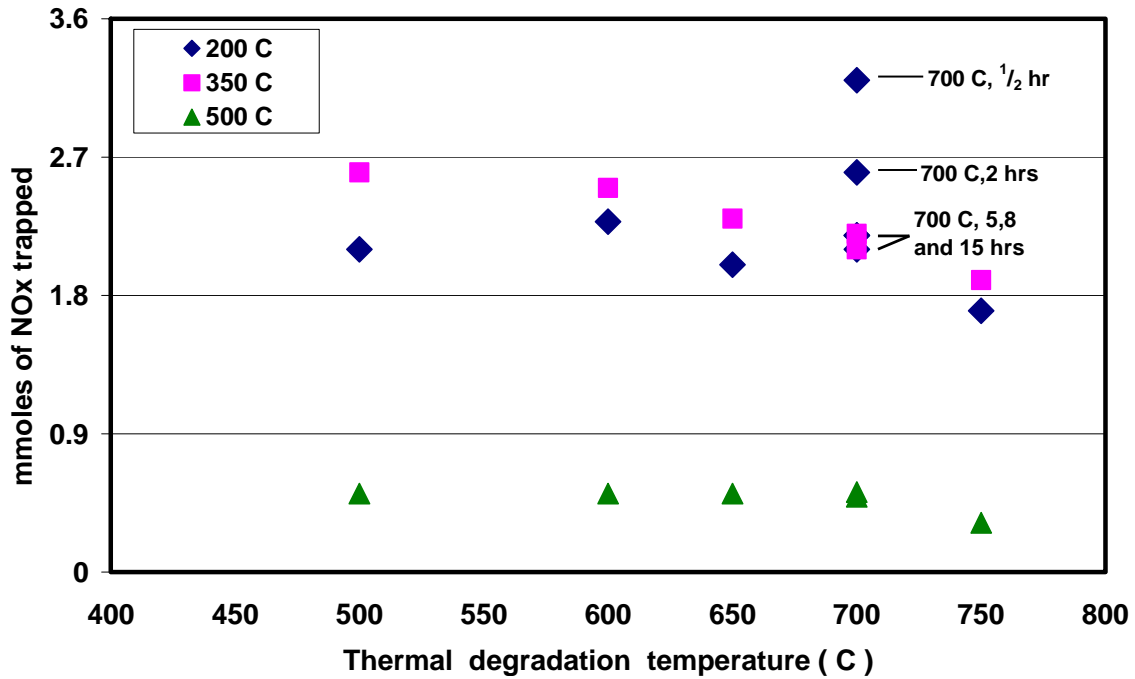
Figure 5-16 Total NO_X storage capacity as a function of temperature and thermal
degradation

There are several reasons that could explain the drop in the NO_X storage capacity

as a function of thermal degradation. One is that there is a reaction between the trapping

components and the washcoat ingredients. A second possibility is the loss of interface

contact between the precious metals and the trapping components because of particle size

growth of both. Furthermore, the drop in NSC could be due to agglomeration of just the

adsorbent material [51].

5.5 Effect of thermal degradation on oxygen storage capacity (OSC)

The OSC of the catalyst was also calculated at different temperatures before and after thermal degradation. The OSC data are shown in Figure 5-17 and also listed in Tables 5-3 and 5-4. In this set of experiments, 10 to 15 cycles were repeated at the 4 standard test temperatures. A lean period of 60 seconds and a rich period of 30 seconds were used, with the lean composition containing 10% O_2, 5% CO_2 and a balance of N_2 and the rich phase containing 1% CO, 5% CO_2 and a balance of N_2. To remove the effect of the water gas shift reaction on the oxygen storage capacity, water was not used in these experiments.
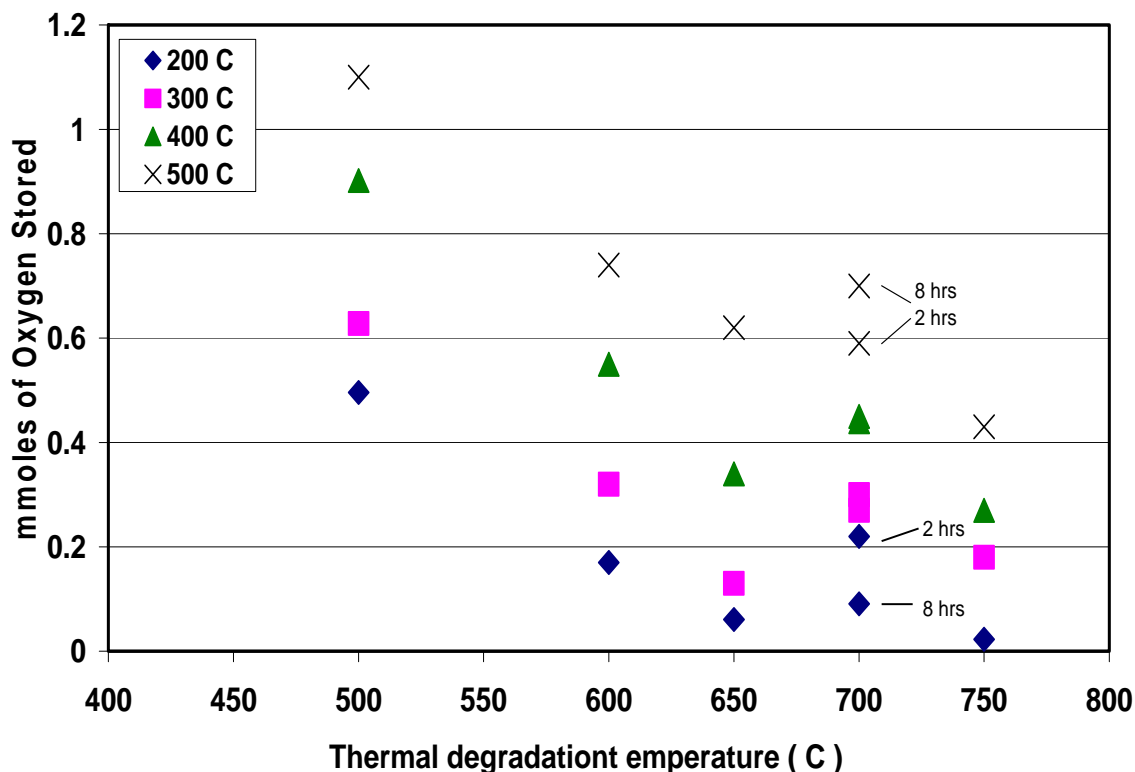
Figure 5-17 Oxygen storage capacity measurements as a function of temperature and thermal degradation

The measured OSC at each temperature consistently decreased with each increase in thermal degradation temperature, except again after the 700°C step. With the shorter exposure at 700°C, the measured OSC increased at 200°C, coincident with the increase in NO_X performance observed during cycling at 200°C. With longer exposure at 700°C, the measured OSC also increased at 400 and 500°C, which also is consistent with improved cycling performance at 400 and 500°C.

These data indicate that an OSC component becomes "activated" with a 700°C treatment, possibly due to redispersion/redistribution. In either case, these data clearly relate back to the improved NO_X performance observed. Ceria for example is a known NO_X storage material at low temperature [91] and if it was to become "activated" then this could explain the 200ºC cycling data. Exposing the sample to higher temperatures or for longer times at 700ºC resulted in decreased OSC.

Table 5-4 Oxygen storage capacities after different aging times at 700°C

Test	Temperature (°C)	½ hr	2hrs	5hrs	8 hrs	15 hrs
OSC (mmoles)	200	0.11	0.22	0.092	0.091	0.098
	300	0.155	0.30	0.29	0.27	0.27
	400	0.34	0.44	0.43	0.45	0.39
	500	0.69	0.59	0.67	0.70	0.45

5.6 Effect of thermal degradation on ammonia formation

Evidence of NH_3 formation as by-product over NSR has been widely reported [79], [80],[92]. It should be pointed out that NH_3 has been labeled as a hydrogen carrier and a reductant participating in the NO_X reduction reaction [75]. Additionally, if the NSR

catalyst is followed by an SCR catalyst [93], the NH_3 produced over the NSR catalyst can used as a reductant source to reduce NO_X to N_2.

The amounts of NH_3 formed during the cycling experiments were calculated as a function of temperature and thermal degradation exposure and listed in Table 5-5. NH_3 was readily observed at the lowest test temperature and increased slightly with thermal degradation. NH_3 release/formation was found to the track the amount of NO_X trapped as a function of thermal degradation at 200°C. Similarly, the amount formed, or observed at the outlet, during 300°C cycling tests also increased with thermal degradation, although there is an apparent discrepancy after the 700°C thermal degradation mode that may be related to the "activation" of a catalyst component as mentioned above.

Table 5-5 Ammonia Formation (mmoles) during the cycling experiments

Temperature (°C)	Reducing Agent $\underline{H_2}$	$\underline{CO}$	Unaged Catalyst	Aged at 600°C	Aged at 650°C	Aged at 700°C (2hrs)	Aged at 700°C (8 hrs)	Aged at 750°C
200	3	0	0.0785	0.0736	0.0736	0.0959	0.100	0.0942
	0	3	0.0016	0	0.0003	0.0057	0.0018	0.0011
	1.25	1.75	0.0194	0.0035	0.0033	0.0525	0.0687	0.0095
300	3	0	0.010	0.0325	0.0442	0.0129	0.0325	0.0670
	0	3	0.011	0.0185	0.0208	0.0112	0.0353	0.0580
	1.25	1.75	0.016	0.0317	0.0196	0.0184	0.0493	0.0727
400	3	0	0.0004	0.0002	0.0012	0.0004	0.0013	0.0024
	0	3	0.0002	0	0.0002	0.0003	0.0005	0
	1.25	1.75	0.0003	0.0001	0.0014	0.0003	0.0001	0.0030
500	3	0	0.0003	0.0006	0.0014	0.0007	0.0015	0.0031
	0	3	0.0004	0.0010	0.0017	0.0012	0.0025	0.0040
	1.25	1.75	0.0008	0.0006	0.0020	0.0017	0.0020	0.0059

At 400ºC, during most tests the NH_3 release was again found to track the NO_X trapped, before and after aging. And again, there is a break in the trend after the 700°C aging, which could be explained by the "activation" of an OSC catalyst component. Crocker and coworkers [94] have observed that the amount of OSC significantly affects NH_3 formation. Overall, with thermal degradation, more NH_3 is formed at the lower operating temperatures and NH_3 release was consistent with NO_X trapped during cycling data.

Chapter 6   Conclusions

This research project had two main objectives:

1. Evaluating the effect of amount and ratio of H_2 and CO reductants on the trapping and reduction performance of a commercial NSR catalyst.

2. Investigating the effect of thermal degradation on the performance of a commercial NSR catalyst.

Overall, the performance of the catalyst improved with each increase in regeneration-phase H_2 concentration. With CO, the same was true, except at 200°C where increasing the CO concentration beyond 1.5% resulted in decreased catalyst performance, which was attributed to CO poisoning of precious metal sites. With mixtures of CO and H_2 at 200°C, the CO poisoning effect outweighed the positive effect of H_2 use. At 300°C, the calculated conversions using either reductant or the mixtures were comparable, with H_2 resulting in slightly improved performance. At 400°C, overall performance was again comparable, but best with the mixtures of reductants, rather than with just H_2. Similar trends were observed at 500°C. NH_3 in the outlet was observed at all temperatures, but increased with decreasing temperature. At 200°C, the amount formed was proportional to the amount of H_2 in the inlet, while at 300 and 500°C, mixtures of CO and H_2 resulted in more NH_3 observed than with just H_2, although the amount of total reductant was maintained.

The performance of the catalyst was also characterized before and after several high-temperature treatments. The characterization included "standard" storage and reduction cycling experiments conducted between 200 and 500°C, evaluating H_2 versus CO and mixtures of H_2 and CO as the reductant source, NO_X storage capacity measurements, oxygen storage capacity measurements, water-gas-shift and NO oxidation reaction extents. For the cycling experiments, there was a steady drop in NO_X conversion after each thermal degradation temperature; except when catalyst was heated at 700°C, where there was an increase in NO_X conversion. For the NO_X storage capacity at 350 and 500°C, a steady drop was observed with each thermal degradation step. There were also decreases in NO_X storage capacity at 200°C after aging at 600 and 650°C, but aging at 700°C resulted in an increase in capacity. There wasn't any significant change in the extent of the water-gas-shift reaction with thermal degradation at high test temperatures whereas a decrease was observed at low temperature. There was a gradual decrease in oxygen storage capacity at test temperatures between 200 and 500°C with each increase in thermal degradation temperature, except again when the sample was degraded at 700°C, where a significant increase was observed. These data indicate that there was redispersion of a trapping material component during the 700°C thermal degradation treatment while the oxygen storage capacity data indicate redispersion of oxygen storage components, therefore we conclude that it is these oxygen storage components that are becoming ''activated'' as trapping materials at low temperature.

Chapter 7: Recommendations

The purpose of this thesis was to evaluate the effect of regeneration mixture properties and thermal aging on the performance of a NSR catalyst. However, there are still some questions that need to be answered. The following are some recommended future opportunities:

- The NO_X source in this study was NO. What would occur if NO_2 was the NO_X source? How would the regeneration characteristics differ with NO_2 used as the NO_X source?

- Similarly, what would be the effect of an upstream oxidation catalyst on the overall NO_X reduction to N_2?

- Would the NH_3 formed be sufficient to feed a downstream SCR catalyst?

- The regeneration mixture used in this study includes CO and H_2. What would be the effect of adding hydrocarbon to the mixture? Would it affect NO_X release and reduction?

- The aging procedures used air and 2% H_2O. What would occur if the gas mixture was more representative?

- This study suggests redispersion/redistribution of OSC components. However, at the present time there is no trusted method to measure the dispersion of trapping components, OSC components and precious metals on these commercial samples.

What is a suitable physical technique that can measure and investigate this redispersion/redistribution?

REFERENCES

[1] Environmental Protection Agency (EPA), http://www.epa.gov/climatechange/scie nce/ recentac.html#ref.

[2] Environmental Protection Agency, http://www.epa.gov/airtrends/sixpoll.html.

[3] C. David Cooper and F.C. Alley. Air Pollution Control: A Design Approach, 3rd Edition, Waveland Press, Prospect Heights, IL, 2002, pp 459.

[4] CleanAIR Systems United States Inc, http://www.cleanairsys.com/airzone-blog/labels/smog-forming%20pollutants.html. ''Feb 22''.

[5] **S**. Hodjati, C. Petit,V. Pitchon, and A. Kiennemann. NO_X sorption–desorption study: application to diesel and lean-burn exhaust gas (selective NO_X recirculation technique). Catalysis Today 59(2000) 323-334.

[6] Chan-Soon Kang , Young-Jae You , Ki-Joong Kim , Tae-hee Kim , Seong- Jun Ahn , Kyong-Hwan Chung , Nam-Cook Park , Shoichi Kimura , Ho- Geun Ahn. Selective catalytic reduction of NO_X with propene over double wash- coat monolith catalysts. Catalysis Today 111(2006) 229-235.

[7] M.A Gómez-García, V. Pitchon, and A. Kiennemann. Pollution by nitrogen oxides: an approach to NO_X abatement by using sorbing catalytic materials. Environmental International, 31(2005)445-467.

[8] Miroslav Radojevic. Reduction of nitrogen oxides in flue gases. Environmental Pollution 102(1998)685-689.

[9] William S. Epling, Larry E. Campbell, Aleksey Yezerets, Neal W.Currier, and James E. Parks II. Overview of the fundamental reactions and degredation mechanisms of NO_X storage/ reduction catalyst. Catalysis Review 46(2004) 163.

[10] C. K. Narula, S. R. Nakouzi, and R. Wu, Jr. C.T. Goralski, Jr., L.F. Allard, Jr. .Evaluation of Sol-Gel Processed BaO.nAl$_2$O$_3$Materials as NO$_X$ Traps. AIChE Journal 47 (2001) 744.

[11] Farrauto R.J., Bartholomew C.H. Fundamentals of Industrial Catalytic, 1st edition, Blackie Academic & Professional: New York, NY, 1997.

[12] Joseph R. Theis, John J. Li, Justin A. Ura and Ronald G. Hurley. The Desulfation Characteristics of Lean NOx Traps. SAE Technical Paper Series 2002-01-0733.

[13] G. W. Graham, H.-W. Jen, O. Ezekoye, R. J. Kudla, W. Chun,a X. Q. Pan, and R. W. McCabe. Effect of alloy composition on dispersion stability and catalytic activity for NO oxidation over alumina-supported Pt–Pd catalysts. Catalysis Letters 116(2007)1-8.

[14] N. Fekete, R. Kemmler, D. Voigtlander, B. Krutzsch, E. Zimmer, G. Wenninger, W. Strehlau, J.A.A. van den Tillaart, J. Leyrer, E.S. Lox and W. Muller. Evaluation of NO$_X$ storage catalysts for lean burn gasoline fueled passenger cars. SAE Technical Paper Series 970746.

[15] G. Ranga Rao, P. Fornasiero, R. Di Monte, J. Ka špar, G. Vlaic, G. Balducci, S. Meriani, G. Gubitosa, A. Cremona, and M. Grazianiy. Reduction of NO over Partially Reduced Metal-Loaded CeO2–ZrO2 Solid Solutions. Journal of catalysis 162 (1996) 1–9.

[16] Sophie Salasc, Magnus Skoglundh and Erik Fridell. A comparison between Pt and   Pd in NO$_X$ storage catalysts. Applied Catalysis B: Environmental 36(2002)145-160.

[17] Hirofumi Ohtsuka and Takeshi Tabata. Roles of palladium and platinum in the selective catalytic reduction of nitrogen oxides by methane on palladium–

platinum-loaded sulfated zirconia. Applied Catalysis B: Environmental 29(2001) 177-183.

[18] Louise Olesson, Hans persson, Erik Fridell, Magnus Skoglundh, and Bengt Andersson. A Kinetic Study of NO Oxidation and NO_X storage on Pt/Al_2O_3 and $Pt/BaO/Al_2O_3$. Journal of physical chemistry B 105(2001)6895-6906.

[19] Rodriquez, F., Juste ,L., Potvin, C., Tempere, JF., Blanchard, G.,and Djegamariadassou,G. NO_X storage on barium-containing three-way catalyst in the presence of CO2.Catalysis Letter 72 (2001)59.

[20] S.Hodjati, K. Vaezzadeh, C. Petit, V. Pitchon, and A. Kiennemann. Absorption/ desorption of NO_X process on perovskites: performances to remove NO_X from a lean exhaust gas. Applied Catalysis B: Environmental 26(2000)5-16

[21] S. Hodjati, P. Bernhardt, C. Petit, V. Pitchon, and A. Kiennemann. Removal of NO_X Part I. Sorption/desorption processes on barium aluminate. Applied Catalysis B: Environmental 19(1998) 209-219.

[22] Liotta, L., Macaluso, A., Arena, G., Livi, M., Centi, G., Deganello, G. A study of the behaviour of Pt supported on CeO2–ZrO2/Al2O3–BaO as NO_X storage– reduction catalyst for the treatment of lean burn engine emissions. Catalysis Today 75(2002) 439-449.

[23] Westerberg B., Fridell E. A transient FTIR study of species formed during NO_X storage in the Pt/BaO/Al2O3 system. Journal of Molecular Catalysis A: Chemical, 165 (2001) 249-263.

[24] Mahzoul H., Brilhac J.F., Gilot P. Experimental and mechanistic study of NO_X adsorption over NO_X trap catalysts Applied Catalysis B: Environmental 20(1999) 47-55.

[25] Todd J. Toops, D. Barton Smith, William S. Epling, Jim E. Parks, William P. Partridge. Quantified NO_X adsorption on Pt/K/gamma-Al_2O_3 and the effects of CO_2 and H_2O. Applied Catalysis B: Environmental 58(2005)255–264.

[26] Fridell Erik, Skoglundh Magnus, Westerberg Björn, Johansson Stefan, Smedler Gudmund. NO_X Storage in Barium-Containing Catalysts. Journal of catalysis 183(1999) 196-209.

[27] Cant, Noel W., Patterson Michael J. The storage of nitrogen oxides on alumina-supported barium oxide. Catalysis Today 73(2002) 271-278.

[28] Prinetto F., Ghiotti G.,Nova I., Lietti L., Tronconi E., Forzatti P. FT-IR and TPD Investigation of the NO_X Storage Properties of BaO/Al_2O_3 and Pt−BaO/Al_2O_3 Catalysts. Journal of Physical Chemistry B. 105(2001) 12732-12745.

[29] Yuejin Li , Stan Roth, Joe Dettling and Tilman Beutel. Effects of lean/rich timing and nature of reductant on the performance of a NOx trap catalyst. Topics in Catalysis. 16/17(2001) 139.

[30] Botas Juan A., Gutiérrez-Ortiz Miguel A., González-Marcos, and M. Pilar. Kinetic considerations of three-way catalysis in automobile exhaust converters. Applied Catalysis B: Environmental 32 (2001)243-256.

[31] L. Limousy , H. Mahzoul , J.F. Brilhac , F. Garin , G. Maire , and P. Gilot. A study of the regeneration of fresh and aged SOx adsorbers under reducing conditions. Applied Catalysis B: Environmental 45 (2003) 169–179.

[32] T. Szailer, J.H. Kwak, D.H. Kim, J.C. Hanson, C.H.F. Peden and J. Szanyi. Reduction of stored NO_X on Pt/Al_2O_3 and Pt/BaO/Al_2O_3 catalysts with H_2 and CO. Journal of Catalysis 239(2006)51.

[33] Amberntsson Annika, Persson Hans, Engström Per, Kasemo Bengt. NO_X release from a noble metal/BaO catalyst: dependence on gas composition. Applied Catalysis B: Environmental 31(2001)27-38.

[34] Liu Zhaoqiong and Anderson James A. Influence of reductant on the thermal stability of stored NO_X in Pt/Ba/Al2O3 NO_X storage and reduction traps. Journal of Catalysis 224(2004)18-27.

[35] Epling William S, Campbell Greg C, Parks James E. The effects of CO_2 and H_2O on the NO_X destruction performance of a model NO_X storage/reduction catalyst. Catalysis Letters 90(2003)45-56.

[36] Isabella Nova, Lidia Castoldi, Luca Lietti, Enrico Tronconi, and Pio Forzatti. On the dynamic behavior of "NO_X -storage/reduction" Pt–Ba/Al2O3 catalyst. Catalysis Today 75(2002)431–437.

[37] David James, Elodie Fourré , Masaru Ishii , and Michael Bowker. Catalytic decomposition/regeneration of Pt/Ba(NO$_3$)$_2$ catalysts: NO_X storage and reduction. Applied Catalysis B: Environmental 45(2003)147–159.

[38] Louise Olsson, Erik Fridell, Magnus Skoglundh ,and Bengt Andersson, Mean field modelling of NOx storage on Pt/BaO/Al2O3. Catalysis Today 73(2002)263–270.

[39] H. Abdulhamid, E. Fridell, and M. Skoglundh, The reduction phase in NOx storage catalysis: Effect of type of precious metal and reducing agent. Applied Catalysis B: Environmental 62 (2006)319-328.

[40] Li Yuejin, Roth Stan, Dettling, Joe Beutel, and Tilman. Effects of Lean/Rich Timing and Nature of Reductant on the Performance of a NOx Trap Catalyst. Topics in Catalysis 16/17(2001)139-144.

[41] Mahzoul H., Gilot, P., Brilhac J.-F., and Stanmore B.R. Reduction of NOx over a NOx-Trap Catalyst and the Regeneration Behaviour of Adsorbed SO2. Topics in Catalysis 16(2001) 293-298.

[42] Bailey O., Dou D., and Denison G. Regeneration strategies for NOx adsorber catalysts. SAE Technical Paper Series 972845.

[43] Annika Amberntsson, Magnus Skoglundh, Martin Jonsson, and Erik Fridell. Investigations of sulphur deactivation of NOx storage catalysts: influence of sulphur carrier and exposure conditions. Catalysis Today 73 (2002) 279–286.

[44] Annika Amberntsson,Magnus Skoglundh, Sten Ljungström, and Erik Fridell. Sulfur deactivation of NOx storage catalysts: influence of exposure conditions and noble metal. Journal of Catalysis 217 (2003) 253–263

[45] Annika Amberntsson, Erik Fridell, and Magnus Skoglundh. Influence of platinum and rhodium composition on the NOx storage and sulphur tolerance of a barium based NOx storage catalyst. Applied Catalysis B: Environmental 46 (2003) 429–439.

[46] Erik Fridell, Hans Persson, Louise Olsson, BjörnWesterberg, Annika Amberntsson, and Magnus Skoglundh. Model studies of NOx storage and sulphur deactivation of NOx storage catalysts. Topics in Catalysi.16/17(2001)1-4.

[47] Fatima Maria Zanon Zotin, Ota´vio da Fonseca Martins Gomes, Cristiano Hono´rio de Oliveira, Arnaldo Alcover Neto, Mauri Jose´ Baldini Cardoso. Automotive catalyst deactivation: Case studies. Catalysis Today 107–108 (2005) 157–167.

[48] F. Rohr, S.D. Peter, E. Lox, M. Ko¨gel, A. Sassi, L. Juste, C. Rigaudeau, G. Belot, P. Ge´lin,and M. Primet. On the mechanism of sulphur poisoning and regeneration of a commercial gasoline NOx-storage catalyst. Applied Catalysis B: Environmental 56 (2005) 201–212.

[49] Zhaoqiong Liu and James A. Anderson. Influence of reductant on the regeneration of SO2-poisoned Pt/Ba/Al2O3 NOx storage and reduction catalyst. Journal of Catalysis 228 (2004) 243–253.

[50] S. Elbouazzaoui, E.C. Corbos, X. Courtois, P. Marecot, D. Duprez. A study of the deactivation by sulfur and regeneration of a model NSR Pt/Ba/Al2O3 catalyst. Applied Catalysis B: Environmental 61 (2005) 236–243.

[51] Todd J. Toops, Bruce G. Bunting, Ke Nguyen, Ajit Gopinath. Effect of engine-based thermal aging on surface morphology and performance of Lean NOx Traps. Catalysis Today 123 (2007) 285–292.

[52] Ch. Sedlmair, K. Seshan, A. Jentys, and J.A. Lercher. Studies on the deactivation of NOx storage-reduction catalysts by sulfur dioxide. Catalysis Today 75 (2002) 413–419.

[53] Erik Fridell, Annika Amberntsson, Louise Olsson, Ann W. Grant, and Magnus Skoglundh. Platinum oxidation and sulphur deactivation in NOx storage catalysts. Topics in Catalysis 30/31 (2004)143.

[54] N. Takahashi, H. Shinjoh, T. Iijima, T. Suzuki, K. Yamazaki, K. Yokota, H. Suzuki, N. Miyoshi, S. Matsumoto, T. Tanizawa, T. Tanaka, S. Tateishi, and K. Hasahara. The new concept 3-way catalyst for automotive lean-burn engine: NOx storage and reduction catalyst. Catalysis Today 27(1996)63.

[55] J. Li, J. Theis, W. Chun, C. Goralski, R. Kudla, J. Ura, W. Watkins, M. Chattha and R. Hurley. Sulfur Poisoning and Desulfation of the Lean NOx Trap. SAE Technical Paper Series 2001-01-2503.

[56] P. Engström, A. Amberntsson, M. Skoglundh, E. Fridell, and G. Smedler. Sulphur dioxide interaction with NOx storage catalysts. Applied Catalysis B: Environmental 22 (1999) 241–248.

[57] K. Taylor.Nitric Oxide Catalysis in Automotive Exhaust Systems. Catalysis Reviews Science and Engineering 35 (1993) 457.

[58] G.W. Graham, H.-W. Jen, W. Chun, H.P. Sun, X.Q. Pan, and R.W. McCabe. Coarsening of Pt particles in a model NOx trap. Catalysis Letters 93 (2004)129.

[59] Joseph R. Theis, Justin A. Ura, George W. Graham, Hung-Wen Jen, John J. Li, William L. Waktins, and Christian T. Goralski Jr. The Effects of Aging Temperature and Air-Fuel Ratio on the NOx Storage Capacity of a Lean NOx Trap. SAE Technical Paper Series 2004-01-1493.

[60] Danan Dou and Owen H. Bailey. Investigation of NOx Adsorber Catalyst Deactivation. SAE Technical Paper Series 982594.

[61] Emrah Ozensoy, Charles H.F. Peden, and János Szanyi. Model NOx storage systems: Storage capacity and thermal aging of BaO/θ-Al2O3/NiAl(100). Journal of Catalysis 243 (2006) 149–157.

[62] Chaitanya K. Narula, Melanie J. Moses and Lawrence F. Allard. Analysis of Microstructural Changes in Lean NOx Trap Materials Isolates Parameters Responsible for Activity Deterioration. SAE Technical Paper Series 2006-01-3420.

[63] Bo-Hyuk Jang, Tae-Hun Yeon, Hyun-Sik Han, Yong-Ki Park and Jae-Eui Yie. Deterioration mode of barium-containing NOx storage catalyst. Catalysis Letters 77(2001) 21.

[64] Ke Nguyen,Hakyong Kim, Bruce G. Bunting,Todd J. Toops, Cheon S. Yoon. Rapid Aging of Diesel Lean NOX Traps by High-Temperature Thermal Cycling. SAE Technical Paper Series 2007-01-0470.

[65] Tama´s Szailer, Ja Hun Kwak, Do Heui Kim, Ja´nos Szanyi, Chongmin Wang, Charles H.F. Peden. Effects of Ba loading and calcination temperature on

BaAl$_2$O$_4$ formation for BaO/Al2O3 NOx storage and reduction catalysts. Catalysis Today 114 (2006) 86–93.

[66] Calvin H. Bartholomew. Sintering kinetics of supported metals: New perspectives from a unifying GPLE treatment. Applied Catalysis A: General, 107 (1993) 1-57.

[67] Yaying Ji, Todd J. Toops, and Mark Crocker. Effect of Ceria on the Storage and Regeneration Behavior of a Model Lean NOx Trap Catalyst. Catal Lett 119 (2007)257–264.

[68] J. Z. Shyu, W. H. Weber, and H. S. Gandhi. Surface Characterization of Alumina-Supported Ceria. The Journal of Physical Chemistry 92(1988) 4965.

[69] J. Szanyi, J.H. Kwak, D.H. Kim, S.D. Burton and C.H.F. Peden. NO2 adsorption on BaO/Al$_2$O$_3$: the nature of nitrate species. Journal of Physical Chemistry B 109(2005)27.

[70] J.M. Coronado and J.A. Anderson. FTIR study of the interaction of NO and propene with Pt/BaCl2 rSiO2. Journal of Molecular Catalysis A: Chemical 138(1999)83.

[71] William S. Epling, Aleksey Yezerets, and Neal W. Currier. The effect of exothermic reactions during regeneration on the NO$_X$ trapping efficiency of a NO$_X$ storage/reduction catalyst. Catalysis Letters 110(2006) 143.

[72] W. Bögner , M. k-timer , B. Krutzsch , S. Pischinger , D. Voigtlgnder, G. Wenninger, F. Wirbeleita, M.S. Brogan, R.J. Brisley, D.E. Webster. Removal of nitrogen oxides from the exhaust of a lean-tune gasoline engine. Applied Catalysis B: Environmental 7 (1995) 153-171.

[73] Louise Olsson, Björn Westerberg, Hans Persson, Erik Fridell, Magnus Skoglundh, and Bengt Andersson. A Kinetic Study of Oxygen

Adsorption/Desorption and NO Oxidation over Pt/Al2O3 Catalysts. Journal of Physical Chemistry B 103(1999) 10433-10439.

[74] J.A. Pihl, J.E. Parks II, C.S. Daw and T.W. Root. Product Selectivity During Regeneration of Lean NOx Trap Catalysts. SAE Technical Paper Series 2006-01-3441.

[75] L. Cumaranatunge, S.S. Mulla, A. Yezerets, N.W. Currier, W.N. Delgass, F.H. Ribeiro, Ammonia is a hydrogen carrier in the regeneration of Pt/BaO/Al2O3 NOx traps with H_2. Journal of Catalysis 246 (2007) 29–34

[76] A. Lindholm, N.W. Currier, E. Fridell, A. Yezerets and L. Olsson. NOx storage and reduction over Pt based catalysts with hydrogen as the reducing agent Influence of H_2O and CO2. Applied Catalysis B: Environmental 75(2007)78.

[77] Jae-Soon Choi *, William P. Partridge, and C. Stuart Daw. Spatially resolved in situ measurements of transient species breakthrough during cyclic, low-temperature regeneration of a monolithic Pt/K/Al2O3 NOx storage-reduction catalyst. Applied Catalysis A: General 293 (2005) 24–40.

[78] L. Castoldi, I. Nova, L. Lietti, and P. Forzatti. Study of the effect of Ba loading for catalytic activity of Pt–Ba/Al2O3 model catalysts. Catalysis Today 96 (2004) 43–52.

[79] T. Lesage, C. Verrier, P. Bazin, J. Saussey, S. Malo, C. Hedouin, G. Blanchard, and M. Daturi. Comparison between a Pt–Rh/Ba/Al2O3 and a newly formulated NO_X-trap catalysts under alternate lean–rich flows. Topics in Catalysis 30/31 (2004) 31.

[80] T. Lesage, C. Verrier, P. Bazin, J. Saussey, and M. Daturi. Studying the NOx-trap mechanism over a Pt-Rh/Ba/Al2O3 catalyst by operando FT-IR spectroscopy. Physical Chemistry Chemical Physics 5(2003)4435.

[81] N. Macleod and R.M. Lambert. In situ ammonia generation as a strategy for catalytic NOx reduction under oxygen rich conditions. Chem. Communications (2003).

[82] H. Abdulhamid, E. Fridell and M. Skoglundh. Influence of the type of reducing agent (H2, CO, C_3H_6 and C_3H_8) on the reduction of stored NO_X in a Pt/BaO/Al$_2$O$_3$ model catalyst. Topics in Catalysis 30/31(2004)161.

[83] Jae-Soon Choi, William P. Partridge, William S. Epling, Neal W. Currier, Thomas M. Yonushonis. Intra-channel evolution of carbon monoxide and its implication on the regeneration of a monolithic Pt/K/Al$_2$O$_3$ NOx storage-reduction catalyst. Catalysis Today 114 (2006) 102–111.

[84] Ahmad Kalantar Neyestanaki, Fredrik Klingstedt, Tapio Salmi, and Dmitry Yu. Murzin. Deactivation of postcombustion catalysts, a review. Fuel 83 (2004) 395–408

[85] S.S. Mulla, N. Chen, L. Cumaranatunge, G.E. Blau, D.Y. Zemlyanov, W.N. Delgass, W.S. Epling, and F.H. Ribeiro. Reaction of NO and O2 to NO2 on Pt: Kinetics and catalyst deactivation. Journal of Catalysis 241 (2006) 389–399.

[86] Shin'ichi Matsunaga, Koji Yokota, Shi-aki Hyodo, Tadashi Suzuki and Hideo Sobukawa. Thermal Deterioration Mechanism of Pt/Rh Three-way Catalysts. SAE Technical Paper Series 982706.

[87] M. Casapu, J.-D. Grunwaldt, M. Maciejewski, A. Baiker, M. Wittrock, U. Göbel, and S. Eckhoff. Thermal ageing phenomena and strategies towards reactivation of NOx- storage catalysts. Topics in Catalysis 42–43(2007)3.

[88] Josh A. Pihl, James E. Parks II and C. Stuart Daw, and Thatcher W. Root. Product Selectivity During Regeneration of Lean NOx Trap Catalysts. SAE Technical Paper Series 2006-01-3441.

[89] Jong-Hwan Lee and Harold H. Kung. Effect of Pt dispersion on the reduction of NO by propene over alumina-supported Pt catalysts under lean-burn conditions. Catalysis Letters 51(1998)1.

[90] Louise Olsson and Erik Fridell. The Influence of Pt Oxide formation and Pt dispersion on the Reactions NO_2 → $NO + {}^1/_2O_2$ over Pt/Al_2O_3 and $Pt/BaO/Al_2O_3$. Journal of Catalysis 210 (2002) 340–353.

[91] Joseph Theis, Justin Ura, Christian Goralski Jr., Hungwen Jen, Eva Thanasiu, Yasmenia Graves, Akihide Takami, Hiroshi Yamada and Seiji Miyoshi. The Effect of Ceria Content on the Performance of a NOx Trap. SAE Technical Paper Series 2003-01-1160.

[92] Anna Lindholm , Neal W. Currier , Erik Fridell , Aleksey Yezerets , and Louise Olsson. NOx storage and reduction over Pt based catalysts with hydrogen as the reducing agent Influence of H_2O and CO_2. Applied Catalysis B: Environmental 75 (2007) 78–87.

[93] Joseph Theis and Erdogan Gulari. A LNT+SCR System for Treating the NOx Emissions from a Diesel Engine. SAE Technical Paper Series2006-01-0210.

[94] Yaying Ji, Todd J. Toops, and Mark Crocker. Effect of Ceria on the Storage and Regeneration Behavior of a Model Lean NOx Trap Catalyst. Catal ysis Letter 119 (2007) 257–264.